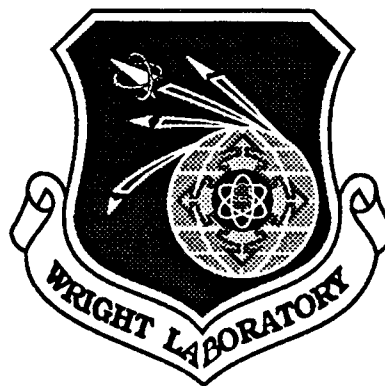


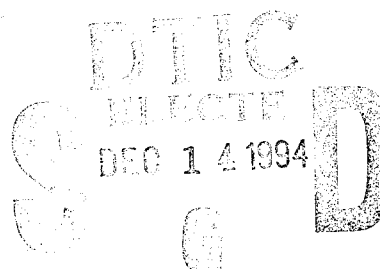
WL-TR-94-2069



**DEVELOPMENT OF A HIGH
TEMPERATURE, HIGH SPEED
DISC LUBRICANT TEST MACHINE**

*DAVID M. NICOLSON
RICHARD S. SAYLES*

**Tribology Section,
Department of Mechanical Engineering,
Imperial College of Science, Technology, and Medicine,
London, SW7 2BX. United Kingdom**



June 1994

Sep 87 - Jun 94

Approved for public release; distribution unlimited.

19941208 014

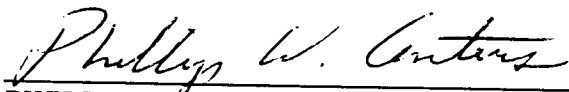
**AERO PROPULSION AND POWER DIRECTORATE
WRIGHT LABORATORY
AIR FORCE MATERIEL COMMAND
WRIGHT-PATTERSON AIR FORCE BASE, OHIO 45433-7251**

REPRODUCTION PROHIBITED

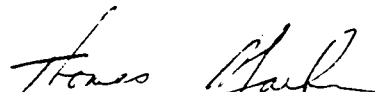
NOTICE

When government drawings, specifications, or other data are used for any purpose other than in connection with a definitely government-related procurement, the United States Government incurs no responsibility or any obligation whatsoever. The fact that the government may have formulated or in any way supplied the said drawings, specifications, or other data is not to be regarded by implication, or otherwise in any manner construed, as licensing the holder or any other person or corporation, or as conveying any rights or permission to manufacture, use, or sell any patented invention that may in any way be related thereto.


This technical report has been reviewed and is approved for publication.



PHILLIP W. CENTERS, Ph.D.
Lubrication Branch
Fuels and Lubrication Division



THOMAS A. JACKSON, Ph.D.
Acting Chief
Lubrication Branch
Fuels and Lubrication Division



LEO S. HAROOTYAN, JR., Chief
Fuels and Lubrication Division
Aero Propulsion and Power Directorate

If your address has changed, if you wish to be removed from our mailing list, or if the addressee is no longer employed by your organization, please notify **WL/POSL**, Wright-Patterson AFB OH 45433-7103 to help us maintain a current mailing list.

Copies of this report should not be returned unless return is required by security considerations, contractual obligations, or notice on a specific document.

| REPORT DOCUMENTATION PAGE | | | Form Approved OMB No. 0704-0188 | |
|--|---|---|---|--|
| Public reporting burden for this collection of information is estimated to average 1 hour per response, including the time for reviewing instructions, searching existing data sources, gathering and maintaining the data needed, and completing and reviewing the collection of information. Send comments regarding this burden estimate or any other aspect of this collection of information, including suggestions for reducing this burden, to Washington Headquarters Services, Directorate for Information Operations and Reports, 1215 Jefferson Davis Highway, Suite 1204, Arlington, VA 22202-4302, and to the Office of Management and Budget, Paperwork Reduction Project (0704-0188), Washington, DC 20503. | | | | |
| 1. AGENCY USE ONLY (Leave blank) | 2. REPORT DATE June 1994 | 3. REPORT TYPE AND DATES COVERED Final 9/01/87 - 6/30/94 | | |
| 4. TITLE AND SUBTITLE Development of a High Temperature, High Speed Disc Lubricant Test Machine | | 5. FUNDING NUMBERS C F49620-87-C-0084 WL/PO PE 62203F AFOSR/EOARD PE 61102F PR 3048 TA 06 WU 51 | | |
| 6. AUTHOR(S) David M. Nicolson Richard S. Sayles | | | | |
| 7. PERFORMING ORGANIZATION NAME(S) AND ADDRESS(ES) Tribology Section Department of Mechanical Engineering Imperial College of Science, Technology, and Medicine London, SW7 2BX United Kingdom | | 8. PERFORMING ORGANIZATION REPORT NUMBER | | |
| 9. SPONSORING/MONITORING AGENCY NAME(S) AND ADDRESS(ES) Aero Propulsion and Power Directorate Wright Laboratory Air Force Materiel Command Wright-Patterson AFB OH 45433-7251 | | 10. SPONSORING/MONITORING AGENCY REPORT NUMBER WL-TR-94-2069 | | |
| 11. SUPPLEMENTARY NOTES | | | | |
| 12a. DISTRIBUTION/AVAILABILITY STATEMENT Approved for Public Release; Distribution is unlimited. | | 12b. DISTRIBUTION CODE | | |
| 13. ABSTRACT (Maximum 200 words) Scuffing and adhesive failure modes are outlined to provide the context for a more detailed review of gear lubrication distinguishing, in particular, elastohydrodynamic and boundary lubrication regimes. The major scuffing theories, are considered against the particular requirements of lubricating at high temperatures and entrainment speeds. Existing lubricant testers are classified and evaluated with respect to their correlation with field experience. The need for a disc machine utilizing mini-discs driven at high speeds is proposed to satisfy both existing and future test requirements. Details of rig design, commissioning and development are detailed together with prototype experience which dictated that "improved repeatability and reproducibility over current methods outweighs incomplete reproduction of the contact cycle." Early "failures" of a similar nature to those experienced in high speed aerospace applications are being used to study the mechanism of high speed (high temperature) scuffing with synthetic lubricants. | | | | |
| 14. SUBJECT TERMS Lubricants, Load Carrying, Test, Turbine Engine, High Temperature | | 15. NUMBER OF PAGES 96 | | |
| | | 16. PRICE CODE | | |
| 17. SECURITY CLASSIFICATION OF REPORT Unclassified | 18. SECURITY CLASSIFICATION OF THIS PAGE Unclassified | 19. SECURITY CLASSIFICATION OF ABSTRACT Unclassified | 20. LIMITATION OF ABSTRACT Unlimited | |

FORWARD

This report describes the research conducted by personnel of Imperial College London England on Contract No. F49620-87-C-0084. The work was performed during the period September 1987 to June 1994.

The work was accomplished under Project 3048, Task, 304806, Work Unit 30480651, High Temperature Mini-Disc Development, with Dr. Phillip W. Centers as the project monitor.

| | |
|--------------------|---|
| Accession For | |
| NTIS | CRA31 <input checked="" type="checkbox"/> |
| DTIC | 173 <input type="checkbox"/> |
| Unannounced | <input type="checkbox"/> |
| Justification | |
| By _____ | |
| Distribution/ | |
| Availability Codes | |
| Dist | Avail and/or Special |
| A-1 | |

Contents

| | | |
|------------------|---|----|
| Chapter 1 | Lubricant load carrying capacity | |
| 1.0 | Background | 1 |
| 1.1 | Gear contact mechanics | 2 |
| 1.2 | Gear lubrication | 5 |
| 1.3 | Gear failure modes | 9 |
| 1.3.1 | Wear | 9 |
| 1.3.2 | Scuffing | 10 |
| 1.3.2.1 | Scuffing theories | 11 |
| 1.3.2.2 | Experience of scuffing in other fields | 13 |
| 1.4 | Review of adhesive wear and scuffing test methods | 15 |
| 1.4.1 | Film strength test machines | 16 |
| 1.4.2 | Simple geometry test machines (Type I Tests) | 17 |
| 1.4.3 | Gear testing machines (Type II Tests) | 17 |
| 1.4.3.1 | The I.A.E gear lubricant test machine | 19 |
| 1.4.3.2 | The F.Z.G gear lubricant testing machine | 20 |
| 1.4.3.3 | The Ryder gear test machine | 21 |
| 1.4.4 | Disc lubricant testing machines (Type III Tests) | 25 |
| 1.4.4.1 | AFAPL disc tester | 28 |
| 1.4.4.2 | The Amsler disc test machine | 28 |
| 1.4.4.3 | Battelle | 28 |
| 1.4.4.4 | Bearing Simulator | 28 |
| 1.4.4.5 | Geared roller tester | 29 |
| 1.4.4.6 | Gear roller tester | 29 |
| 1.4.4.7 | High temperature ep tester | 29 |
| 1.4.4.8 | Mini-disc | 30 |
| 1.4.4.9 | Imperial/Mobil 3.5" hydrostatic disc machine | 30 |
| 1.4.4.10 | Society of Automotive Engineers' disc test machine | 31 |
| 1.5 | The implications for LCC testing with developments in transmission lubricants and materials | 33 |
| Chapter 2 | Mini-disc configuration and design | |
| 2.1 | Design objectives | 39 |
| 2.2 | Ryder gear contact parameters | 41 |
| 2.2.1 | Ryder simulation | 42 |

| | |
|--|----|
| 2.3 Bearing simulation using discs | 47 |
| 2.4 Testing costs | 48 |
| 2.5 General arrangement of mini-disc test rig | 49 |
| 2.5.1 Drive-train | 52 |
| 2.5.2 Support and loading of discs | 53 |
| 2.5.2.1 Gas bearings | 54 |
| 2.5.2.2 Hybrid tilting pads | 55 |
| 2.5.2.3 Pivot design | 61 |
| 2.5.2.4 Test head lubrication | 62 |
| 2.5.2.5 Ancillary lubrication | 62 |
| 2.5.3 Sealing | 63 |
| 2.5.4 Heating | 66 |
| 2.5.4.1 Insulation | 67 |
| 2.5.5 Instrumentation | 68 |
| 2.5.5.1 Torque measurement | 68 |
| 2.5.5.2 Temperature measurement | 69 |
| 2.5.5.3 Speed measurement | 70 |
| 2.5.5.4 Disc load | 70 |
| Chapter 3 Results and test programme | |
| 3.1 Summary of commissioning and preliminary testing | 72 |
| 3.2 Results of tests to date | 72 |
| 3.3 Requirements for future testing and analysis | 75 |
| References | 86 |

List of Figures

| | | |
|-------------|--|-------|
| Figure 1.1 | Ryder gear tooth contact cycle using measured flank profiles | 2 |
| Figure 1.2 | Lubricant regimes | 5 |
| Figure 1.3 | Coefficient of friction versus specific film thickness | 6 |
| Figure 1.4 | Wear regime | 10 |
| Figure 1.5 | IAE gear test machine | 19 |
| Figure 1.6 | FZG gear testing machine | 20 |
| Figure 1.7 | Cross section of Ryder gear test machine | 22 |
| Figure 1.8 | Effect of tooth hunting | 23 |
| Figure 1.9 | Ryder tooth loading | 24 |
| Figure 1.10 | Gear contact simulation by discs | 26 |
| Figure 1.11 | Imperial / Mobil disc machine | 31 |
| Figure 1.12 | SAE disc machine | 32 |
| Figure 1.13 | Bulk lubricant temperature with projected aircraft speed | 33 |
| Figure 1.14 | Helicopter main gearbox lubricant development | 34 |
| Figure 1.15 | Candidate lubricant fluids for elevated temperature | 35 |
| Figure 2.1 | Disc sliding velocity versus load for constant PVs | 42 |
| Figure 2.2 | Thermal behaviour of the Ryder test according to Olver's model | 43 |
| Figure 2.3 | Thermal behaviour of mini-disc according to Olver's model | 44 |
| Figure 2.4 | Predicted effect of speed upon disc scuffing | 45 |
| Figure 2.5 | Practical dN rating | 47 |
| Figure 2.6 | Mini-disc versus Ryder testing costs | 48 |
| Figure 2.7 | Mini-disc specimen | 49 |
| Figure 2.8 | General arrangement of mini-disc test rig | 50,51 |
| Figure 2.9 | Schematic of drive-train | 52 |
| Figure 2.10 | Gas bearing | 54 |
| Figure 2.11 | Hydrostatic pad with integral piston | 55 |
| Figure 2.12 | Pivoted pad journal bearing after Michell and hybrid version | 56 |
| Figure 2.13 | Pad design optimisation routine | 58 |
| Figure 2.14 | Hybrid pad performance | 59 |
| Figure 2.15 | Sketch of hybrid pad | 60 |
| Figure 2.16 | Final and prototype hybrid pads sectioned at middle station | 61 |
| Figure 2.17 | Schematic of labyrinth seal | 64 |
| Figure 2.18 | Design of labyrinth seal | 65 |

| | | |
|-------------|---|----|
| Figure 2.19 | Induction heating of AMS 6260 and silicon nitride discs | 66 |
| Figure 2.20 | Schematic of torque measurement | 68 |
| Figure 2.21 | Disc temperature measurement by infra-red emission | 69 |
| Figure 3.1 | 'Conventional' scuff | 77 |
| Figure 3.2 | Surface topography of mini-disc after running-in | 78 |
| Figure 3.3 | Surface topography of scuffed mini-disc | 79 |
| Figure 3.4 | Preliminary scuffing results with high speed mini-disc | 80 |
| Figure 3.5 | Log file 10/11/93 | 81 |
| Figure 3.6 | 'High speed' scuff | 82 |
| Figure 3.7 | Surface topography of 'high speed' scuff | 83 |
| Figure 3.8 | Axial bands of 'polished mini-disc | 74 |
| Figure 3.9 | Log file 11/11/93 | 84 |
| Figure 3.10 | Log file 16/11/93 | 85 |
| Figure 3.11 | Alternative approaches to assess of scuffing envelope | 76 |

List of Tables

| | | |
|------------------|--|-----------|
| Table 1.1 | Lubricant film strength testing machines categorised by type | 16 |
| Table 1.2 | Parameters for IAE, FZG and Ryder gear test machines | 18 |
| Table 1.3 | Disc machine operating conditions | 27 |
| Table 2.1 | Specimen configurations | 39 |
| Table 2.2 | Ryder gear contact parameters | 41 |
| Table 2.3 | Recessed hydrostatic, hydrodynamic and plain bearing parameters | 56 |

Chapter 1

Lubricant Load Carrying Capacity

1.0 Background

A key requirement in the development of transmissions is the need to increase specific power, i.e. torque and/or angular velocity per unit mass, without impeding upon reliability.

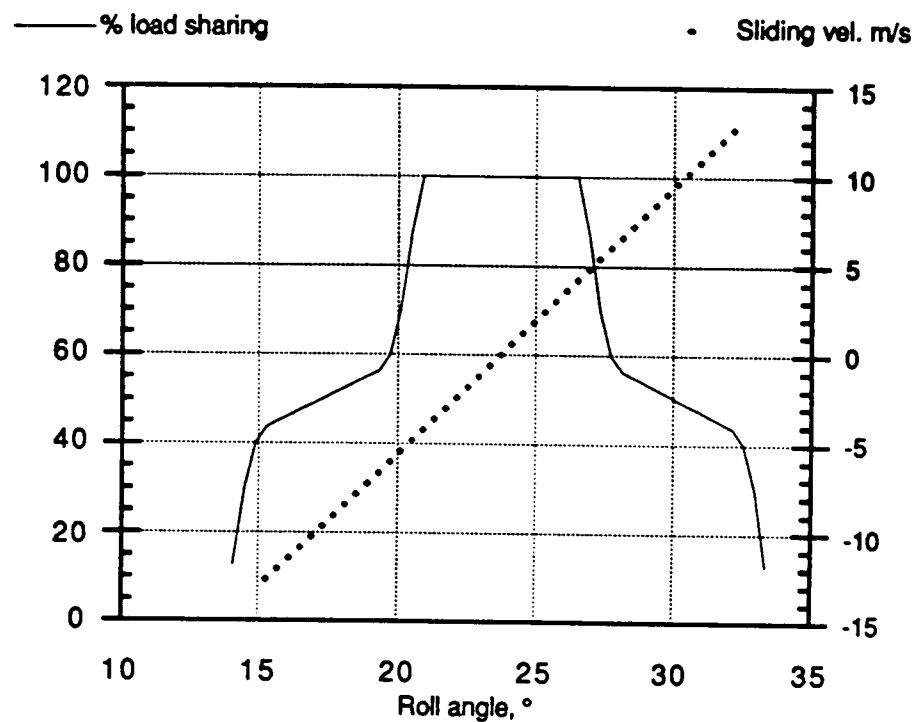
Existing test methods are inadequate in predicting certain failure mechanisms, such as scuffing, and have resulted in the need to develop alternative load carrying capacity tests. Load carrying capacity is one measure of lubrication efficacy.

This report outlines the design and construction of a mini-disc rig to evaluate scuffing, together with test results undertaken at Imperial College, London on behalf of Wright Patterson airforce base (WPAFB).

1.1 Gear Contact Mechanics

Tooth contact loads vary during meshing and the relative motion between the teeth comprises both sliding and rolling at different points within the meshing cycle. This cycle is illustrated in Figure 1.1 from maximum negative sliding¹ at engagement, through zero at the pitch point (i.e. pure rolling) to maximum positive sliding at disengagement.

Figure 1.1 Ryder Gear Tooth Contact Cycle Using Measured Flank Profiles
(Courtesy of Eaton Transmissions Ltd)



¹ Sliding is termed as the difference between the respective rolling velocities of meshing teeth. For sliding to be positive, convention dictates that both rolling and sliding are in the same direction.

Static contact analysis data was employed to produce Figure 1.1, hence no allowance was made for dynamic effects, alignment or pitch errors which will superimpose transient loads.

In transmitting power and relative motion between geared shafts, tooth contact is non-conformal. For a rectangular contact² of width l , the mean contact stress can be defined as:

$$\sigma_{\text{mean}} = \frac{\text{Load}}{\text{contact area}} = \frac{W}{2 \times b \times l} \quad (1)$$

where:

$$b = \sqrt{\frac{4 \times W \times R'}{\pi \times l \times E^*}} \quad (2)$$

$$R' = \left\{ \frac{1}{R_1^2} + \frac{1}{R_2^2} \right\}^{-1}$$

$$E^* = \left\{ \frac{1 - \nu_1^2}{E_1} + \frac{1 - \nu_2^2}{E_2} \right\}^{-1}$$

R_1 & R_2 are radii of teeth at point of contact, E_1 and E_2 , ν_1 and ν_2 are moduli and Poisson's ratios respectively.

Given $\sigma_y \propto \text{hardness}$:

$$W_{\text{allow}} = \frac{(\text{hardness})^2}{E^*} \times R' \times l \quad (3)$$

Hence the optimum material parameter is one of high ($\text{hardness}^2/E^*$), whilst the relative radius, R' , varies with roll angle.

Besides allowable contact stress, the geometry of the tooth means that there will also be a tensile stress at the root fillet due to bending. If the tooth is modelled as a cantilever then from:

² In practice tooth contact is ~ elliptical but of high aspect ratio in spur gears. For simplicity this has been approximated to a nominal line contact for the purposes of this study.

$$\sigma = \frac{M \times y}{I} \quad (4)$$

it can be shown, AGMA (1965) that

$$W_{allow} = fn(hardness \ \& \ geometry) \quad (5)$$

where geometry embraces tooth shape, thickness and root fillet.

The root bending stress is tensile and occurs on the surface whilst the maximum compressive stress is sub-surface and therefore constrained, $\sigma_c > \sigma_b$, typically 1.2 GPa cf. 0.5 GPa for performance gears.

In practice, the teeth are heat treated which modifies the argument above, insofar as the material is no longer homogeneous whilst the contact is not smooth but occurs over numerous discrete asperities.

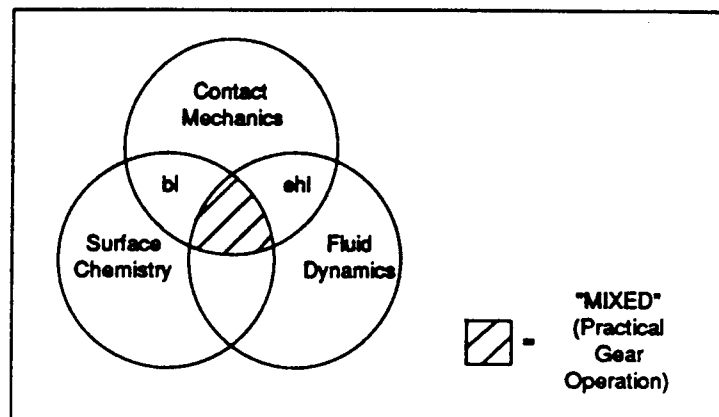
In addition, tooth meshing is dynamic which affects both tooth loading and introduces fatigue where toughness is paramount. Nevertheless the analysis does provide an insight into the requisite material parameters for gears.

1.2 Gear Lubrication

Whilst traction can be improved by increasing the equivalent modulus, E^* , in order to reduce the area of contact, in practice much more is to be gained from lubrication. Three regimes, shown in Figure 1.2 are broadly distinguishable corresponding to the variation in contact conditions illustrated in Figure 1.1:

- Boundary (bl)
- Mixed
- Full Elastohydrodynamic lubrication (ehl)

Figure 1.2 Lubricant Regimes



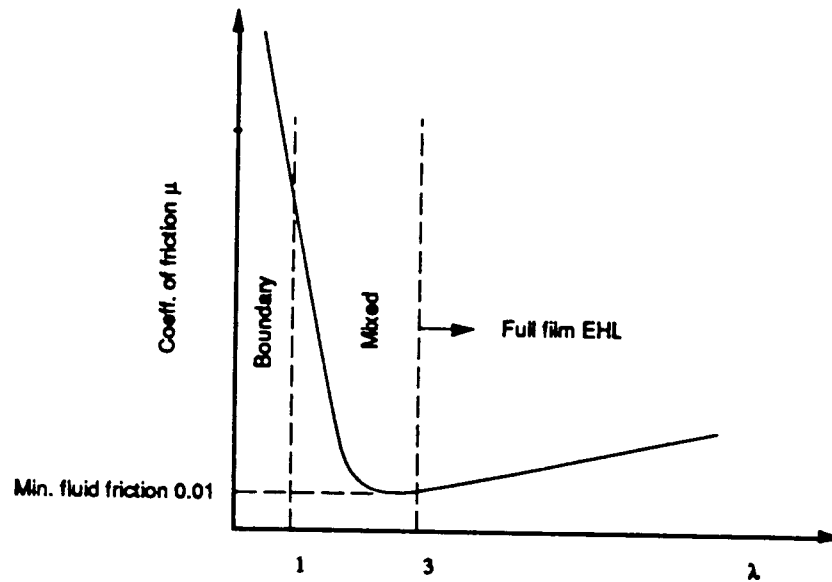
Boundary lubrication is that which “cannot be attributed to the bulk viscous properties of the lubricant, but arises from a specific solid lubricant interaction”.

Boundary lubrication lowers traction. This is achieved by the creation of low shear strength interfacial films appropriate to the severity of the contact (temperature, pressure and sliding speed) reducing adhesion and traction.

The mechanism and interaction of fluid and material parameters is complex and dominated by the physical and chemical properties of the surfaces in contact. Increased rotational speed assisted by better finish, improved geometry or higher lubricant inlet viscosity, will

enable a full elastohydrodynamic film to develop via a mixed regime as illustrated in Figure 1.3.

Figure 1.3 Coefficient of Friction versus Specific Film Thickness



$$\lambda = \frac{h}{\sqrt{(\sigma_1)^2 + (\sigma_2)^2}} \quad (6)$$

where

h = film thickness

σ_1, σ_2 = r.m.s roughness

Elastohydrodynamics extends the applicability of classical hydrodynamics to non-conformal surfaces. This is achieved through the elastic deformation of the contacting surfaces and enhanced lubricant viscosity that arises under extreme pressure.

Under these conditions, the minimum film thickness between two rollers (\approx two spur teeth) has been defined empirically by Dowson & Higginson (1966) as:

$$h_{min} = 2.7 \times \frac{U^{0.7} \times \eta^{0.7} \times \alpha^{0.54} \times R^{0.43}}{\left(\frac{W}{l}\right)^{0.13} \times E^{0.03}} \quad (7)$$

where

$U = U_1 + U_2$, U_1 & U_2 are peripheral velocities of bodies 1 & 2 respectively

From Equation (7) it is evident that the minimum film thickness is strongly influenced by the entrainment speed, U , the inlet viscosity, η , and the pressure viscosity coefficient, α . Gear geometry and speed dictate the entrainment speed. Lubricant rheology determines the inlet viscosity and pressure viscosity coefficient, largely according to temperature. The optimum film thickness is that which just, completely separates the surfaces.

In practice the influence of temperature upon viscosity is substantially greater than upon the pressure viscosity coefficient and it is therefore the viscosity index which is optimised.

The benefits of operating under full elastohydrodynamic conditions would mean complete separation of the tooth surfaces. However, in practice, low rotational speed and/or weight, preclude this.

It may be concluded that distinguishing between regimes depends upon whether shear is predominantly within the fluid film or within the surface layers. Transition between regimes depends upon specific operating conditions such as gear type and arrangement, material, loading, accuracy, finish, lubricant, lubrication and cleanliness.

Hence effective gear design needs to take into account:

- i. Gear size in relation to load carrying capacity³ and resistance to scuffing⁴
- ii. Allowable contact stress and resistance to pitting
- iii. Tooth size to ensure adequate bending strength
- iv. Cost

³ Scuffing is used as the criterion of LCC whilst operating in the Mixed Regime of Figure 1.2, and is the transition from *mild acceptable wear* to *catastrophic wear*

⁴ The term *scuffing* is used throughout rather than the American usage of *scoring*.

Where advanced transmissions are concerned (i), (ii) and (iii) are of primary concern in maximising specific power and reliability. This is sought by maximising Load Carrying Capacity and/or speed⁵ through optimising geometry, dynamics, material, lubricant etc.

This study is primarily concerned with the nature of extensive adhesive wear as a result of combined boundary and elastohydrodynamic lubrication failure.

⁵ Hsing (1974) importance of LCC upon transmission weight where 50% of commercial life cycle costs are attributable to fuel (\propto weight) and Cocking (1984) high ratio final stage configuration

1.3 Gear Failure Modes

The AGMA classifies gear failure modes as follows:

- *Wear*
- *Scuffing*
- *Interference*
- *Surface fatigue*
- *Plastic flow*
- *Fracture*
- *Process Related*
- *Compound*

Gear failure is frequently multifarious and such distinctions are primarily a means of characterisation. For the purpose of this report *wear* and *scuffing* are reviewed. Scuffing often manifests itself as *gross wear*.

1.3.1 Wear

If the lubricant film between meshing teeth during running is insufficient to separate the surfaces, asperity contact will lead to wear. Wear can be categorised as:

- polishing
- moderate
- excessive

Polishing wear is the most frequently observed where low speed gears operating in a boundary regime combine asperity contact with extreme pressure (ep) action.

Moderate wear can occur at gear tips and roots, where gears are insufficiently hard and ep action inadequate. Prevention is possible by using either a more viscous or active lubricant or by changing the operating conditions, i.e. geometry, surface finish, load, etc.

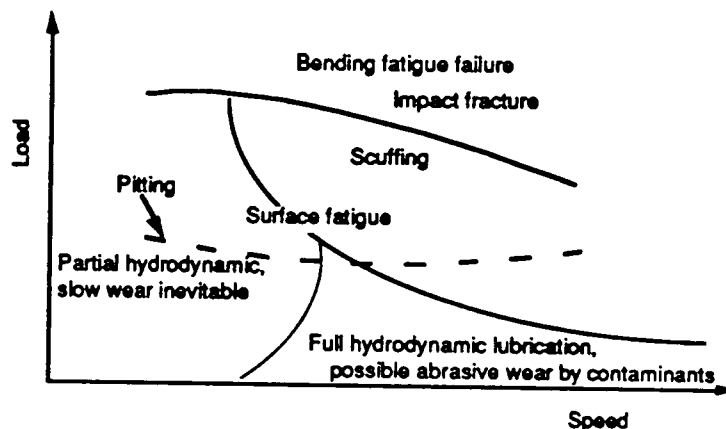
If wear is allowed to become excessive the reduction in tooth thickness and/or creation of crack initiation sites will eventually impair tooth bending strength.

Two further types of wear are of note: *abrasion*, two or three-body, and *corrosion*. Ineffective lubricant filtration promotes two body abrasion, whilst condensation, for example, can cause corrosive wear.

Acceptable levels of wear vary. For example, what is considered acceptable for automotive gears, is likely to be excessive for a set of precision instrument gears. Wear during 'running-in' is invariably considered beneficial.

Wear regimes can be depicted in terms of load-speed plots as shown in Figure 1.4.

Figure 1.4 Wear Regimes, Shell (1964)



1.3.2 Scuffing

Scuffing is defined by the AGMA (1980) as "gross adhesive wear, characterised by tooth asperity contacts welding and tearing". It is usually the result of tooth damage associated with defective lubrication. Localised scuffing, for example, can be caused as a result of tooth misalignment, form errors, inadequate tip relief or excessive dynamic loading. In contrast to other types of lubrication-related tooth failure which take time to develop,

scuffing occurs precipitously⁶ and is therefore of primary concern. Unless caught early on and rectified, scuffing will render a gear set totally un-serviceable.

Very light scuffing, termed *frosting*, can either heal completely if conditions change, or remain limited to the root. If allowed to develop, material loss above and below the pitch line will destroy the tooth profile, create noise and vibration, and may lead eventually to tooth fracture.

1.3.2.1 Scuffing theories

Scuffing mechanisms can be summarised as a combination of Blok's critical temperature criterion and Dyson's failure of ehl. The remaining hypotheses are to a greater or lesser extent based or derived from these, Dyson (1975).

Blok attributes gear failure to a critical temperature, comprising the sum of the bulk (skin) temperature and the flash temperature rise in the contact, θ_f , which may for a given material/lubricant combination be written as:

$$\theta_f \propto \left\{ \frac{\mu \times W \times (v_1 - v_2)}{(B_1 \sqrt{v_1} - B_2 \sqrt{v_2}) \times \sqrt{2b}} \right\} \quad (8)$$

where:

μ = coefficient of friction

W = load per unit length

v_1, v_2 = sliding velocity of bodies 1 & 2

B_1, B_2 = thermal constant of bodies 1 & 2

b = contact half-width, Ref. Equation (2)

⁶ 'Fatigue scoring' phenomena investigated by MacPherson (1972) is one of surface micro-pitting fatigue causing scuffing.

As v_1 and $v_2 \propto n$, rpm of pinion

$$\frac{v_1 - v_2}{\sqrt{v_1} - \sqrt{v_2}} \propto \sqrt{n} \quad (9)$$

hence

$$\theta_f \propto \mu \times W^{\frac{3}{4}} \times n^{\frac{1}{2}} \quad (10)$$

which, if μ is constant may be rewritten,

$$(n)^{\frac{2}{3}} \times W = \text{constant} \quad (11)$$

which is similar to the PV_s criteria⁷, namely:

$$n^2 \times W = \text{constant} \quad (12)$$

Dyson's theory, on the other hand, is based on the lambda concept, namely, if the ratio of film thickness to composite surface roughness is less than unity, then failure of ehl and scuffing are more likely to occur.

Since ehl is strongly affected by lubricant inlet viscosity, any reduction in viscosity will increase the level of asperity contact and, in turn, reduce inlet viscosity through thermal feedback. The localised lubricant films between contacting asperities, known as micro-ehl will collapse in the absence of high ambient pressure created by the macro-ehl hence a film separating the surfaces no longer exists.

Thus while Blok's criterion is one of critical contact temperature, that of Dyson's is critical inlet temperature. Empirical evidence over the validity of either theory varies according to the source and test method employed. However, their use is widespread in the absence of

⁷ PV_s after Almen (1942), the product of the mean Hertzian pressure and the sliding velocity, where $P \propto \sqrt{W}$ and $V_s \propto n$ hence $PV_s \propto W n^2$. Grosberg (1977) notes the exponent varies between -1 and +2 according to the source.

better alternatives⁸. Implicit in this empiricism is the difficulty in predicting the onset of scuffing, especially where formulated lubricants are concerned.

In practice, boundary films complicate matters and any adequate scuffing theory must explain both the failure of elastohydrodynamic and subsequent failure of the boundary film. Final analysis indicates that it is the wear of the boundary film that dictates the actual onset of scuffing, or equally, recovery where the coefficient of boundary friction is low enough to permit the ehl film to re-form.

It is usually possible to ensure scuffing is avoided by refining the surface finish, modifying the tooth profile, improving lubricant additive or cooling. However, in some circumstances it may be necessary to redesign the gear. For example, a finer pitch will reduce the extent of sliding, albeit for a reduction in tooth bending strength. Increased lubricant viscosity is not necessarily beneficial, as viscous shear heating can lead to a reduced film besides increasing traction.

1.3.2.2 Experience of scuffing in other fields

Scuffing can occur in engines between piston-ring and bore, and on occasion between piston-skirt and bore. Experience has led to empirical designs for both piston and ring, subject to:

- *application* : rate of pressure rise, bore distortion, rubbing speed, and temperature.
- *material* : ring and liner compatibility, and finish.
- *lubricant* : additives.

For example, piston-ring chromium plating and cross-honing of the bore can be combined with an appropriate lubricant additive to mitigate against scuffing, Avery (1967) & Neale (1974). Neale (1971) notes that piston ring scuffing is not common in service as considerable effort is expended during development in prevention.

⁸ For example, AGMA (1965) advocates a flash temperature of 145°C for AMS 6260 spur gears hardened to 60Rc and lubricated with an ester to Mil-L-7808.

Scuffing can also occur between cams and tappets, Dyson (1961). The dynamics are more complex than those of piston-ring and bore, as rotation of the tappet tends to reduce the flash temperature and help renew the contact surface, whilst the contact geometry and friction vary with cam rotation. Once again application, material and lubricant influence the likelihood of scuffing. For example, historically chilled cast-iron cams and tappets have been used to resist scuffing. More recently active lubricants and overhead cam designs, which reduce valve train loads, have enabled alternative materials which are more resistant to pitting to be used successfully.

Assessed under Blok's criterion; typical flash temperatures at 5000 rpm are of the order of 180°C, but can be as high as 350°C, with friction coefficients around 0.08. Designs are also frequently assessed on PV_s with typical values in the region of 3.5 GPam/s. Flash temperatures for piston-ring and bore are of the same order as between cam and tappets, but significantly higher ambient temperature means that asperity contact is particularly undesirable.

Although scuffing per se is not experienced with rolling element bearings, a form of adhesive wear, known as smearing, is sometimes observed where there is significant sliding. Prime locations are between:

- the cage and rolling elements
- the flange and roller contacts in roller bearings
- the inner race and elements in high speed lightly loaded bearings

1.4 Review of Adhesive Wear and Scuffing Test Methods

At the turn of the century lubricant testing was largely confined to viscosity, specific gravity, flash point and colour, Hyde (1922). An oil's suitability for any particular application would be derived from either experience or journal testers such as the Thurston or Ingram & Stapfer, Hurst (1911). Although the property of oiliness was observed it was not until refined mineral oils gained wider acceptance as lubricants⁹ that attempts were made to identify its nature.

Early film strength lubricant test machines such as the Napier, similar in configuration to the Timken, were developed as the advent of hypoid gearing¹⁰ added impetus to the demand for ep and subsequently anti-wear additives, Musgrove (1944).

The course of lubricant development has led to a proliferation of lubricant testers employing numerous configurations to assess lubricant performance without the cost and complexity of field service testing.

Such tests tend to rate lubricants according to specific operating conditions, including:

- *Film Strength*
- *Corrosion*
- *Compatibility* (e.g. with elastomeric seals and gear case materials)
- *Deposition*
- *Foaming*
- *Oxidation and thermal stability*
- *Wear*

⁹ Frequently on account of other properties, such as better oxidation resistance.

¹⁰ Many early failures of hypoid gears could be traced to insufficient rigidity of the assembly, but even when rigidly mounted, satisfactory operation required a suitably active lubricant.

1.4.1 Film Strength Test Machines

Ease of monitoring test parameters, accelerated testing and reduced test-cost promotes laboratory over field testing. However, extreme caution must be taken in correlating results against full-scale service, Macpherson (1986) and Wolf (1932).

In view that the research undertaken on behalf of WPAFB is primarily concerned with scuffing, film strength test methods/machines have been reviewed in isolation with respect to assessing lubricant Load Carrying Capacity.

Laboratory test methods used to assess wear and scuffing performance can be categorised into three types of lubricant test machine:

- Simple Geometry Testing Machines: those using simple geometric test specimens under pure sliding conditions (referred to as Type I Tests).
- Gear Test Machines: those using gears as the test specimen (referred to as Type II Tests).
- Disc Test Machines: those using discs to simulate a particular point on the path of contact (referred to as Type III tests).

Table 1.1 Lubricant Film Strength Testing Machines Categorised by Type

| TYPE | | FAILURE CRITERIA | STANDARD |
|-------------|---|--|--------------------------------------|
| I | Pin & 'V' block (Falex) | specific wear seizure | ASTM D-2670 ASTM D-3233 |
| I | Block & ring Timken test | specific wear seizure | IP 240 ASTM D-2509 |
| I | 4-Ball m/c (Shell-Seta, Falex) | specific wear seizure | IP 239 ASTM D-2783 ASTM D-4172 |
| I | Almen | seizure | - |
| I | Alpha LFW-1 -Timken | specific wear | ASTM D-2714 |
| II | Ryder Gear m/c | specific area scuffed | ASTM D-1947 |
| II | FZG Gear m/c | specific wear specific area scuffed | IP 334 DIN 51 354 |
| II | IAE Gear m/c | initial scuff specific area scuff | IP 166 |
| III | Amsler disc machine | specific wear initial scuff | - |
| III | SAE disc machine | specific wear initial scuff | Fed. Test Std 791 mthd 6501.1 |
| III | Imperial/ Mobil Coryton disc machine | specific wear initial scuff | - |

1.4.2 Simple Geometry Testing Machines (Type I Tests)

Convenience and the relative ease by which parameters can be monitored accounts for the widespread use of Simple Geometry Testing Machines. The limited correlation with field experience can be attributed to inadequate reproduction of service conditions in a laboratory environment and the complexity and diverse nature of practical systems.

No attempt is made to simulate the gear contact cycle or any part of it. The motion is one of pure sliding and contact geometry varies with run-time although the Falex test does attempt to partly cater for the change in contact conditions by specifying a run-in procedure.

The limitation of pure sliding is a common feature of Type I tests and has been tackled by various researchers, such as Brix (1946) who modified the Timken configuration to oscillate one rotating disc against a self-aligning plate to introduce rolling.

1.4.3 Gear Testing Machines (Type II Tests)

Gear Testing Machines use spur gears as test specimens to determine the relative load carrying capacity of lubricants with power re-circulating on the four-square principle. This allows torque to be "locked" into the system, whereby the power required is merely that needed to overcome system losses.

The operating conditions of Gear Testing Machines are pre-determined to ensure that the mode of failure is invariably scuffing with increased torque. Gear tests are used to compare relative performance of one oil to another, rather than an absolute measure of performance.

There are three key differences between the various types of gear machines:

- the method of applying the load, during running or static
- whether or not the teeth hunt
- the extent to which the lubricant bulk temperature is controlled

Table 1.2 outlines the gear and operating parameters for the major types of Gear Testing Machines.

**Table 1.2. Gear and Operating Parameters for IAE, FZG¹¹ and Ryder
Gear Test Machines**

| Gear test machine | IAE | IAE | IAE | FZG, A | FZG, C | RYDER |
|---------------------------------------|-----------|-----------|-----------|---------|---------|--------------------|
| Pinion speed, rpm | 2000 | 4000 | 6000 | 2175 | 2175 | 10000 |
| No. of teeth, pinion/gear | 15/16 | 15/16 | 15/16 | 16/24 | 16/24 | 28/28 |
| Addendum mod. coef. x p | 0.375 | 0.375 | 0.375 | 0.8635 | 0 | 0 |
| Addendum mod. coef. x G | 0.494 | 0.494 | 0.494 | -0.5 | 0 | 0 |
| tip relief, pin./Gear μm | 12.7, 7.6 | 12.7, 7.6 | 12.7, 7.6 | 0 | 0 | 5-10 ¹² |
| Pressure angle | 26.317 | 26.317 | 26.317 | 22.5 | 22.5 | 22.5 |
| Face width, m | 4.77E-3 | 4.77E-3 | 4.77E-3 | 20.1E-3 | 20.1E-3 | 6.35E-3 |
| Test Oil temperature, °C | 60 | 70 | 110 | 90 | 90 | 74 |
| Test oil flow, ml/min | 284 | 568 | 568 | Dip | Dip | 270 |
| Initial Load, N | 127 | 127 | 127 | 90 | 90 | 93 |
| Load - stress increment ¹³ | 64N | 64N | 64N | 185MPa | 185MPa | 93N |
| Running period, min | 5 | 5 | 5 | 15 | 7.5 | 10 |
| Rest period, min | 5 | 5 | 5 | A/R | A/R | 10 |
| Max sliding velocity m/s | 3.96 | 7.92 | 11.89 | 3.96 | 3.6 | 11.89 |
| Pitch line velocity m/s | 8.4 | 16.7 | 25.1 | 8.3 | 8.3 | 46.74 |

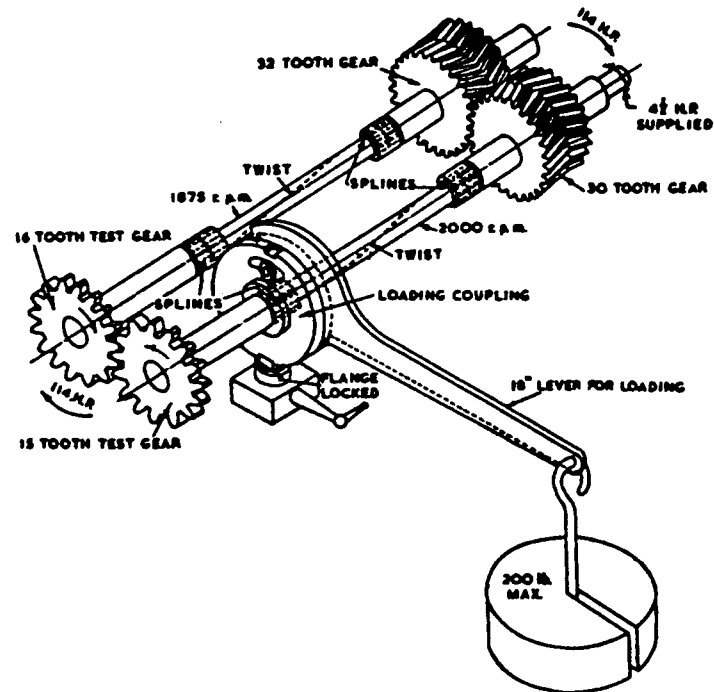
¹¹ In addition to the conditions detailed in Table 1.2 the IAE gear test can also be carried out at 200°C, at either 2000 rpm or 6000 rpm.

¹² Intriguingly gears were originally specified without tip relief on the grounds that it did not improve repeatability, Ryder(1959). Figure 1.9 indicates that the tip relief now specified is relatively insignificant.

¹³ IAE & Ryder are pitch line loads, FZG is crown tooth stress.

1.4.3.1 The Institute of Automotive Engineers' (IAE) gear test machine

Figure 1.5 IAE Gear Test Machine. Mansion (1952)



The IAE gear test stipulates a total of four determinations running two pairs of gears, testing both forward and reverse faces. The gears operate at an extended centre, giving rise to a high pressure angle and consequently increased relative sliding.

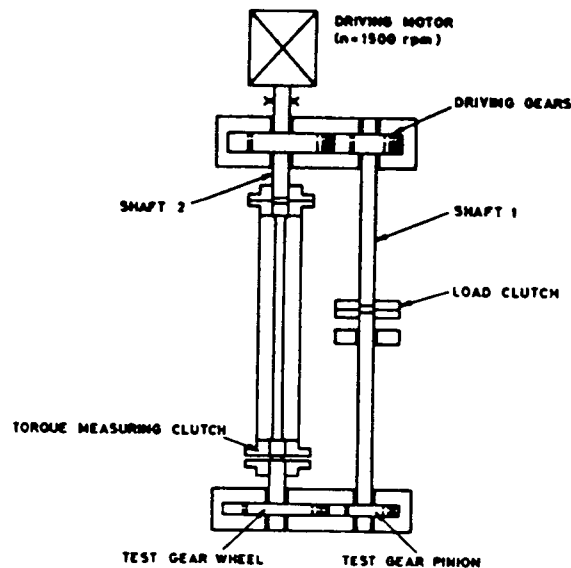
The test is interrupted between each load stage for a visual inspection of the teeth. If less than 60% of the face area above the pitch line is scuffed, the tooth load is increased by locking additional torque into the system whilst the rig is static. In the event that only one face is damaged this is deemed an initial failure load. Complete failure requires that both face and counter face are damaged. Hence, an average failure load is derived from eight failure values, initial and complete.

Whilst flowrate and initial temperature of the test lubricant are controlled, no provision is made for cooling. However the interruptions between each load stage will allow the gears to cool. 4.5 litres of test lubricant are required for each run.

1.4.3.2 The FZG (Forschungsstelle für Zahnräder und Getriebebau¹⁴) gear lubricant testing machine

The FZG gear test machine shown in Figure 1.6 is similar to the IAE test machine. Two gear profiles have been standardised, detailed as "A" and "C" in Table 1.2. The pinion of profile "C" has a long addendum to increase the extent of sliding which is necessary to test fully formulated oils.

Figure 1.6 FZG gear testing machine, IP 334/80



A step loading sequence is applied in twelve unequal load stages from 100-16,000N, equivalent to equal increments of Hertzian stress up to 2.3 GPa. As with the IAE test the torque is altered whilst the rig is static.

¹⁴ Laboratory for Gear research, TU München.

An immersion heater is used to raise the sump temperature to 90°C before the test commences. The gears hunt and are dip lubricated. At each load stage the gears are inspected for scuffing and weighed for wear whilst the lubricant is cooled back to 90°C. The failure load is that at which the wear rate increases dramatically, i.e. it is necessary to be able to distinguish between load stages of low and high wear.

As with the IAE test, both faces of the teeth are used for rating purposes. Discrepancies between forward and reverse results may occur when testing active lubricants, and ratings are considered suspect if they differ by more than one load stage for a given machine.

The particular strength of the FZG test is attributed by Olver (1993) to be the cooling of the test lubricant back to 90°C between each load stage. This ensures that each stage starts from a common bulk temperature.

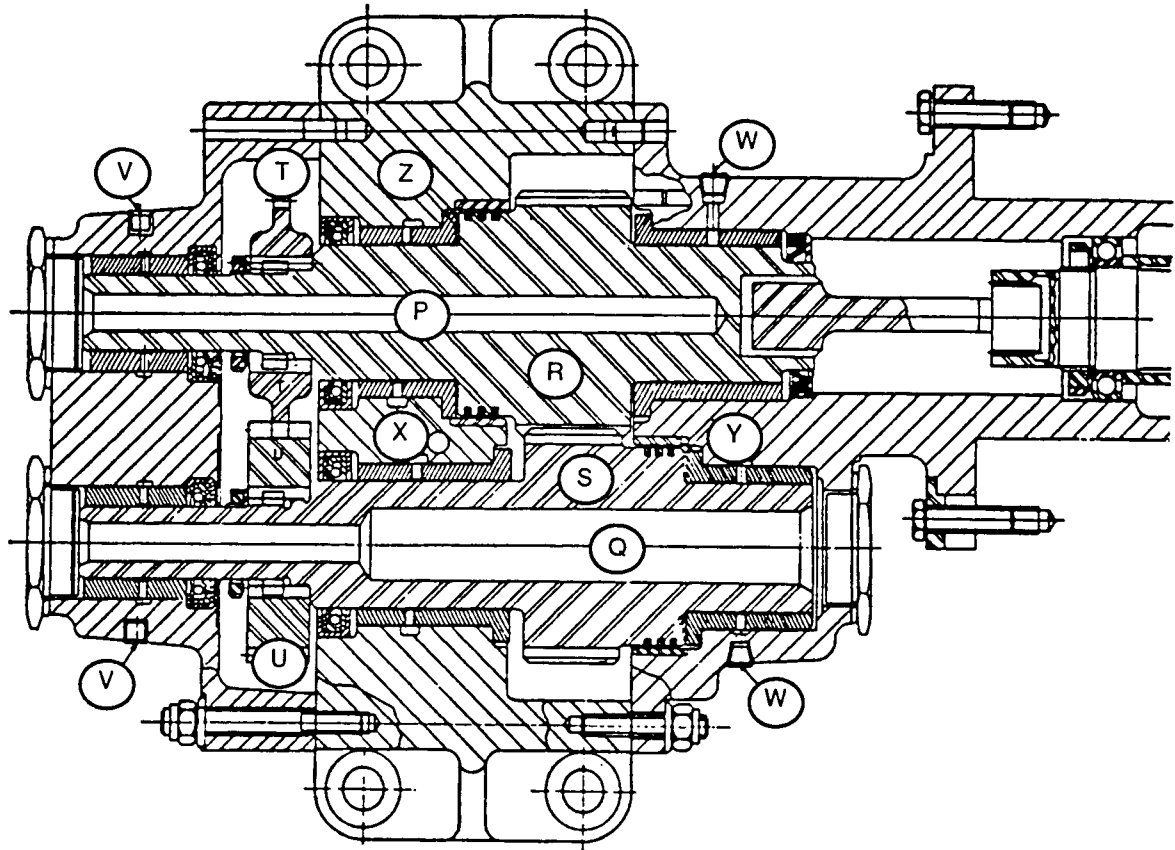
1.4.3.3 The Ryder gear test machine

ASTM D 1947, or the Ryder test as it is more commonly known, is illustrated in Figure 1.7. Torque is introduced into the four-square arrangement by applying hydraulic pressure during running to produce an axial load on the helical slave gears. At the end of each load stage, the torque is released when the test is interrupted for inspection of the teeth.

Both the Erdco & WADD gear test machines are similar in configuration and operation, and both comply with ASTM D 1947-77. The WADD gear test machine is, in essence, a development of the Ryder. Improvements in material and design permit operation up to 30,000 rpm and 370°C.

The test head is arranged to use only 500 ml of test lubricant, with a separate lubricant supply being used for the remainder of the test-rig which is maintained at $74\pm3^{\circ}\text{C}$. However, there is no provision for cooling of the test lubricant and despite rapid recirculation and exposed pipework it is suggested that in practice it rises well above 74°C in the higher load stages and this has considerable influence upon lubricant performance.

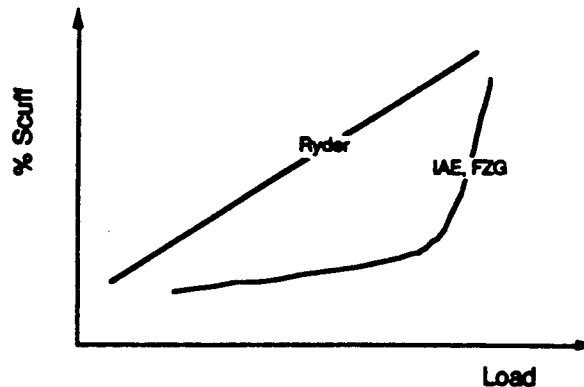
Figure 1.7 Cross Section of Ryder Gear Test Machine. ASTM (1947)



| | | | |
|---|--------------------|---|-------------------------|
| P | Drive Shaft | V | Support oil in |
| Q | Driven Shaft | W | Support and load oil in |
| R | Slave Gear | X | Support and load oil in |
| S | Slave Gear | Y | Load chamber |
| T | Test Gear (narrow) | Z | Load chamber |
| U | Test Gear (wide) | | |

Scuffing frequently occurs at a fairly low load in the Ryder test as a consequence of the lack of tooth hunting. The spread of damage is more gradual than in either the FZG or IAE gear test machines, as illustrated in Figure 1.8.

Figure 1.8 Effect of Tooth Hunting. Benzing (1964)



Ryder recognised that the frequent occurrence of scuffing under very low loads remained limited to the tips and did not develop until the later load stages. In order to discriminate lubricant performance he arbitrarily defined the criterion for failure as 22.5% of total tooth area scuffed, which is equivalent to two thirds of the teeth scuffed over one third of their working area, Ryder (1959). In practice, it is necessary to apply load stages beyond those required for Ryder's 22.5% criterion to identify the failure load stage with any confidence. For certain active lubricants this can prejudice subsequent testing on the reverse side.

Each pair of gears are tested on both flanks as per the IAE test. If only two determinations are made, i.e. a single pair of gears, repeatability stipulates that scuffing loads do not differ by more than 13.8 kN/m at 95% confidence levels. Whereas if four determinations are made then the average of each pair should not differ by more than 9.75 kN/m.

Reproducibility between installations specifies that single observations taken at two positions must agree within 13.8 kN/m at 95% confidence levels, whilst the averages must agree within 11.6 kN/m.

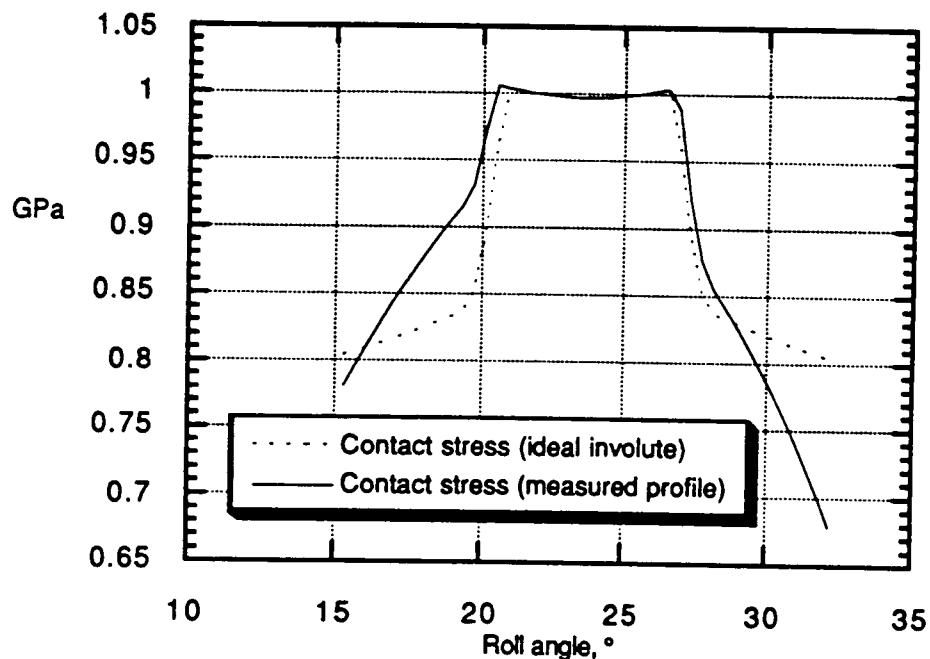
Load ratings are usually quoted relative to a standard reference oil, for example; Mil-L-7808 is rated at 88% of Ref. Oil C which has a failure load of 73 kN/m based upon four determinations.

The difficulties in meeting these conditions have been reviewed by various authors. For example, work by Kelley (1953) showed that an increase in surface roughness of 0.25

microns r.m.s can decrease load carrying capacity by 25% and misalignment of only 0.005 radians can decrease the load carrying capacity by 35%. Carper (1971) demonstrated that tip relief of only 10 microns, which is within the Ryder gear tolerance, can increase the load carrying capacity by some 50%. More recently, Wilson (1987) detailed the problems experienced by Sier Bath, a subsidiary of Alcor, in matching the performance of the original Pratt & Whitney gears despite close attention to tolerance.

Furthermore, analysis of measured tooth profiles has revealed premature engagement of the Ryder teeth under load, in advance of conjugate action. This would account for the localised scuffing experienced at low load stages and will affect repeatability. (This is not apparent from Figure 1.9 as roll angle is used as the abscissa).

Figure 1.9 Ryder Tooth Loading. (Courtesy of Eaton Transmissions Ltd)



1.4.4 Disc Lubricant Testing Machines (Type III Tests)

Although Merritt (1935) is credited¹⁵ for the first use of a disc test machine in gear simulation, the concept had been around for several years in the form of the Amsler disc machine¹⁶. In fact Martin (1916) demonstrated an awareness of the concept, through the use of rigid cylinders to simulate tooth contact, in his paper on the theory of involute gearing. Whenever or whoever first employed discs for lubricant evaluation the approach remains valid today and is cogently summarised by Mansion in his discussion of Evans' (1941) paper:

"it is desirable to test ep lubricants under something more approaching service conditions than is offered by most of the so-called ep testing machines (yet) it must be understood that the involute gear in whatever form, is recognised to be far from ideal as a test specimen, since, even by the most accurate gear grinding methods the reproducibility of form falls far short of what can be achieved on any type of circular specimen. There is also, of course, the disadvantage of cost".

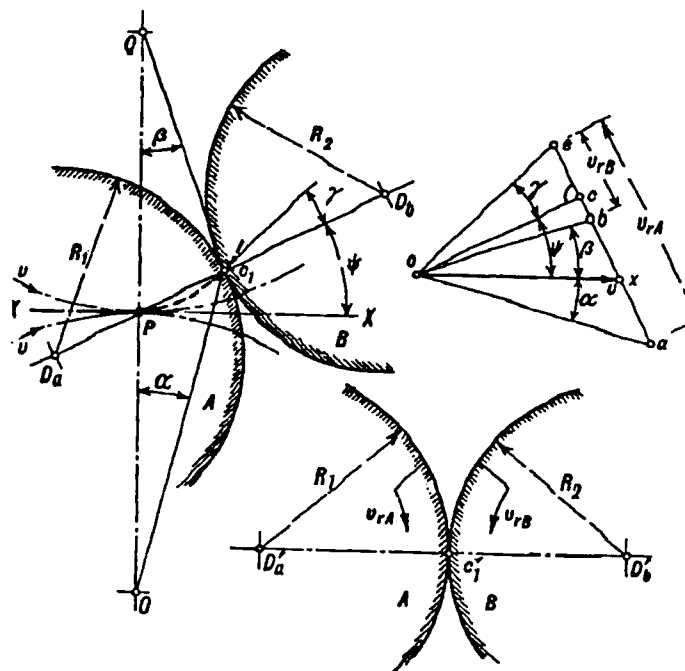
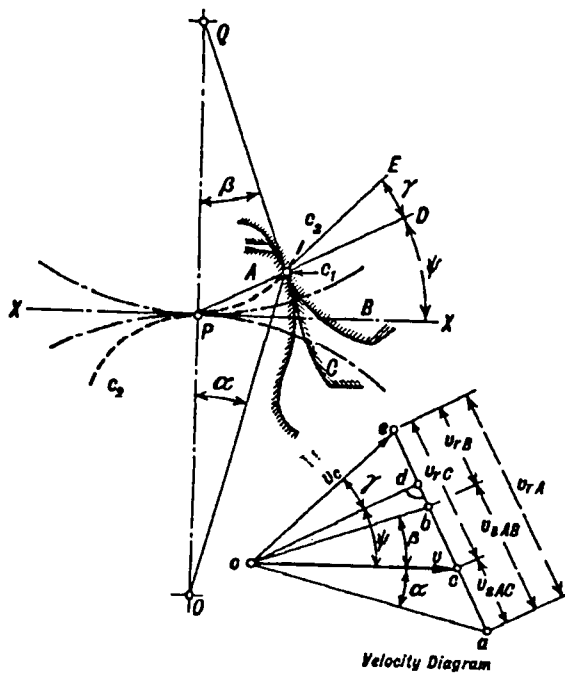
Disc lubricant testing machines (Type III tests) are a compromise between simple geometry testing machines and gear testing machines, partially simulating gear contact. Figure 1.10 overleaf illustrates that a pair of discs can be used to reproduce contact conditions at any particular position of a gear's meshing cycle.

The discs must be rotated at the same angular velocity as the pinion and gear respectively, and the disc radii equal those of the gear tooth profile at the point of simulated contact. The relative radius of curvature of the two discs is the same as that of the pinion and gear. Gear kinematic simulation is incomplete insofar as contact conditions vary during the meshing cycle whilst the relative surface motion of the discs remain constant. The main attributes of the disc lubricant testing machine are the greater control over operational and system parameters.

¹⁵ Cameron (1966), Dowson (1966) & Johnson (1987)

¹⁶ Amsler disc m/c 1922 ref. Machinery (1948) and Automobile Engineer (1948)

Figure 1.10 Gear Contact Simulation by Discs. Merritt (1942)



Numerous disc test machines have been developed for research purposes. The major disc machines and their salient characteristics are reviewed in Table 1.3.

Table 1.3 Disc Machine Operating Conditions

| <i>Machine Ref.</i> | <i>Disc dia. & (track-width), mm</i> | <i>S/R %</i> | <i>P₀ GPa</i> | <i>V₁ m/s</i> | <i>V₂ m/s</i> | <i>PV_s¹⁷ GN/ms</i> | <i>Geometry</i> | <i>Lub.</i> | <i>Temp max °C</i> |
|---|--|------------------------------|--------------------------|--------------------------|---------------------------------------|--|---------------------------------------|-------------|--------------------|
| <i>AFAPL Carper (1972) & Rao (1981)</i> | 100.2 | 0-100 | 2.8 | 3.7-17.5 | 3.7-17.5 | 31.7 | ellipse crown 472mm | jet | 150 |
| <i>Amsler O'Donoghue (1966)</i> | 35, 17.5 (3.175) | 0-100 | 2.4 | 0-1.8 | 0-0.9 | 1.7 | line | jet | see text |
| <i>Battelle Orcutt (1962), Sibley (1961) & Schlosser (1963)</i> | 76.2 | zero unless disc rad. varied | 0.8 | 0-4.8 | as V ₁ | - | ellipse crown 381mm | dry lub A/R | 1100 |
| <i>Bearing simulator Bell (1970)</i> | 18 | zero unless disc rad. varied | 2.8 | 0-18.9 | as V ₁ | - | Asym. ellipse 279mm, 10° crown, taper | jet | 279 |
| <i>Geared roller tester Benedict (1961)</i> | 45.7, 30.5 (10.2) | 13 | 1.0 | 0-19 | .33V ₁ -1.33V ₁ | 24.1 | line | dip | 204 |
| <i>Gear roll tester Jackson (1960)</i> | 63.5 (6.35) | 0-96 | 1.1 | 0-33 | 0.58 | 1.3 | line | jet | 370 |
| <i>High temp. ep tester Hopkins (1962)</i> | 50.8 | 58-100 | (4.0) | 1.25-3.7 | 0-33 | 9.9 | ellipse crown 381 or 914 mm | | 370 |
| <i>Mini-disc Nicolson (1988)</i> | 19 (6.35) | 0-100 | 1.2 | 0-5.5 | 0-5.5 | 4.4 | line | jet | 150 |
| <i>I.C. Mobil Cameron (1971)</i> | 82.5 (6.35) | 0-98 | 1.0 | 0.2-21 | 0.2-21 | 14 | line | splash/jet | 150 |
| <i>SAE Van der Minne (1937)</i> | 48.5, 48.5 (12.7) | 54, 87, 91 | 2.0 | 5.0 | 0.25, 0.34, 2 | 6.7 | line | dip | see text |

The key distinctions between these disc test machines and their application are discussed below:

¹⁷ Conditions for maximum PVs @ arbitrary, notional 50% S/R, defined here as $(V_1 - V_2)/(V_1 + V_2)$

1.4.4.1 AFAPL

The Air Force Aero Propulsion Laboratory (AFAPL) disc machine uses 100.2 mm diameter discs of 4724 mm crown radius. Although this produces an elliptical contact, the aspect ratio is sufficiently high as to approximate to a nominal line contact. This rig is versatile, for example, both discs can either be driven independently or coupled via a toothed belt, Carper et al (1972) and Rao (1981). Ku et al (1976) and Lane (1979) carried out extensive parametric testing on the AFAPL disc machine which has provided considerable data.

1.4.4.2 The Amsler disc test machine

The Amsler disc test machine has overhung shafts at 52.8 mm nominal centres and driven through opposite ends. Discs can be of any size commensurate with the centre distance between the shafts. Test lubricant is jet fed at 1 cm³/sec and no control over temperature is provided. Whilst there is no standard test procedure it is usual to run-in at minimum speed and load. Torque is measured by means of a pendulum device and wear rate ascertained either by weight loss or reduction in the outer diameter of the ring. Discs may be re-finished for re-use, O'Donaghue (1966).

1.4.4.3 Battelle

The Battelle disc machine employs adjustable clearance tilting pad journal bearings for radial support and spring loaded single ball thrust bearings for axial positioning, Wilson (1959), Sibley (1961), Orcutt (1962) and Schlosser (1963). The disc shafts are geared together via a timing belt and motive power is provided by an air turbine. One bearing housing is restrained solely by a strain gauged cantilever for traction measurements. Film thickness measurements are made with a collimated x-ray from either side or end elevations. The disc enclosure is heated by radiant heating lamps up to 1100°C. One quart of test lubricant, separate from the main oil supply, is required. Alternatively a solid lubricant may be tested using either air or inert gas as a supply stream.

1.4.4.4 Bearing simulator

Bell (1970) devised a small disc machine with independently driven shafts to simulate high speed ball bearing kinematics. In common with many disc machines, ring discs are

shrunk onto shafts and loaded together by means of a cantilever beam arrangement. A variety of heating methods, including induction heating of the discs, are combined to reach temperatures of 315°C, Parker (1971) and Kannel (1974).

1.4.4.5 Geared roller tester

Benedict (1961) and Leach (1965) investigated gear fatigue and scuffing using ring discs pressed onto parallel shafts at three inch centres and linked by eccentric phasing gears. The lower disc being dip lubricated supplies the contact. The discs are loaded pneumatically.

1.4.4.6 Gear roller tester

The Gear Roller tester, patterned after that designed by Zandt and Kelley (1953), was used by Jackson et al (1960) to investigate gear scuffing at elevated temperatures using 2.5 inch diameter discs, where one disc rotated at a fixed speed of 175 rpm and the other at a variable speed up to 10,000 rpm. Electrical heating of the disc enclosure and pre-heating of the test lubricant enabling independent control over disc and lubricant temperature up to 370°C.

Jackson used a variation of Kelley's (1953) novel operating procedure whereby after run-in, a load near the scuffing limit was applied before the speed was then increased until failure.

1.4.4.7 High temperature E.P. tester

Hopkins' (1962) High Temperature ep tester required a mere 60 ml sample of test lubricant by immersing the discs in a close fitting heated reservoir. The discs were overhung on vertically arranged shafts, one disc being restrained to around 100 rpm and the other driven up to 1400 rpm. Loading was achieved by displacing one of the drive shafts so that it inclined relative to the other. The heavily crowned discs would reduce the effect of this misalignment.

1.4.4.8 Mini-Disc

Nicolson (1988) used a mini-disc test machine, a precursor to this work, to simulate gear scuffing. The rod-like specimens had a thicker central section which comprised a 0.75" disc and a tang on the bottom face mated with the drive shaft via an Oldham coupling. The simplicity of the specimen design permitted close control over their manufacture.

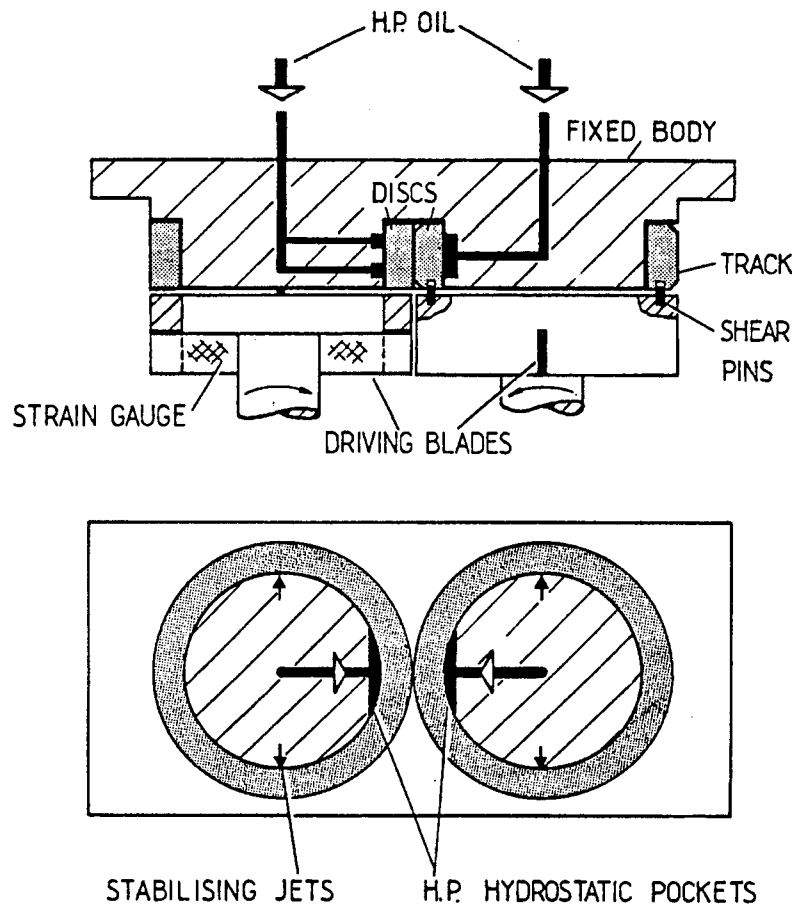
1.4.4.9 Imperial / Mobil 3.5" hydrostatic disc machine

The Imperial/Mobil disc machine was designed by Cameron & Macpherson (1971) to tackle the perennial problem of ensuring nominal line contact between discs. 82.5 mm diameter bearing inner races were used as test specimens. These were slipped over rigid fixed mandrils with hydrostatic pockets to both locate and load the rings together, as shown in Figure 1.11.

Torque, inclusive of bearing losses, hydrostatic load, shaft speeds, and temperature were instrumented. A typical operating procedure comprises a run-in under nominal load for 15 minutes, incremented by 445N every five minutes thereafter until scuffing is indicated. Six litres of test lubricant are required for operation.

Later versions of the Imperial / Mobil hydrostatic Disc Machine combined one of the hydrostatic pads with a piston to increase disc load to over 1kN/m and replaced splash lubrication of the contact with an oil jet.

Figure 1.11 Imperial / Mobil Disc Machine. Cameron & MacPherson(1971)

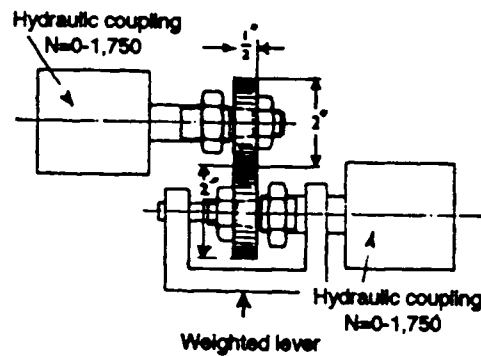


1.4.4.10 The Society of Automotive Engineers (SAE) disc test machine

The SAE disc test machine, illustrated in Figure 1.12, is based upon an earlier design used by the United States Bureau of Standards according to Neely (1936). The test is exceptional in having been assigned a standard.

Two Timken T48651 externally re-ground outer-raceways employed as test pieces are straddle-mounted between taper roller bearings on parallel horizontal shafts. After a 30 second run-in, load is applied automatically until either scuffing is detected or the maximum load of 2.7 kN reached. Both 'endurance' wear testing and shock loading at 350 N per second can be evaluated, West (1946).

Figure 1.12 SAE disc Machine. Van der Minne (1937)



Some SAE test machines have been modified to include calibrated oil jets with thermostatic heating rather than rely upon dip lubrication to splash the top specimen. This prevents overheating of the top specimen which can lead to material softening. Considerable care over finish (not greater than 0.25 microns R_a), ring concentricity (within 12.7 microns), and alignment is required to minimise experimental scatter, Boner (1971).

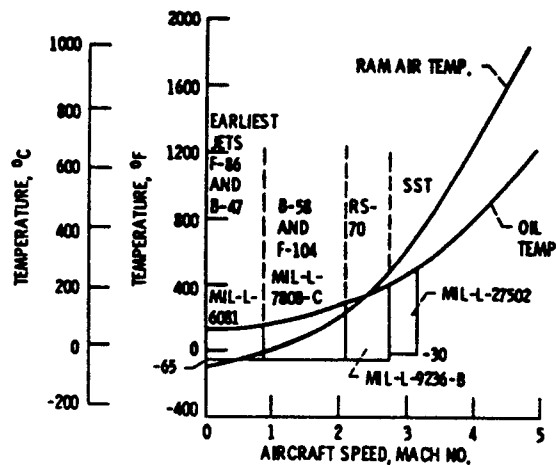
1.5 The implications for LCC testing with developments in transmission lubricants and materials

Previous sections have outlined the nature and basis upon which lubricant load carrying capacity is currently assessed. Although net LCC performance is determined by both material and lubricant in combination it is convenient to consider each separately.

Transmission lubricants can broadly be distinguished between those for which LCC is of primary concern, such as certain helicopter main gear boxes, and those for which LCC is secondary to, say, thermal capacity, for example turbine power take-offs.

Figure 1.13 illustrates that turbine lubricant development has been driven by the rise in ambient operating temperatures for increased turbine efficiency. Although these lubricants have been formulated to include both ep and anti-wear additives it is their thermal performance that has been optimised.

Figure 1.13 Bulk lubricant Temperature with Projected Aircraft Speed

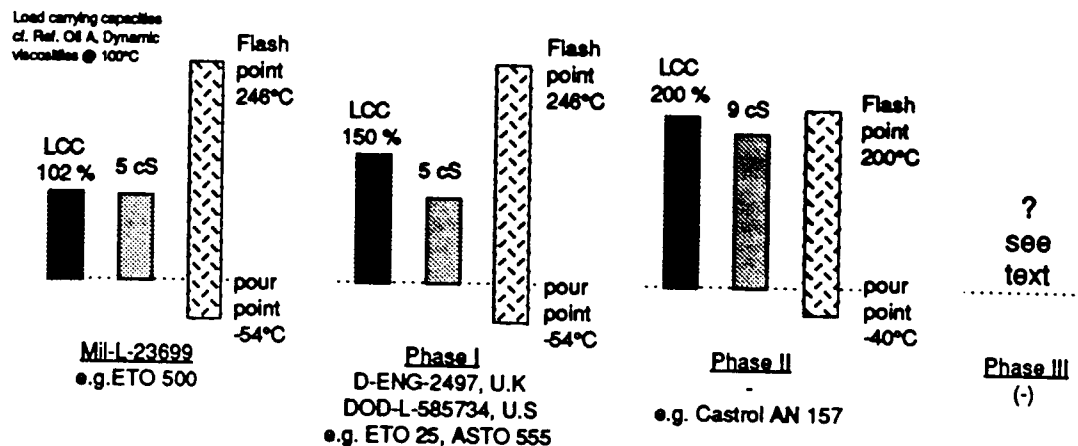


At present the approach is to provide thermal barriers between the turbine and adjacent transmission components as well as extensive cooling. These incur a weight penalty which will increase if the rise in bulk operating temperatures continues. For example, it

can be seen from Figure 1.13 that as flight speeds exceed mach 2.5 the ram air temperature exceeds the bulk oil temperature which will restrict cooling capacity to fuel utilisation. This is of particular relevance in view of the renewed interest in the Supersonic Transport (SST) program.

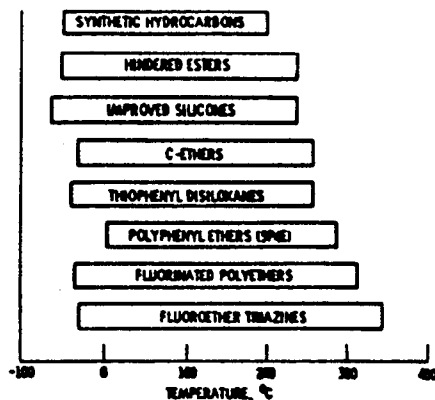
Compared with turbine lubricant development, lubricant development primarily with respect to LCC is more recent, indeed the first dedicated helicopter main gear-box lubricant specification is still undergoing qualification as Phase II shown in Figure 1.14. Previously, such considerations have been secondary to supply logistics and economics which led to the widespread use of turbine lubricants, e.g. Phase I, despite excess thermal capacity at the cost of LCC.

Figure 1.14 Helicopter main gearbox lubricant development



Phase III in Figure 1.14 is as yet only conjecture but it is surmised that it will be a common lubricant to both turbine and transmission, combining LCC with thermal performance. With this in mind high temperature candidates which are reviewed with LCC in mind:

Figure 1.15 Candidate lubricant fluids for elevated temperature. Loomis(1982)



Hindered polyol ester, range -51°C to 240°C, a formulated version of this based upon pentaerythritol aimed at meeting spec. Mil-L-27502 exhibits good lubrication ability and fair fire resistance however it requires a foaming depressant and the possibility of extending its thermal operating range still further is questionable. (Compared with the dibasic ester of Phase II, lower VI)

Polyphenyl ethers, range -4°C to 288°C, a five ringed polyphenyl ether based fluid, formulation includes tricresylphosphate for anti-wear. Despite both high temp stability and auto-ignition temperature, its high pour point requires the use of a diluents such as trichloroethylene but it has been used successfully in a military gas turbine.

Fluorinated polyethers, range -34°C to 360°C, again demonstrate excellent temperature stability although this is marred by toxicity above 260°C as well as the nature of "some highly halogenated materials to react violently with aluminium and magnesium alloys at high shear stresses" Dupont (1988), most aerospace gearboxes include such alloys.

Fluoroether triazines, range -30°C to 343°C, exhibit excellent stability, non-flammable and are good boundary lubricants. They exhibit improved low temperature properties compared to the Polyphenyl ethers and are not corrosive at high temperatures. Problems of high volatility and poor fluidity at low temperatures are being solved but even in quantity production these fluids will be so expensive as to limit their applicability and fail to justify their development costs.

Other candidates include; *improved silicones*, range -61°C to 240°C , which despite outstanding VI, temperature coefficient of viscosity, have limited fire resistance and boundary lubricating ability and *C-ethers* (including those blended with *thiophenyl disiloxanes* to enhance the pour point) which were deficient in lubricating ability as well as sludging during engine tests. Although synthetic hydrocarbons are comparatively widely used and have excellent boundary and rheological properties they have poor fire resistance and are oxidatively stable only to 200°C so their potential is limited unless used in an inert system. Alternative methods of lubrication at elevated temperature also include solid and/or dry lubrication and two phase lubrication. These are outside the scope of this work.

Although transmission temperatures have not risen in unison with turbine temperatures this is largely due to extensive cooling in the absence of transmission materials which are able to withstand extended operation above 120°C . This approach is steadily becoming less tenable as the weight penalty incurred by cooling will only increase as power ratings rise. There are also specific requirements, such as that for helicopter main gearboxes to be able to withstand 'once-off excursion' to 300°C in the event of lubricant loss. The lack of suitable materials has previously meant providing a back-up lubricant supply in combination with secondary reservoirs instead.

The nature of gear tooth contact reviewed in §1.1 whereby an intrinsically tough material is heat-treated to provide the requisite surface hardness must therefore be reconciled with operation at elevated temperature. In the case of helicopter main gearboxes the rise in gear temperature is envisaged to around 150°C but for transmission take-offs the aim must be taken as the bulk lubricant temperature insofar as this would eliminate the need for thermal barriers and extensive cooling.

Low and medium alloy carburising gear steels such as S82 or AISI 9310 start to temper above 140°C which has been approached in two ways; (i) alloying to reduce decomposition of martensite for example CBS 600 and (ii) alloying to promote secondary hardening through the precipitation of alloy carbides, for example CBS 1000. Unfortunately, although secondary hardening increases to a maximum around 500°C this coincides with minimum toughness.

Davies (1989) reviews two alternatives which show promise, nitriding and binary hardening. Nitriding alloys are temper-resistant but tend to exhibit lower core strength and shallower case depth than carburising alloys but a combination of the two, hence the

term 'binary' achieves adequate case depth, temper resistance, hardness and residual stress distribution.

Gear performance is also being improved by smelting refinements such as vacuum arc remelt (VAR) and manufacturing refinements such as shot-peening. Inevitably these will affect LCC although scuffing resistance is likely to benefit most from increased hot hardness.

Coatings are already extensively used to promote running-in and combat scuffing in gears, Woodley(1977) and Nicholson (1981). At present these are either sacrificial or modify the surface, yet potential exists for hard coatings such as titanium nitride, provided problems regarding finish and adhesion¹⁸ can be overcome.

The pattern of alloy steel development for transmissions has followed that pioneered for high temperature bearing steels. Alternative transmission materials to are likely to follow this path as temperatures continue to rise, whilst emphasising the need for toughness and the particular requirements of LCC in resistance to scuffing.

¹⁸ Inadequate adhesion can often be traced to excessive mismatching of the moduli and Poissons' ratios for the coating and substrate.

Chapter 2

Mini-Disc Machine Configuration & Design

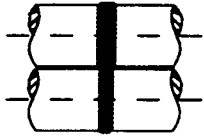
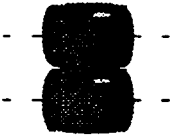
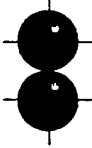
2.1 Design Objectives

Three specimen configurations: mini-disc, spherical roller and ball were considered against the following criteria prior to design

- *Contact shape*
- *Bearing size & speed*
- *Contact pressure*
- *Lubricant flow*
- *Temperature*
- *Environment*

The advantages and disadvantages of each configuration are shown in Table 2.1

Table 2.1 Specimen Configurations

| <u>CONFIGURATION</u> | <u>ADVANTAGES</u> | <u>DISADVANTAGES</u> |
|---|---|---|
| <p>(a) mini-disc</p>  | <ul style="list-style-type: none"> •Line contact can be achieved. •Crowning allows elliptical contact. | <ul style="list-style-type: none"> •Drive alignment avoids high speed instability. •Non-standard specimen geometry. •Relatively high contact loads and rig power required. |
| <p>(b) spherical roller</p>  | <ul style="list-style-type: none"> •Elliptical contact. •Inherent dynamic stability. •Standard specimen geometry (though not yet for silicon nitride). | <ul style="list-style-type: none"> •Alignment of drive for high speed operation. •Difficult to produce accurately. |
| <p>(c) ball</p>  | <ul style="list-style-type: none"> •Inherent dynamic stability. •Standard cheap and accurate specimens. •Low contact loads and power required. •Coupling for high speeds easier than either (a) or (b). | <ul style="list-style-type: none"> •Only 'point' contact. •Contact geometry changes during running, (extended tests). |

Whilst the ball arrangement would have been the least difficult approach it was considered inappropriate because the resulting 'point' contact changes substantially with running and is unrepresentative of spur tooth contact. This also applies to the spherical roller despite the high aspect ratio of the contact normal to the rolling motion. Consequently the disc is considered the most appropriate because of nominal line contact yet, if required, the discs can be crowned to produce an elliptical contact.

The aspect ratio of the contact becomes progressively lower with increased load, hence reliance upon contact stresses to achieve scuffing, often close to the material yield point is a poor solution. Load carrying capacity needs to be assessed at speeds (and temperatures) that obviate the need for such unrealistic contact stresses.

In seeking to meet these criteria together with the objectives outlined in Chapter 1 it was concluded that in the interests of both flexibility and cost, a high speed and high temperature mini-disc machine should be constructed which would allow testing as closely as possible to an ideal operating ceiling of 2.5×10^6 dN and 400°C .

These design objectives were onerous in that they represented a four-fold increase in temperature range and twenty-fold increase in speed over previous designs. Furthermore, prior work by Nicolson (1988) under U.S.A.F contract F49620-86-C-0059, revealed the difficulty in achieving correlation with the Ryder test which itself exhibits poor repeatability.

This chapter outlines the configuration and design of the mini-disc machine to correlate with the Ryder meshing cycle and encompass future requirements for load carrying capacity testing.

2.2 Ryder Gear Contact Parameters

Using a finite element contact model to simulate the Ryder gear contact cycle, measured tooth profiles under realistic bending have been compared with 'ideal' involute teeth in Table 2.2. No allowance has been made for either tooth bending or profile deviation and contact stresses are based upon smooth equivalent cylinders with no regard for tip effects.

Table 2.2 Ryder Parameters

| | LPC 'model' | LPC 'ideal' | 22.5% 'ideal' | LPSTC 'ideal' | LPST 'model' | PITCH POINT | HPSTC 'ideal' | HPSTC 'model' | 22.5% 'ideal' | HPC 'ideal' | HPC 'model' |
|----------------------------|---|----------------|------------------|------------------|-----------------|----------------|------------------|------------------|------------------|----------------|----------------|
| roll angle° | 13.69 | 14.90 | 16.51 | 18.99 | 20.90 | 22.50 | 25.83 | 26.50 | 31.80 | 32.59 | 33.38 |
| r1, mm | 10 | 11 | 12 | 14 | 15 | 16 | 19 | 19 | 23 | 23 | 24 |
| r2, mm | 24 | 23 | 22 | 20 | 19 | 18 | 16 | 15 | 11 | 11 | 10 |
| rel. rad. | 7.0 | 7.3 | 7.7 | 8.2 | 8.4 | 8.5 | 8.4 | 8.4 | 7.5 | 7.3 | 7.1 |
| S/R | -42% | -37% | -30% | -20% | -12% | -5% | 9% | 12% | 34% | 37% | 41% |
| V _s , m/s | -15.08 | -13.26 | -10.84 | -7.12 | -4.25 | -1.85 | 3.15 | 4.15 | 12.11 | 13.29 | 14.48 |
| Load, N | 381 | 1202 | 1424 | 3000 | 3000 | 3000 | 3000 | 3000 | 1348 | 1202 | 381 |
| Hertz GPa | 0.44 | 0.76 | 0.81 | 1.14 | 1.12 | 1.12 | 1.12 | 1.12 | 0.79 | 0.76 | 0.44 |
| PV _s , GN/ms | 6.62 | 10.08 | 8.74 | 8.10 | 4.78 | 2.07 | 3.52 | 4.66 | 9.62 | 10.11 | 6.30 |
| notes | (i) LPC- Lowest point of contact, HPSTC- Highest point of single tooth contact etc. 'model' refers to loaded tooth profile, 'ideal' neglects both tooth bending and profile variation from ideal involute. (ii) Rao (1981) quotes maximum average Hertzian stress for Ryder of 1.0 GPa. (iii) There is, strictly, zero load at the Highest or Lowest Point of Contact, the figure used for the loaded, measured profile is that node nearest, in order to provide a value for PV _s . | | | | | | | | | | |

Table 2.2 highlights the difficulty in reproducing the Ryder contact conditions. For example a slide/roll ratio (S/R) of 37% was used in the preliminary work by Nicolson (1988) as representing the position of maximum PV_s (LPC & HPC 'ideal') where the discs were driven at fixed speeds. However, as Table 2.2 illustrates, this varies when actual loaded gear profiles are considered, and makes the choice of a single set of contact conditions upon which to base simulation somewhat arbitrary. Equally, Ryder's failure criterion of 22.5% tooth area scuffed does not provide a precise and therefore convenient meshing point¹⁹.

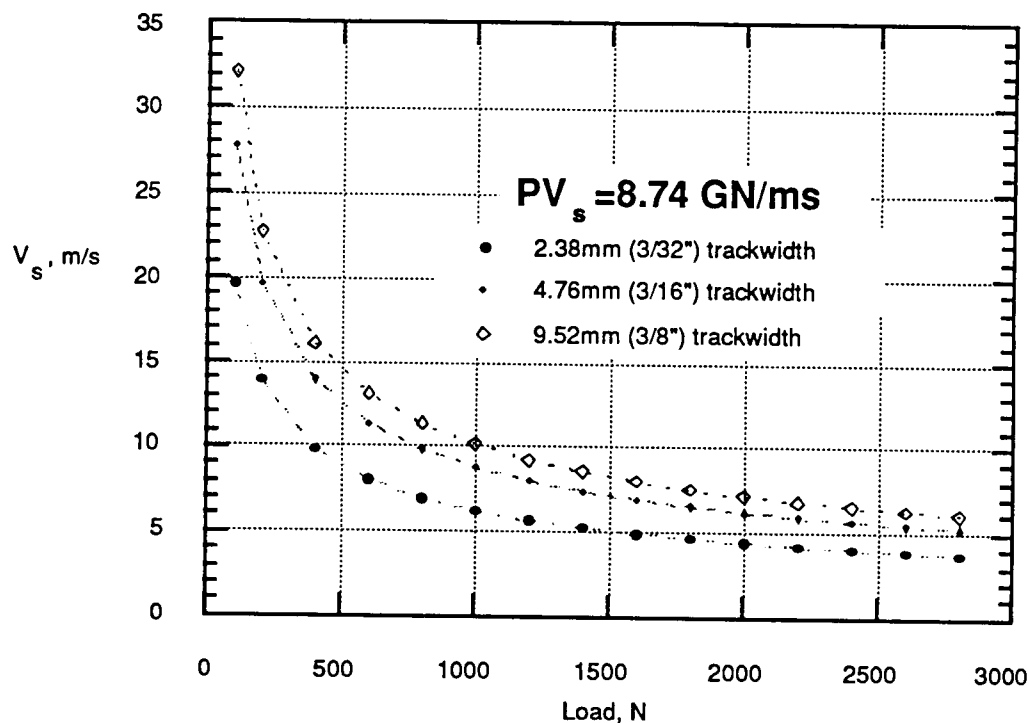
¹⁹ Both the HPSTC and the HPC, are commonly used as datums for simulation. The actual location of scuffing onset is affected by profile modification, tip relief, tooth section and pressure angle.

2.2.1 Ryder Simulation

It is apparent from the discussion of Ryder parameters that these are less tightly defined than might be first construed. Olver (1991) demonstrated that scuffing performance is strongly influenced by disc geometry, speed and load. These aspects are considered insofar they might best be arranged to achieve similar scuffing performance to that experienced with the Ryder test.

Figure 2.1 illustrates that if PV_s for a 19mm (3/4") diameter disc machine is matched against the last part of the tooth to be scuffed, namely 8.74 GN/ms²⁰, the load required diminishes with sliding speed.

Figure 2.1 Disc Sliding Velocity versus Load for Constant PV_s



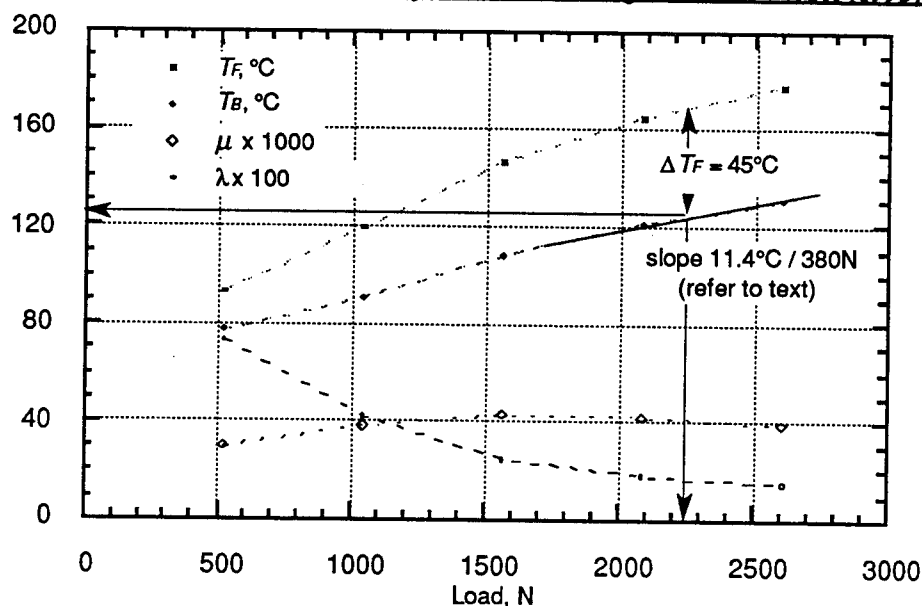
²⁰ The location of the 'tails' of the 22.5% scuff were calculated theoretically by assuming that scuffing progressed at unequal rates from root and tip thereby reaching the pitch line simultaneously. However, the analysis has produced two different values of PV_s , corresponding to upper and lower scuffing boundaries.

The applied load, and in turn load capacity needed for the supporting bearings, varies according to the track width chosen. It is evident, however, that a load capacity in excess of 200N is required which would entail speeds in excess of 40,000 rpm if the disc entrainment velocity is matched to that of the Ryder contact. It should also be noted that the use of 3/4" diameter discs does not match the precise relative radii at any point of the Ryder tooth contact. This reduces the theoretical smooth contact width by approximately 25%, but as a roughness in the order of 1 μ m rms, at typical scuffing loads, would increase the contact width by about 25%, it is not thought to be significant.

PV_s is only one method of comparison, scuffing severity is frequently assessed using critical temperature criterion which suggests that total contact temperature should be contrived to be the same for both disc and Ryder to enhance correlation.

The Ryder gears were assessed using a model written by Olver (1993). Olver's model is an extension of the principles he reported in 1991 to explain scuffing in different sized disc machines. In essence, it is a thermal feedback model where the heat capacity and heat transfer characteristics of a particular system and its geometry can be accommodated along with the more conventional lubricant properties and contact parameters needed to determine steady-state film properties.

Figure 2.2 Thermal Behaviour of the Ryder Test according to Olver's Model (1993)



The results illustrated in Figure 2.2 must be qualified as the thermal coefficients and surface area of the test head were estimated. The predicted 11.4°C rise per 380N load stage fortuitously agrees with that measured by Benedict (1968) of 12°C. Figure 2.2 illustrates that for a reference oil failure load of 2200 lb/in, corresponding to a load of 2260N, the model predicts a flash temperature, T_F of 45°C and bulk temperature, T_B of 125°C where

$$T_B = \frac{(T_s + T_p)}{2} \quad (13)$$

where T_g & T_p are gear and pinion temperature respectively

It is this particular condition for which simulation has been sought, using 19mm (3/4") discs rotating at speeds v_1 & v_2 equivalent to the Ryder HPSTC.

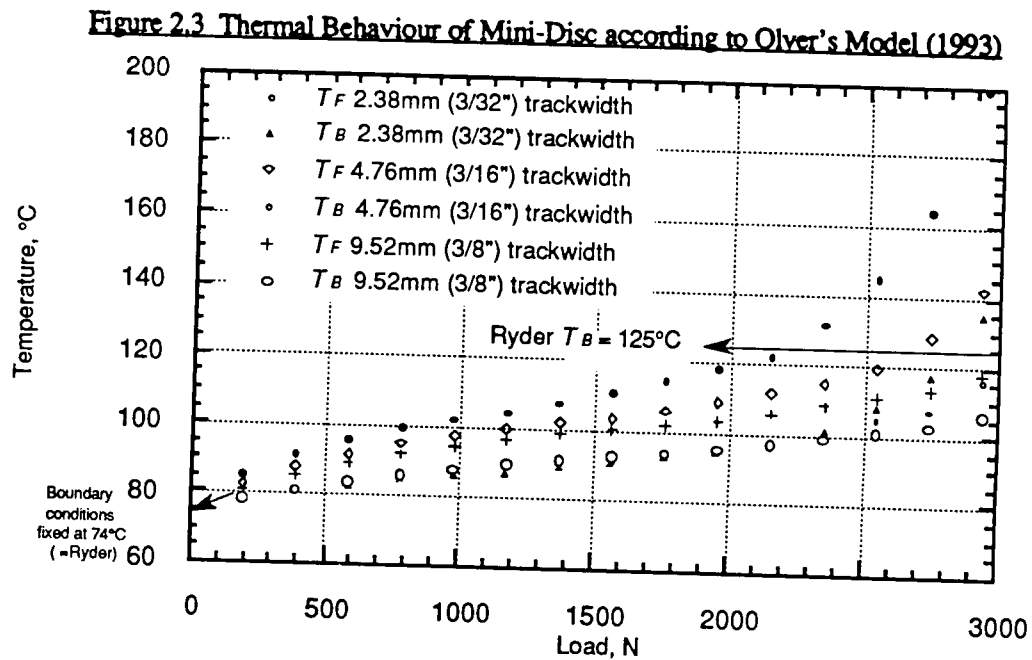
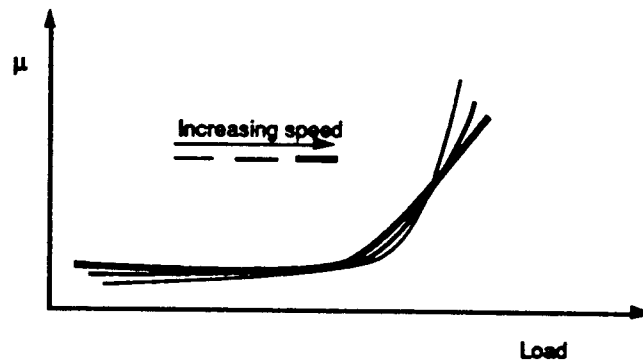


Figure 2.3 indicates that ΔT_B and ΔT_F are matched by using disc track widths of approximately 4mm and 2950N. For a wider track width the bulk temperature is of greater importance, conversely for the narrower track the flash temperature is of overriding importance. It should be stressed that this approach attempts to map only one failure condition, thus for a different reference oil and hence failure load one would

anticipate a different optimum track width. Equally, it may be purported that the contact point simulated should not be the HPSTC but the 'tail' of the 22.5% scuffed area as used in replicating load intensity.

The effect of increased speed upon scuffing, as predicted by Olver's model is shown in Figure 2.4. The onset, as determined by the coefficient of friction, occurs earlier at high speed but the rate, $\partial\mu/\partial N$, is lower.

Figure 2.4 Predicted Effect of Speed upon Disc Scuffing



The traction model used by Olver is based upon that of Bair (1982)²¹ where μ is proportional to temperature subject to limiting shear stress.

Within the model:

$$T_F \propto \mu \times \sqrt{v} \quad (14)$$

hence if μ initially falls with speed, as shown in Figure 2.4, T_F need not necessarily rise with increasing speed. However, the heat generated:

$$Q \propto \mu \times v \quad (15)$$

hence Q could still be rising. Meanwhile the model heat transfer coefficient, upon which heat dissipation depends, will also rise with speed:

²¹ Surface roughness and lubricant strongly influence the model, the roughness used was that of run-in Ryder gears whilst the lubricant was an ester corresponding to the reference oil.

$$h \propto \sqrt{v}$$

(16)

It should be noted that the entrainment velocities are high, 6m/s rising to 90m/s. The less rapid scuff at higher speeds may be explained by conventional ehl theory; if there is sufficient film to separate the surfaces then it will be due to the speed rather than viscosity which will be extremely low. Any further increase in temperature with increasing load will have relatively little effect upon viscosity and hence feed back in reduced film thickness.

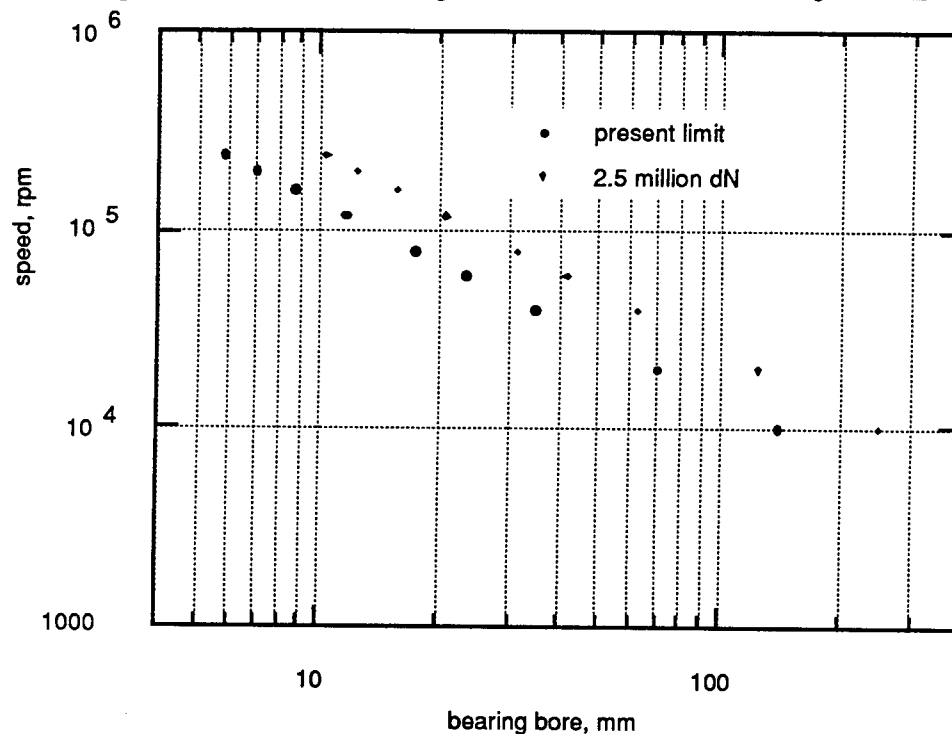
Superficially either the load intensity or critical temperature criteria are applicable but in practice the onset of scuffing is affected by additional parameters. Additive response, for example, is not incorporated into the critical temperature hypothesis.

No attempt has been made to replicate the relative contact whereby gross conformity might become significant, Sayles et al (1981) and Archard (1973). Furthermore no attempt has been made to simulate the transient nature of the contact cycle but, "the desire for correlation with the Ryder must be set against the inherently poor repeatability of the gear test".

2.3 Bearing Simulation Using Discs

The primary objective of simulating gear scuffing has already been discussed although this is not to disregard possible bearing simulation. The dN rating illustrated in Figure 2.5, despite wide usage, fails to take proper account of size and centrifugal effects. Nonetheless it provides an indication of both the present envelope and future test requirements.

Figure 2.5 Practical dN Rating. Hamrock (1981) after Bamberger (1971)



At high speed the centrifugal force experienced by the rolling elements leads to outer race control. In essence the inner and outer contact angles are no longer equal and significant slip occurs at the inner race. It will be apparent that as the inner race contact is elliptical it would be necessary to crown the discs to achieve a contact of similar aspect ratio, and cone the discs for asymmetry. From Bell (1970) these parameters are envisaged to be: 10" (250mm) crown, 10° cone taper and 2200lbf (10kN) applied load at 10,000 rpm. The rig should cater for axial load caused by the disc taper.

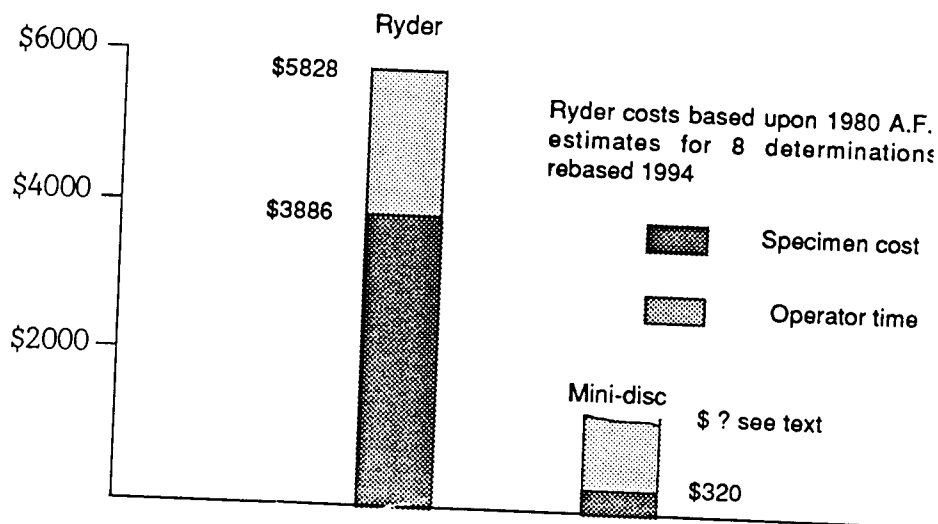
2.4 Testing Costs

The simplicity and size of the specimen minimises sample costs and enhances potential for manufacture in a wide variety of materials and finishes. These factors are likely to become even more significant in future, however, a major component of load carrying capacity testing costs are related to manpower and the extent of testing necessary to achieve acceptable repeatability. Figure 2.6 is an estimate of the testing costs incurred for eight Ryder and mini-disc determinations.

Rao (1981) postulated disc repeatability would be such as to reduce the number of determinations for qualification testing to just three, instead of eight as required by the Ryder. If so, and this can only be borne out by experience, then the cost benefits of the mini-disc would be substantial.

Where exotic or novel materials are concerned, assuming such materials can be procured in a form suitable for gear manufacture, cost benefits are likely to be even more marked.

Figure 2.6 Mini-disc versus Ryder testing costs

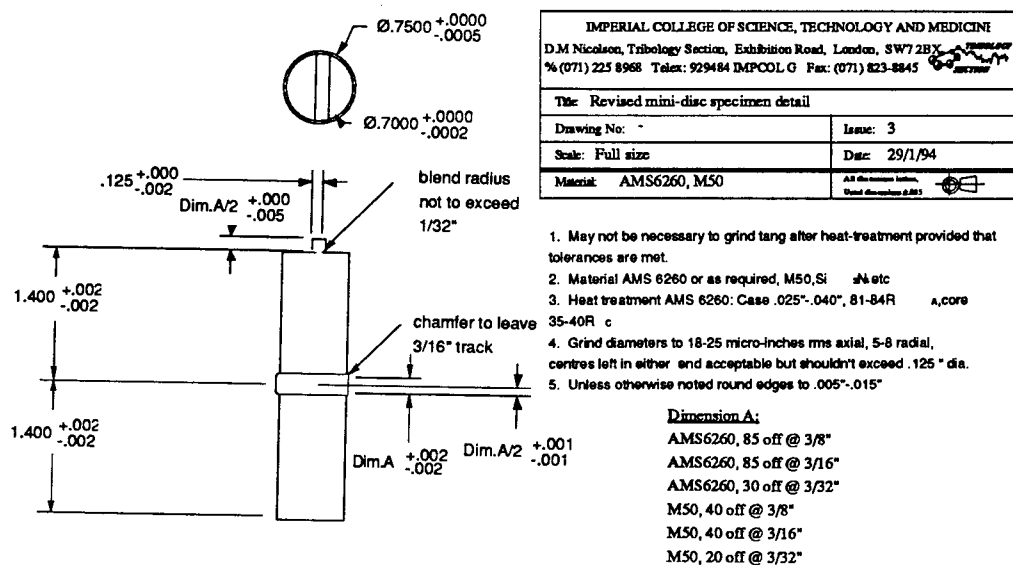


No allowance for specimen recycling has been included because of the disadvantage incurred by reduced disc diameter, however recycling may become viable for exotic materials such as silicon nitride which at present, under limited order quantity, cost around \$400.

2.5 General Arrangement of Mini-Disc Test Rig

Preceding sections confirm both the feasibility and attractions of using moderately narrow track, small diameter discs driven at high speed. This section presents an overview of the mini-disc and general arrangement, followed by a detailed description of the principal elements. Figure 2.7 illustrates the mini-disc specimen.

Figure 2.7 Mini-Disc Specimen



For any given pair of specimens, one has a wider track to reduce end effects. The disc specimens are driven via opposite ends whilst supported by hybrid bearings as shown in Figure 2.8 and Figure 2.9 overleaf. These are mounted in a hinged 'nut-cracker' which enables the two discs to be loaded and provides ready access to replace the specimens. Heated test fluid is fed to the hybrid bearing pads and the contact by a precision gear pump which is located directly beneath the test enclosure. The test enclosure forming the sump.

Figure 2.8 (a) General Arrangement of Mini-Disc Test Rig

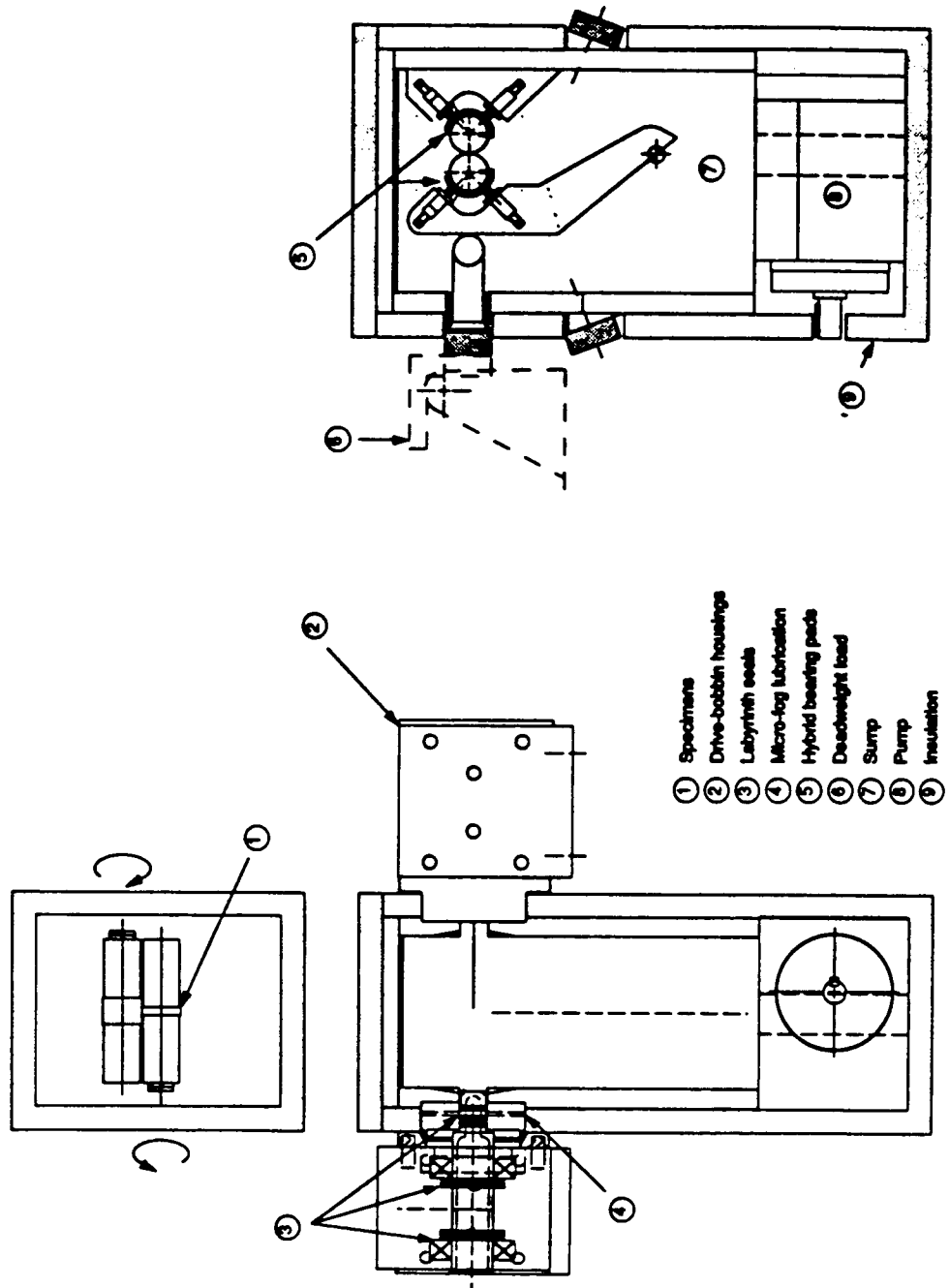
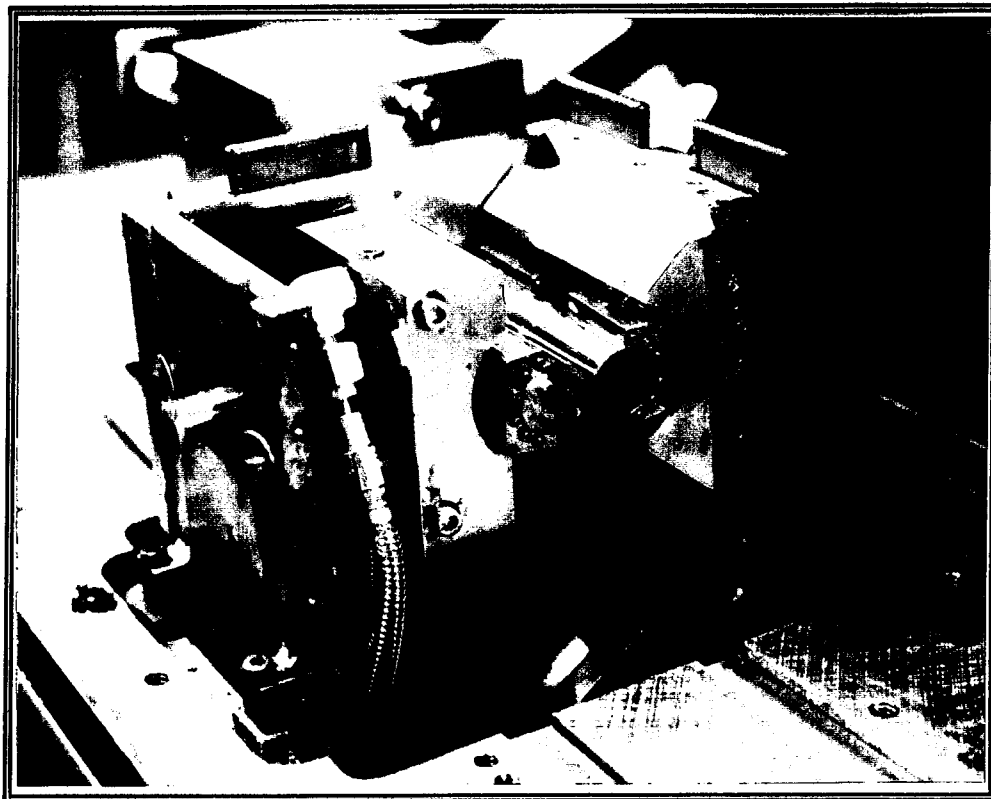
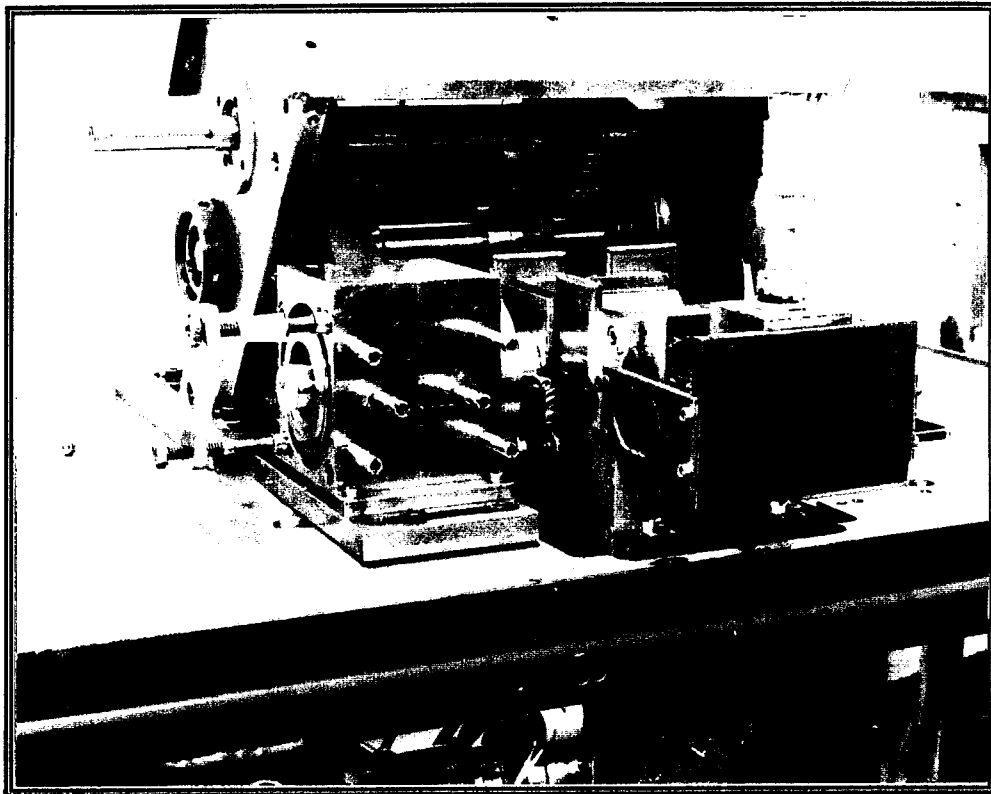


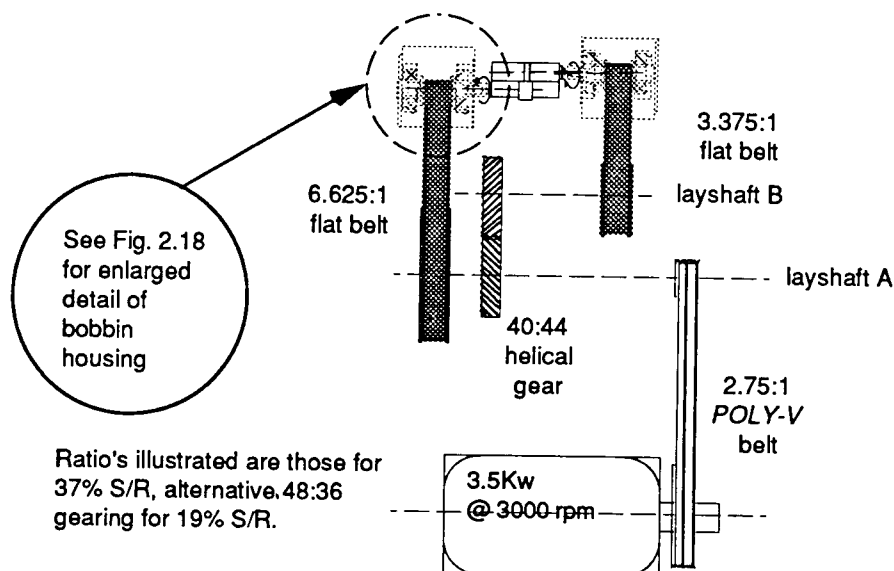
Figure 2.8 (b) General Arrangement of Mini-Disc Test Rig



2.5.1 Drive-train

The layout of the drive-train is shown in Figure 2.9 , with that of the bobbin housing in Figure 2.18 in § 2.5.3.

Figure 2.9 Schematic of Drive-train



For simplicity a single, variable speed drive motor has been used in a four-square arrangement so that the power required is merely that absorbed in the disc contact and bearings. Layshaft 'A' is driven via a *poly-v* belt and layshaft, 'B', coupled to 'A' via a pair of unequal helical gears to reverse the relative rotation²².

As rotational speeds up to 100,000 rpm were envisaged, a high final drive ratio has been used in combination with a minimal driven pulley diameter using flat belts. These transmit adequate power at more conventional speeds together with the ability to cope with the high speed and small bend radius. The belts specified comprise woven polyester impregnated with neoprene. The flat belts drive the bobbin spindles which are mounted between pre-loaded deep-groove bearings pre-tested to 90,000 rpm.

²² It is recognised that vibration can affect scuffing & fatigue performance, Smith & Macpherson (1978), but meshing frequencies of the layshaft gears are outside those considered critical.

Distinction needs to be drawn between the onset of catastrophic scuffing and partial seizure followed by recovery. This is done by denoting a limiting coefficient of friction in the disc contact at which the transmission is rated, $\mu = 0.2$, and accepting significant slip thereafter. The extent of slip is monitored via specimen speeds as detailed in § 2.5.5. Tension is critical with flat belts. The entire layshaft assembly is keyed perpendicular to the driveline axes and layshaft 'B' can be rotated around 'A' which enables each belt to be tensioned individually. Tension is applied by a strain gauged cantilever after it was discovered that measuring lateral deflection of the belts was inadequate.

The bobbin spindle ends have been machined to provide a tang to drive each specimen via an Oldham coupling. Initial attempts to avoid the need for a 'floating' coupling by driving the specimen directly, using two shear pins, did not meet with success and caused excessive labyrinth wear described in § 2.5.3.

With the aim of ensuring each drive spindle remained concentric with its respective disc axis, the bobbin housings were initially attached to each jaw of the 'nut-cracker' ²³. However, in practice this was not found to be sufficiently rigid. Instead the discs were loaded statically in the 'nut-cracker' which was shimmed appropriately to allow for running clearance, and the drive components aligned with the disc axes before being rigidly clamped.

2.5.2 Support and Loading of Discs

Mounting the specimens in an overhung arrangement, as used by Bell (1970) amongst others, was considered inappropriate because the specimens needed to be ground on their respective drive shafts to ensure concentricity. This would largely nullify the advantages of the mini-disc simplicity and prove less conducive to even loading of the contact. The rod shape and independent support of the mini-disc is designed to avoid this problem. Whilst this geometry would be maintained it was proposed that gas be used as the means of support instead of hydrostatic journal bearings used previously.

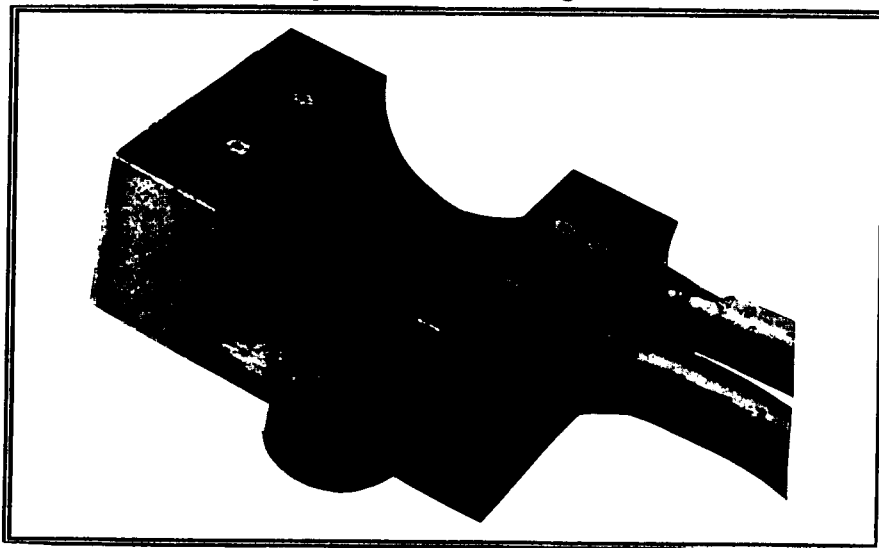
²³ Ref. circ't rpt FY1455-87-03006/D1, 1st yr 'Dev. of high speed, high temperature mini-disc m/c'

2.5.2.1 Gas bearings

The benefit of gas lubrication is that bearing performance is largely independent of temperature²⁴, test lubricant and speed. Use of gas would also permit more effective control over lubricant feed to the contact, including the extent of lubricant starvation which is of particular interest. Furthermore, the gas may be used to control the environment surrounding the discs, providing an atmospheric blanket. Despite a low specific load capacity, which invariably means that clearances are significantly less than liquid lubricated bearings²⁵ frictional losses are extremely low. This is desirable when measuring traction coefficients.

Considerable effort was expended in attempting to achieve sufficient load capacity using hybrid gas bearings. One version is illustrated in Figure 2.10. Despite the attractions of using gas it did not prove possible to achieve adequate load capacity without resorting to excessive flowrates. It was concluded that although this approach was theoretically feasible using a hybrid tilting pad arrangement and given sufficiently stringent tolerances, the margin was inadequate when differential expansion between the discs and pads, transient loads and debris were included. Consequently the test fluid would have to be used for disc support.

Figure 2.10 Gas Bearing



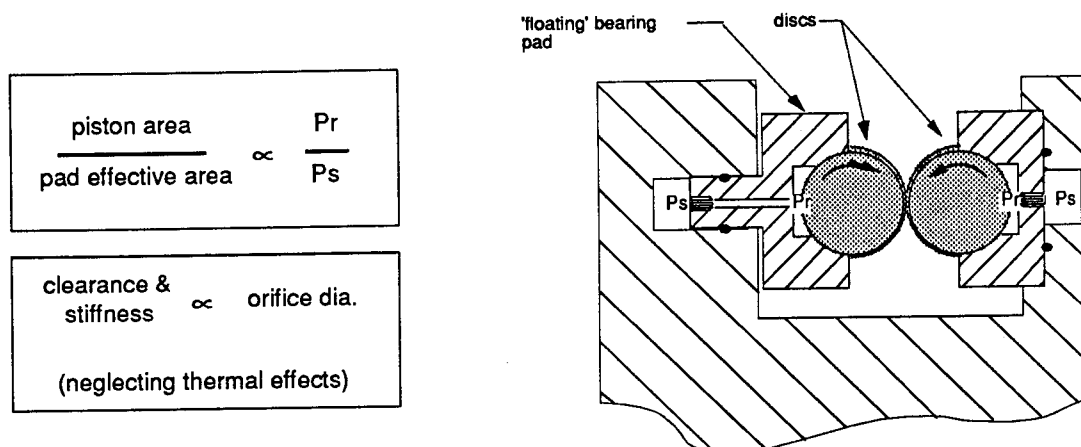
²⁴ In contrast to liquids, air or nitrogen increase in viscosity of the order of 200% between 20-400°C.

²⁵ Journal bearing friction $\propto \eta / c$, (laminar flow for a given geometry & speed) whereas load capacity $\propto \eta / c^2$ hence for similar spec. load, if $\eta_{oil} = 100 * \eta_{air}$, then $c_{oil} = 10 * c_{air}$: c =clearance, η =viscosity.

2.5.2.2 Hybrid tilting pads

Figure 2.11 illustrates the hydrostatic pad developed by Olver (1991) from Macpherson's (1972) original design. Mini-discs supported in this way have been run successfully at PV_s of 13.3 GN/ms testing formulated lubricants at 125°C. This arrangement provides ease of loading via control of the supply pressure, P_s , together with disc self-alignment. Furthermore, if a fixed displacement pump is used in conjunction with a pressure relief valve, the pad film thickness is largely independent of the applied load, given that the pump delivery is sufficient and both thermal and dynamic effects are ignored.

Figure 2.11 Hydrostatic Pad with Integral Piston.

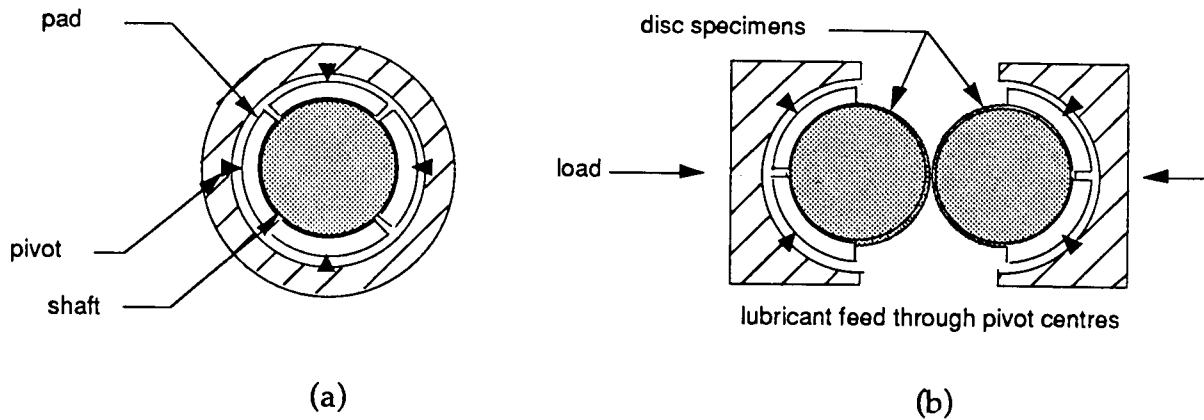


However, the performance of a prototype based upon this design was not satisfactory, confirming the previous mini-disc experience when running fluids of low viscosity. Moreover, at high speeds recessed hydrostatic pads become markedly less effective, Mohsin (1981), and significant eccentricity occurs between the drive and disc axes due to dynamics. In order to satisfy the wide range of fluid viscosity, disc speed and temperature, hybrid tilting pads were proposed.

The plain tilting pad invented by Michell in (1905) became synonymous with thrust applications but he recognised their equal potential as journal bearings proposing the segmented multi-pad arrangement illustrated in Figure 2.12 (a). For the wide operating

range envisaged a hybrid variant of Michell's tilting pad bearing would be necessary as illustrated in Figure 2.12 (b).

Fig. 2.12 (a) Pivoted pad hydrodynamic journal bearing after Michell (1937) and (b) hybrid mini-disc configuration



Design optimisation of hybrid bearings is not straight forward, for example, optimising static load capacity at minimum power requires that the ratio of frictional losses to pumping power, K , should lie between 1 and 3 whilst the optimum recess location is at quarter station²⁶. Simultaneously, as load capacity is a function of the recess area, this should be maximised commensurate with maintaining adequate sill width to prevent excessive flow. These objectives must, however, be reconciled with dynamic optimisation for which no recesses are preferred and the optimum value of K lies between 3 and 12, Koshal (1981). Table 2.3 highlights this quandary.

Table 2.3 Recessed Hydrostatic, Hydrodynamic and Plain Hybrid bearing parameters

| Parameter | Recessed hydrostatic bearing | Pressure-fed hydrodynamic bearing | Plain hybrid bearing |
|--|------------------------------|-----------------------------------|----------------------|
| suggested land-width ratio | 0.25 | 0 or 0.5 | 0.1 |
| suggested power ratio, K ²⁷ | 1.0 | 40.0 | 3.0 |
| min. | 3.0 | | 12.0 |
| max. | | | |
| feed geometry | 4-6 recesses | axial or circumferential groove | plain, double entry |

²⁶ $a/L = 0.25$, as shown in Figure 2.16

²⁷ $K = 3-6$ where max temperature rise is important, 3-12 for maximum tolerance band.

In designing a hybrid bearing it is usual to specify dynamic load and diameter, assume a length to diameter ratio and power ratio, K , in order to determine the supply pressure²⁸. After confirmation that this is sufficient to support the static load, a numerical solution is used to determine the operating clearance according to the fluid viscosity before verifying the flowrate and stiffness. In the event that one of these parameters is inappropriate either for manufacture or performance, then first the clearance and subsequently the supply pressure must be altered and the process repeated. Equally, a different viscosity may be considered. However, this may affect the temperature rise experienced by lubricant passing through the bearing and in turn affect stiffness where orifices are used, Rowe (1983).

In order to assess performance and optimise the hybrid bearing design a program was written, based upon that of Spikes (1983) incorporating both tilt and hydrostatic jacking. A finite difference method outlined in Figure 2.13 overleaf was used to solve Reynolds' equation for the pad pressure field. This provided the design illustrated in Figure 2.15, the performance of which is presented in Figure 2.14. Attention is drawn to both the large l/D as well as the shallow recesses. The unusually large recesses are due to the pivot redesign, whereby the projected pivot area must be less than that of the recesses to ensure the pad functions correctly at start-up. Expediency dictated an isoviscous approach without allowance for local variation in viscosity, hence there is an over-estimate of bearing performance at high speeds where there is the apparent margin in load capacity.

The program was also used to assess the effect of manufacturing inaccuracy upon performance such as that of incorrect recess location.

²⁸ Optimum load capacity is achieved for $0.4 < P_r/P_s < 0.7$

Figure 2.13 Pad Design Optimisation Routine

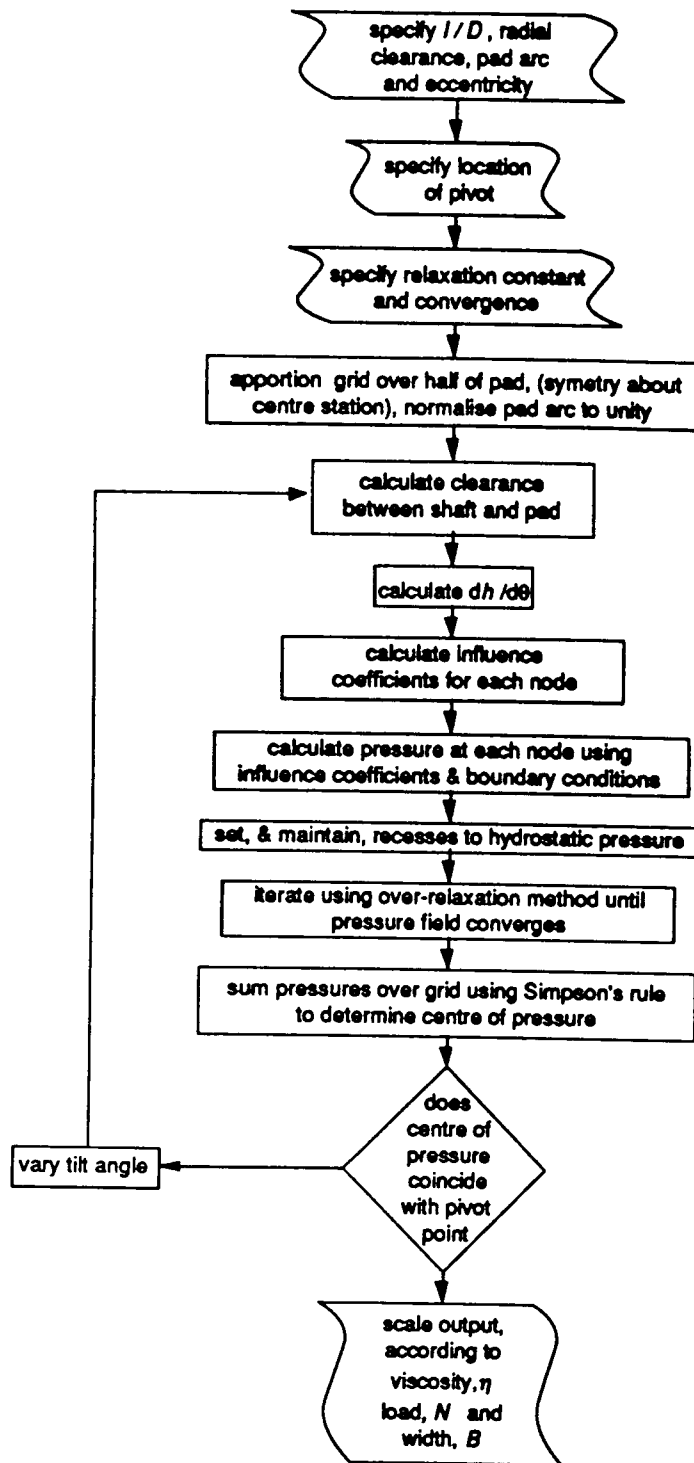
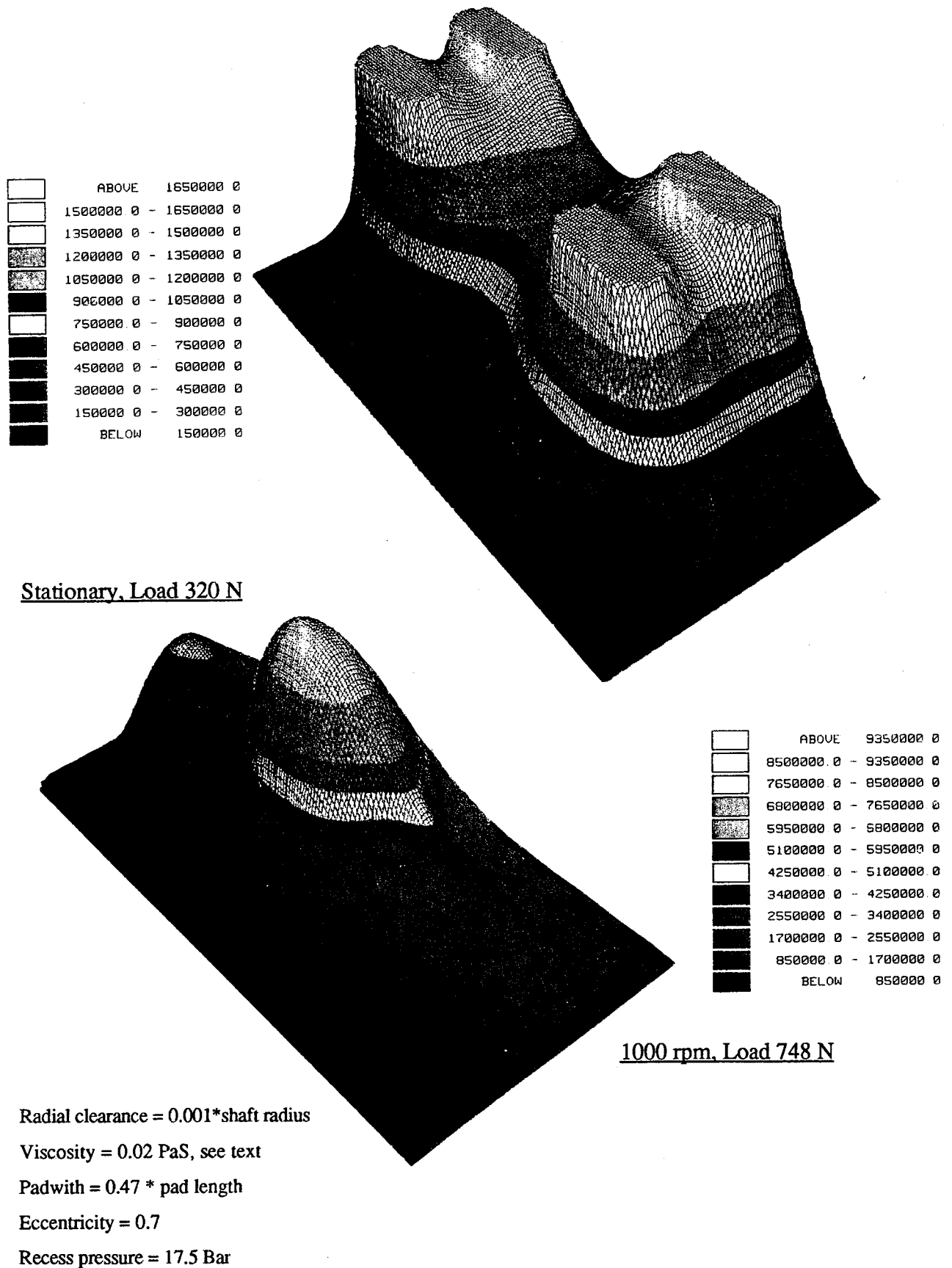
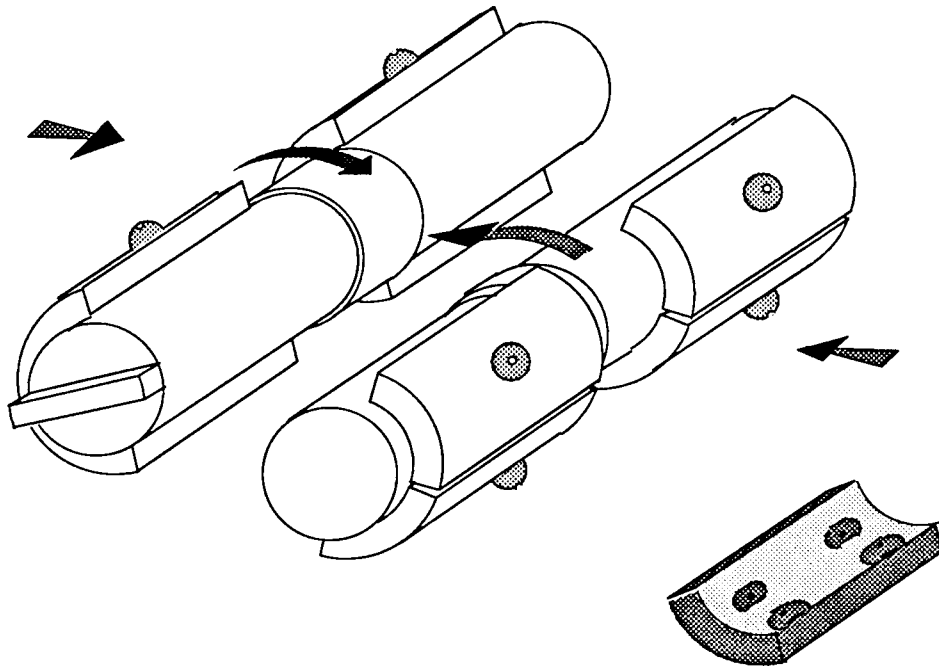


Figure 2.14 Hybrid Pad Performance, Predicted Isoviscous Pressure Profiles



cf. 2.7 KN @ 5000 rpm & 12.6 KN @ 25000 rpm

Figure 2.15 Sketch of Hybrid Pad

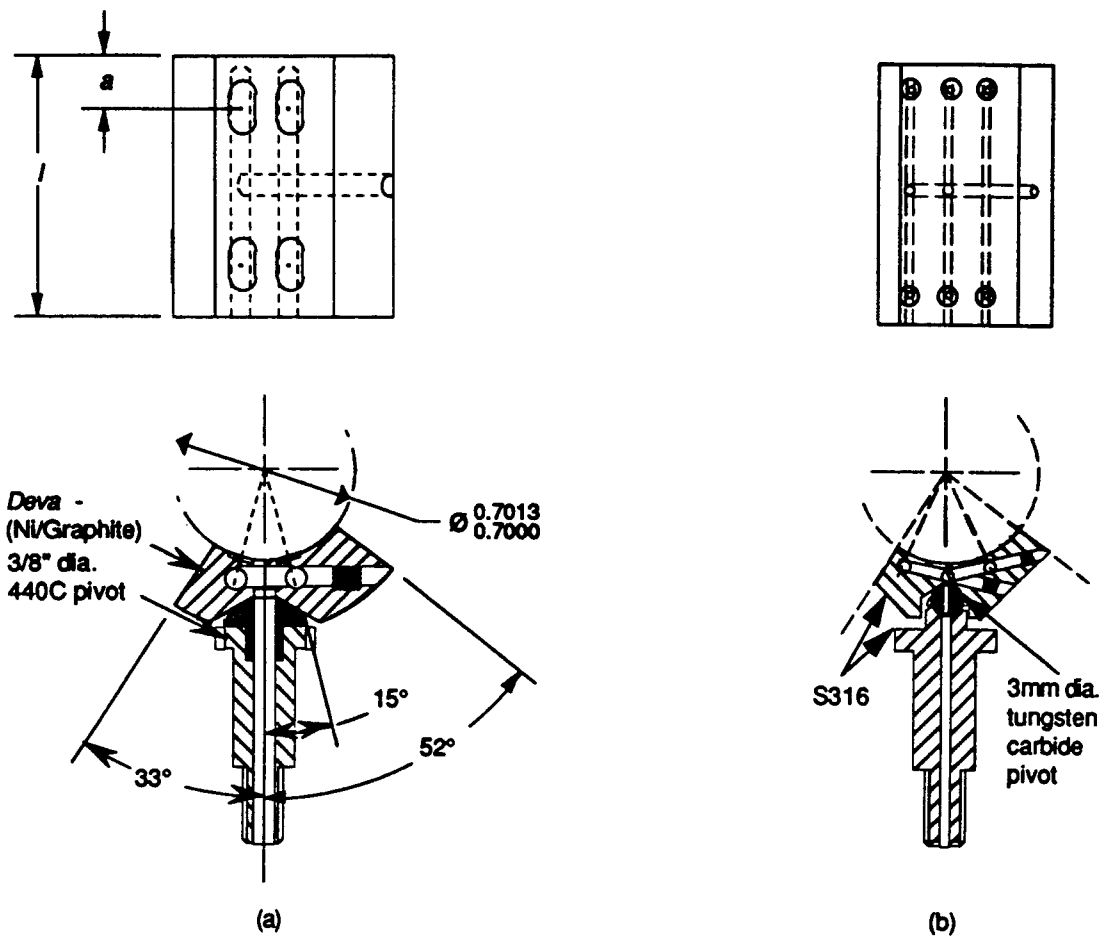


2.5.2.3 Pivot design

The pivot design was reassessed after the tungsten carbide pivots shattered during operation.

Figure 2.16 Final (a) and Prototype (b) Hybrid Pad

Sectioned at Middle Station



In modifying the design, see Figure 2.16, the tungsten carbide balls were replaced with 440C 'mushrooms' and the pad material altered to *Deva*, a proprietary, sintered material composed of nickel and graphite. This softer pad material was necessary to ensure the counter-bore in the pad would still yield to provide a conformal seal with the pivot despite the increased ball diameter. *Deva* also offered markedly superior dry sliding properties

for the journal face in the event of over-load. However, in consequence of this modification, the pads could no longer be held onto their pivots in a manner akin to a *Dzus* fastener. Instead, fine gauge wire links the pads together, providing a cradle to retain the pads when changing specimens. It is suggested that a method of individually attaching the pads loosely to their pivots is incorporated into the design.

2.5.2.4 Test head lubrication

The desire to use gas for supporting the discs without resorting to use of the test fluid was attempted partly because of anticipated limited fluid availability and difficulty in specifying a suitable pump. One-shot lubrication was impractical whilst any pump would have to cope with the range of temperature, exotic nature of the proposed fluids and delivery. Entrapped gases and debris bode ill for rapid recirculation implicit with the small test fluid volume.

After due consideration a compact chemical gear pump was specified. Manufactured out of stainless steel²⁹ and rated to cope with the range of viscosity and temperature. The pump's performance was reliant upon tight clearances so thermal gradients had to be avoided. The pump was modified with cross-drillings to accept cartridge heaters and the bearings replaced with plain carbon bushes.

Test lubricant is fed to a nozzle directed into the disc entrainment, although alternative locations can be readily implemented.

2.5.2.5 Ancillary lubrication

The drive-bobbin spindles and layshaft gears are lubricated separately from the test-head by an oil mist. This is fed to nozzles, located adjacent to the bearing and layshaft gear entrainment, which force the mist to coalesce and lubricate. It is necessary to ensure that the mist is prevented from encroaching the test enclosure and contaminating the test lubricant. Consumption is regulated by the air flow and the mixture by a needle-valve.

²⁹ The additional cost & complexity of manufacturing both the pump and test enclosure out of Hastelloy was not warranted as corrosive fluid candidates would be of limited interest.

2.5.3 Sealing

The design of the seals changed during the course of test rig development. Initial use of gas hybrid bearings entailed the use of a labyrinth sealing arrangement.

The labyrinth seal interposes a 'tortuous flow path between high and low pressure regions by means of a series of non-contacting restrictors and separating chambers'. The function of the restrictors is to convert the pressure head into kinetic energy which is then dissipated throughout the chambers. They are particularly suitable for high temperature service although by comparison with face seals, leakage rates are generally greater.

Labyrinth design is a compromise between maximising the number of throttlings per unit length and minimising the kinetic carry-over with an adequate pitch. No allowance is necessary for rotational effects at the speeds envisaged.

The most widespread method of analysis follows that of Martin (1908) which calculates the leakage by considering the restrictors as a series of annular orifices,

for which the mass flow per unit area is:

$$\frac{\dot{w}}{A} = \left(\frac{p_o}{\sqrt{\frac{RT_o}{g}}} \right) \times \beta \times F_{\infty} \times K \quad (17)$$

where the labyrinth factor:

$$\beta = \sqrt{\frac{1 - \left(\frac{p_a}{p_o} \right)^2}{N - \ln \left(\frac{p_a}{p_o} \right)}} \quad (18)$$

where:

A = annulus area

g = gravitational constant

F_{∞} = kinetic carry-over, empirical function of geometry

K = average flow coefficient

N = number of restrictions

P_o = upstream pressure

P_n = downstream pressure

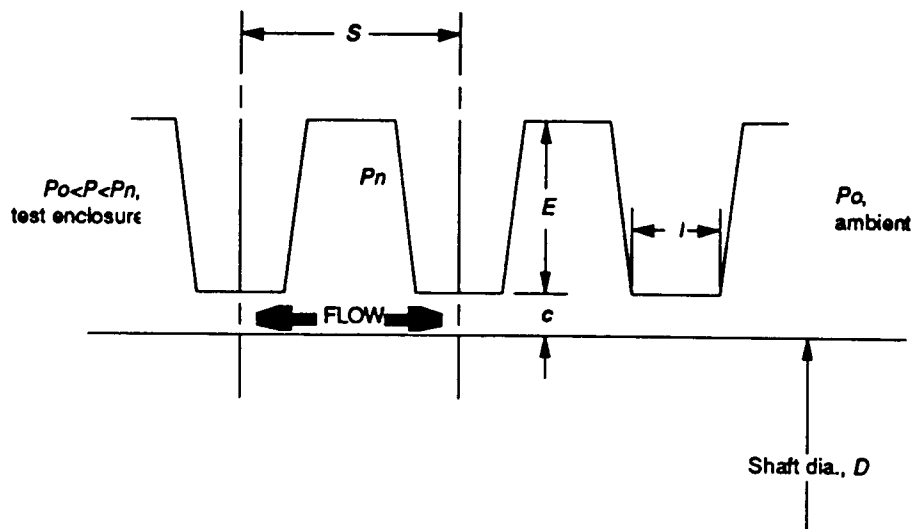
R = Universal gas constant

T_o = Absolute temperature

\dot{w} = mass flowrate.

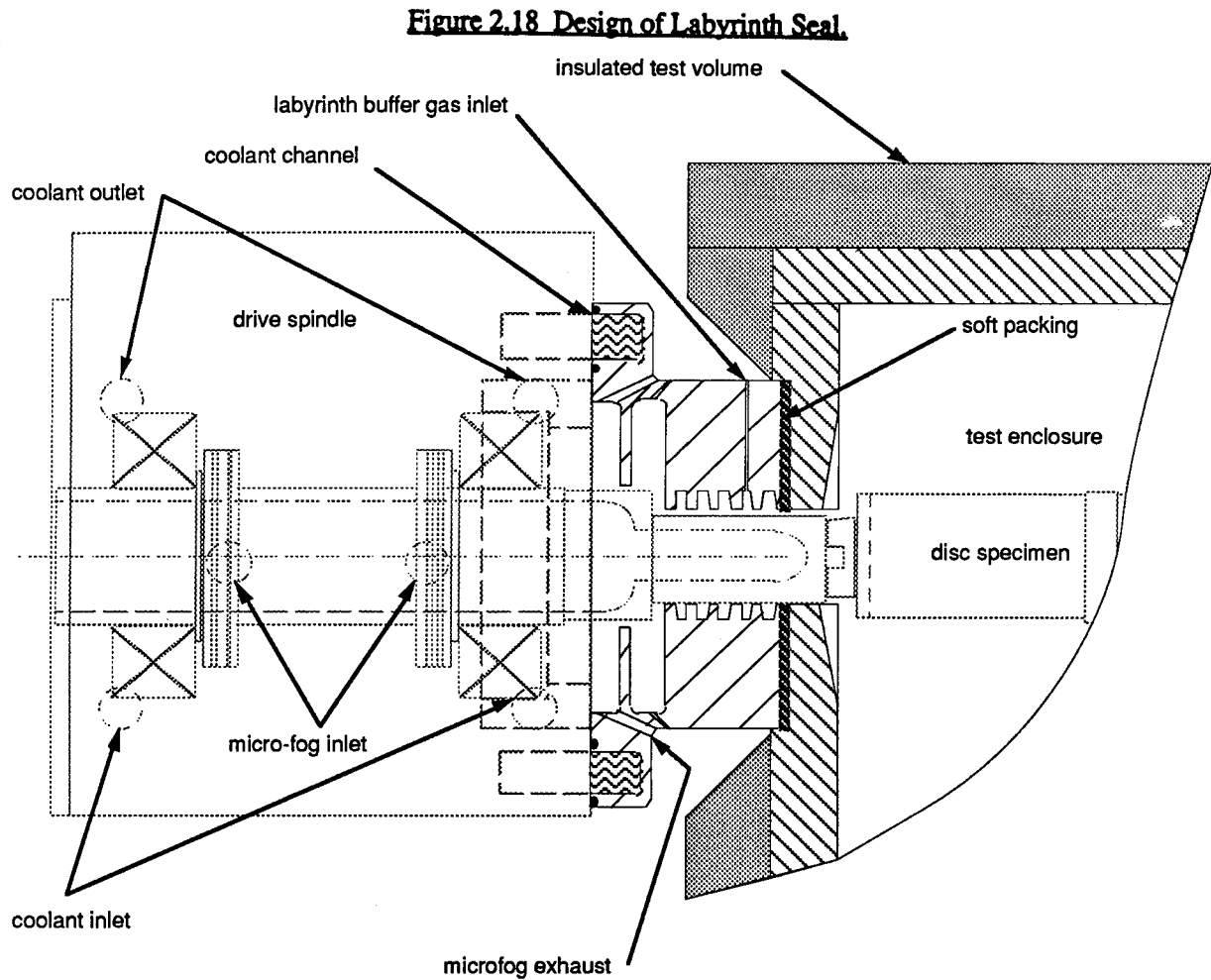
The schematic in Figure 2.17 is based upon the formalised method of General Electric's Fluid Flow Division (1973)³⁰, showing two back-to-back labyrinths incorporating a buffer gas. The test enclosure is maintained at a pressure slightly above ambient, which allows the exhaust to be scrubbed via a simple trap.

Figure 2.17 Schematic of Labyrinth Seal



³⁰ This is an empirical modification to Martin's (1908) method to include kinetic carry-over, Vermes(1961), and annulus performance, Bell (1957).

Figure 2.18 shows the design of the labyrinth used.



Wear between the drive shaft and journal due to movement of the shaft led to excessive leakage. However, before rectification could be sought the hybrid gas bearings were disbanded in favour of using hybrid tilting pads. Consequently lip seals were fitted which permitted the bobbin housing to be mounted closer to the specimen, thereby reducing the overhang. For elevated temperature operation, these will have to be replaced with suitable face seals.

2.5.4 Heating

One of the implications of limited test fluid volume and small disc mass is that any increase in frictional dissipation within the contact will increase the bulk temperature both rapidly and dramatically and the heat source should be able to respond accordingly.

Induction heating was considered as a prime candidate, particularly as the majority of the heating effect takes place in the surface layers. However the desire to use ceramic discs, Figure 2.19, being neither magnetic nor conductive, would have required the use of a susceptor. Furthermore this method makes no provision for heating or cooling the test fluid prior to entrainment.

Figure 2.19 Induction Heating of AMS 6260 and Silicon Nitride Discs



Radiant heating of the lubricant supply was tentatively applied using infra-red focused onto a thin-walled capillary feed. However, the change from hybrid gas to hybrid fluid pads meant that the test fluid could be used to distribute heat between both specimens and enclosure. Consequently the test fluid is heated by four 250W cartridge heaters contained

within the pump. Heating elements set into the sides of the test enclosure provide a further 2.5 KW.

A *ceram*³¹ window in the back of the test enclosure allows the discs to be radiantly heated independently of the test fluid. This also provides access for a thermal imager.

Previous work by Nicolson (1988) suggested that cooling might be required and a take-off between the pump and manifold was provided, despite the penalty of increased test fluid volume. This has been used for additional fine filtration during the commissioning.

2.5.4.1 Insulation

Microtherm insulation encased in glass-fibre was used extensively on account of its low conductivity, 0.02 W/m²K compared with ~ 0.2 W/m²K for glass insulation, which has minimised the distance between the bobbin housing and test enclosure.

³¹ Exhibits low infra-red absorption

2.5.5 Instrumentation

Torque, temperature and speed are all logged during operation using an A→D, and Macintosh PC. The loading cycle is software controlled via the A→D which adds flexibility.

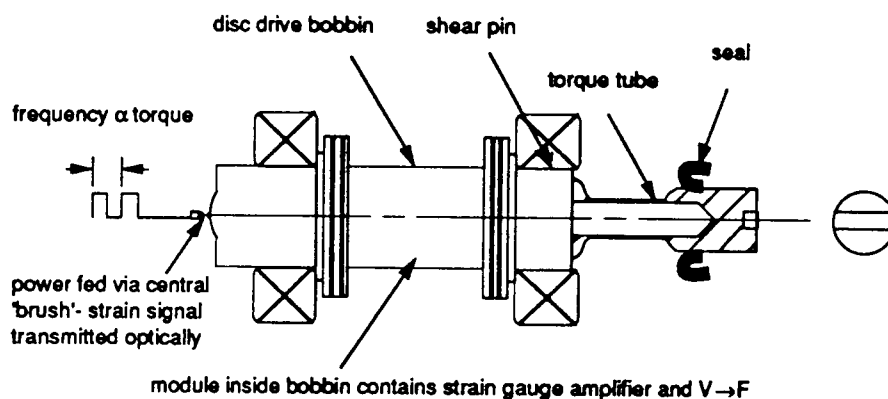
2.5.5.1 Torque measurement

Disc traction is measured, inclusive of the pad losses, with a torsion tube and strain-bridge incorporated into the slower of the two drive spindles, as shown in Figure 2.20. The bridge potential is converted to a modulated a.c. signal and transmitted via a light emitting diode to a stationary photo-electric diode. This signal is amplified and partly fed back via a central brush to provide module power. The remainder is reconverted to indicate the strain potential. Feeding part of the signal back via a brush has allowed a phase-locked loop to be used to compensate for thermal effects.

The use of signal telemetry avoids noise which is inherent with high speed slip-ring sets.

Calibration is limited to static dead-weight.

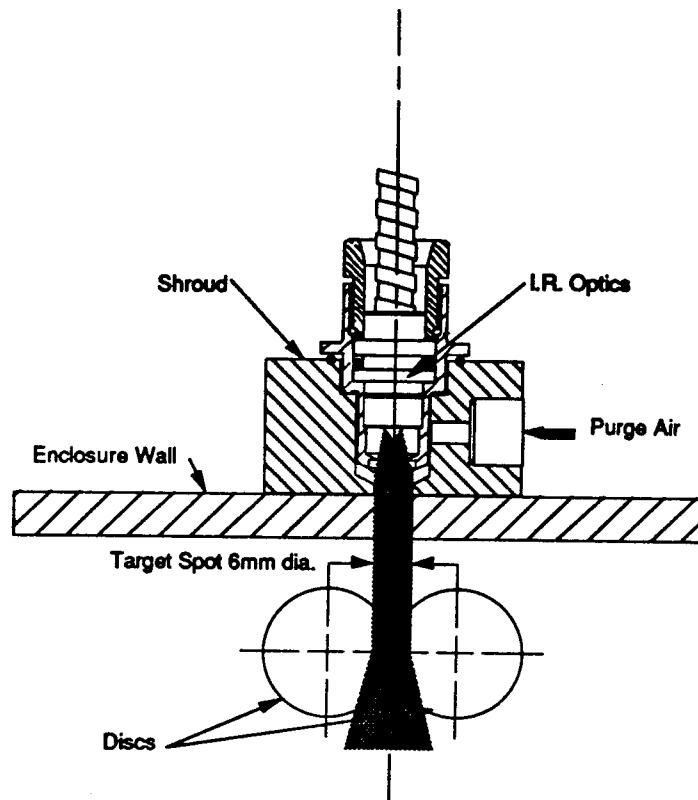
Figure 2.20 Schematic of Torque Measurement



2.5.5.2 Temperature

Thermocouples are located in both the sump and fluid supply jet although trailing thermocouples have not been used as it is questionable whether these are effective in determining disc surface temperature, particularly at high speed. Embedded thermocouples have been calibrated with surface temperatures by Carper (1972), amongst others, but this method was not considered feasible here. Instead, an infra-red camera has been used as shown in Figure 2.21, calibration of which confirmed the relative insignificance of the lubricant film/spray, although the dynamic emissivity of the contact is rather more open to conjecture.

Figure 2.21 Disc temperature measurement by infra-red emission



2.5.5.3 Speed

Disc speed is continuously variable although the slide to roll ratio is pre-determined by the choice of layshaft gears. Magnetic induction pick-ups are used to measure individual disc speeds and the lower layshaft, which allows the extent of slip to be monitored. Provision for software to control the speed has been incorporated. Calibration is verified using an oscilloscope.

2.5.5.4 Disc load

Disc load is applied by squeezing the 'nut-cracker' via a lever arm and actuator, refer to Figure 2.8. The strain in the arm is monitored to provide a feedback loop for the actuator and indication of the applied disc load. A compression spring between the arm and actuator allows fine tuning of the system stiffness.

Permutations in loading cycle, such as rate, step or ramp are controlled by software which drives the actuator.

CHAPTER 3

Results and test programme

3.1 Summary of commissioning and preliminary testing

In the course of rig development and commissioning a considerable amount of 'testing' has been carried out albeit without the level of parameter control that constitutes formal load carrying capacity testing. These preliminary results are reviewed with the proviso that more extensive testing is due to be carried out and it would be premature to draw too many conclusions before these are complete³².

To date endurance testing at temperatures above 180°C has not been attempted due to the nature of the shaft seals however there does not appear to be any reason why this aspect cannot be rectified to match the envisaged operating envelope with that of entrainment speed³³.

3.2 Results of tests to date

In the interests of providing a valid comparison between the preliminary work Nicolson (1988) and that being developed by MTI, New York, it was decided to provisionally use 37% slide to roll. AMS 6260 discs, as per Figure (2.7), have been used throughout. The lubricant is an ester to Mil-L-23699B.

A sample of the test specimens have been subjected to topographical and SEM including taper microsection analysis both before and on completion of testing.

Tests were performed by increasing the load stepwise whilst running. In some cases, particularly at higher speeds the expected 'run-away' as illustrated in Figure 3.1, with dramatically increased torque was not registered. This is not to state that an initial scuff did not occur, only that it as it did not develop in the 'conventional' low speed manner and seize. Instead substantial wear is experienced by the slower disc which in combination with localised plastic deformation created polished smearing, referred to henceforth as 'high speed scuffing'.

Figure 3.2 shows the nature of the disc surface prior to failure after running in.

³² The reader is referred to the author's PhD thesis which is in the course of preparation (June '94)

³³ To date, V_{\max} 45000 rpm

Figure 3.3 illustrates the typical or 'conventional' scuff experienced at low speed and high load; a speckled and substantially distressed surface as a result of extensive plastic flow. This particular failure occurred at 10,000 rpm³⁴ and 1700 N and will be used as a basis for comparison.

Figure 3.4 depicts all the results and thus includes failures of 'conventional scuffing' as well as 'high speed scuffs' described above. In deference to convention and the absence of a significantly better alternative³⁵, these have been plotted as load versus speed however detection of the 'high speed scuff' was by no means consistent as illustrated by Figure 3.5 which makes interpretation subjective in terms of a failure load. Although, as expected, there is a fall in scuffing load with speed, some of the narrow, 1/8" track discs have a higher LCC than the 1/4" track discs, in contradiction with both Olver's model (1993) and prior experience. Preferential additive action is unlikely to be responsible as this is a formulated oil and the scatter in the results suggests repeatability should be the first target.

Figure 3.6 illustrates the nature of the 'high speed scuff'. The worn slower disc is apparently polished although as Figure 3.7 makes evident, this is erroneous. The mean length of the surface scratches observed is approximately 100 µm, which is in accord with two body abrasion where the length of scratch in disc 2 created by either an asperity or particle embedded in disc 1 is given by;

$$scratch = \left(\frac{|rpm1 - rpm2|}{rpm1} \right) \times 2b = \left(\frac{2 \times S/R}{1 + S/R} \right) \times 2b \quad (19)$$

where $2b$ = contact width, S/R = slide to roll ratio and $rpm 1$ & $rpm 2$ = disc speeds.

The faster disc is mottled matt and largely unworn with the exception of a single band. From a taper microsection, it is actually very similar to that of the 'conventional' scuff of

³⁴ Speeds refer to faster, narrow track disc.

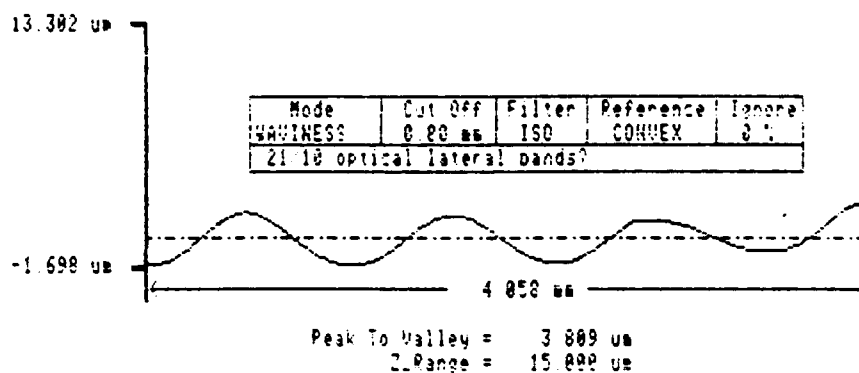
³⁵ Future planned testing will attempt to represent such results on a diagram covering regimes of operating parameters which relate to differing outcomes of an initial scuff.

Figure 3.3, whilst the surface layer is approximately 50 Vickers harder than the case prior to running, evidence of work hardening during plastic flow.

The single furrow of material worn in the faster disc by the slower was frequently experienced with this disc machine at or above 15000 rpm. Wear of the slower disc by the faster is common in disc machines testing lubricant load carrying capacity but the furrow and 'polishing' are either uncommon or unreported.

In addition, regular axial bands were visible on some of the 'high speed scuffs'. Figure 3.8 illustrates those present on 'polished' discs run at 7000 rpm (15000 rpm mating disc). Though visible on some of the higher speed tests they were less pronounced.

Figure 3.8 Axial bands on 'polished' Mini-Disc



Disc rotating at 116 Hz, bands approximately 1.2 mm apart therefore generated at ~ 6 kHz. Layshafts A & B at 36 Hz & 34 Hz respectively hence tooth meshing frequency 1.5 kHz. No evidence of bands on counter face rotating at 250 Hz, (15000 rpm)

Nominal PV_s of the 'conventional scuff', Figure 3.3 was 5.3 GN/ms compared with 8.5-9.4 GN/ms and 4.5 GN/ms for Figures 3.7 and 3.6 respectively confirming the difficulty of using this criterion. Flash temperatures have not been calculated as these results were acquired prior to modifications to increase torque measurement sensitivity.

The log file of Figure 3.9 corresponds with the 'high speed scuff' of Figure 3.6 and illustrates the gradual increase in temperature and traction, as observed by armature power. This may be compared with the much more evident nature of the slow speed 'conventional' scuff Figure 3.1 which is the major objective for increasing torque sensitivity. In ascertaining the effect and importance of cooling, Figure 3.10 illustrates the

dramatic run-away. The appearance of the failed discs were extremely similar to those of Figure 3.6, namely that the low speed disc wore severely.

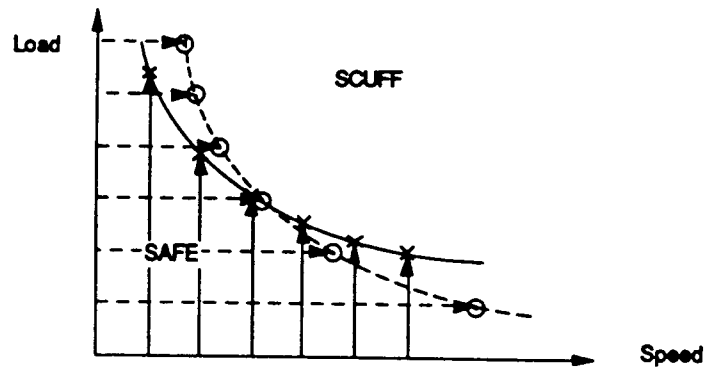
3.3 Requirements for future testing and analysis

Load capacity testing by implication involves applying progressively higher loads until some criterion of surface failure is reached, this is invariably accompanied by an increase in traction, temperature and noise. Whilst it is equally true that the same failure phenomenon can be induced if the sliding speed or temperature is increased, the majority of load carrying capacity tests are reported as functions of load and speed, and the remaining conditions specified where known. The transition diagrams of Begelinger (1976) & Salomon (1976) are notable in their attempt to discern between the prevailing conditions immediately before scuffing and, equally significant, their extension to look at the effect of other parameters.

Any particular test device will have its own signature, but every effort should be made to minimise its influence. The design of the mini-disc rig has been aimed at ensuring the widest possible operating envelope combined with the greatest possible control over parameters such as specimen consistency and alignment since the surfeit of plausible explanations of scuffing, and in many cases apparent experimental contradiction suggest that it is necessary to map out scuffing performance extensively i.e. considering all parameters if an insight is to be gained into the phenomena.

As load is increased, whether or not scuffing occurs will depend the extent to which beneficial modification of the surface occurs during the loading sequence. Of particular significance for this test machine, in view of its unusual configuration, is its ability or otherwise to absorb power during incremental loading in view of the low inertia, small disc and limited fluid. To address this it is proposed to attempt to map scuffing envelopes, for a variety of initial conditions, both along the load ordinate and speed abscissa where it is anticipated that the boundary will differ as illustrated in Figure 3.11.

Figure 3.11 Alternative approaches to assess scuffing envelope for Load/Speed



A common failing of much disc machine testing reported is the lack of duplication, since repeatability is both prime objective of this work and a justification widely used in favour of disc testing it is proposed to test sufficient samples at the same nominal conditions to permit this aspect to be quantified.

Subject to these results as well as constraints of manpower and funds, it is then proposed to increase the temperature range of the disc-rig further in order to assess ceramic disc performance.

Conclusions

Preliminary tests have shown that conventional low speed/ high load scuffing as shown by Nicolson (1988) can be achieved with the developed rig. In addition the rig's ability to push conditions and particularly speeds further has shown that there may be a transitional scuffing mode of failure which does not immediately lead to seizure. This aspect warrants further study in terms of a comprehensive map of scuffing and, in particular, whether limited recovery is possible at high speed.

In setting these objectives it should also be possible both to quantify repeatability as well as the reduction in test costs.

Figure 3.1 'Conventional' scuff. Nicolson (1988)

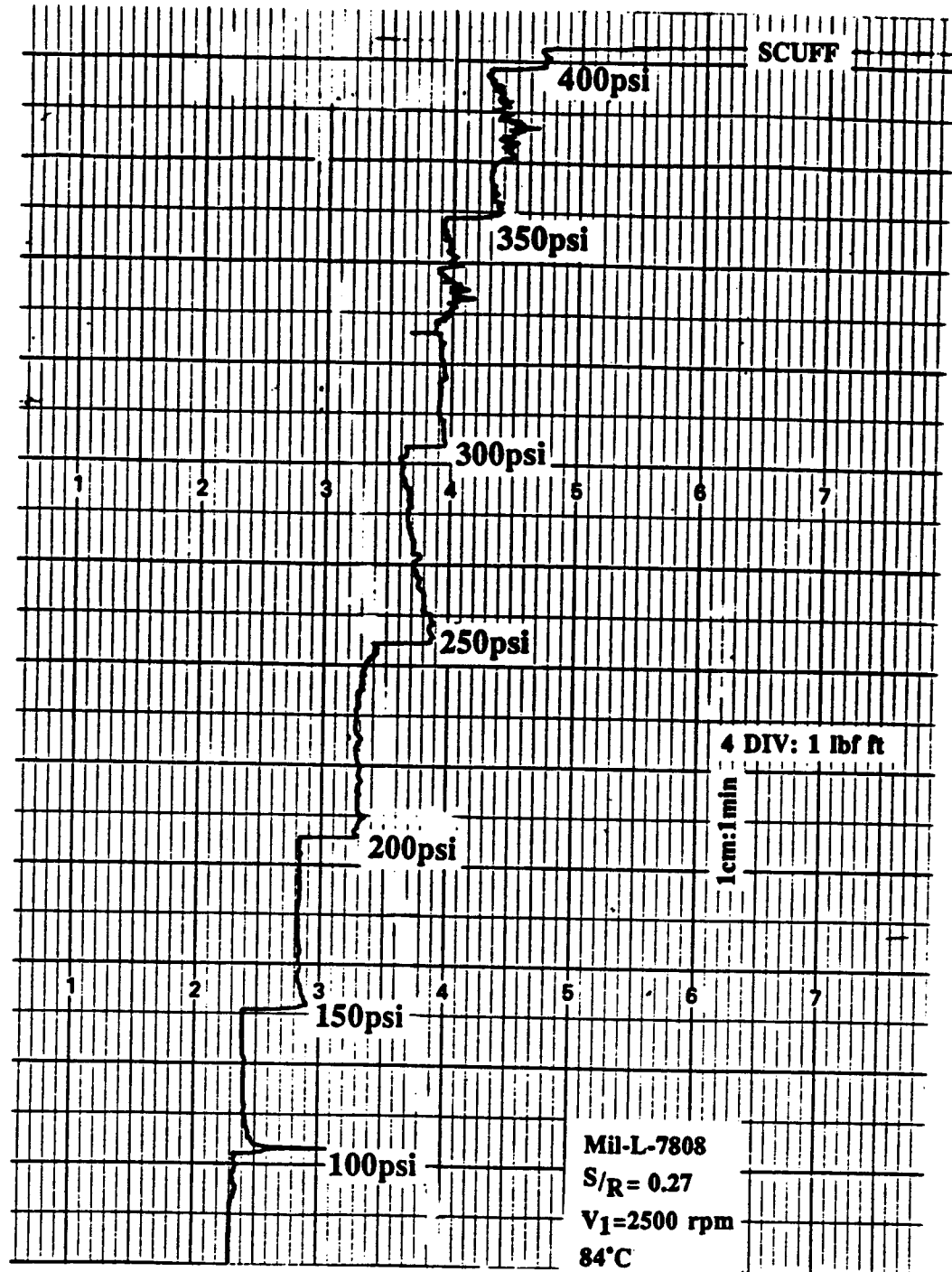
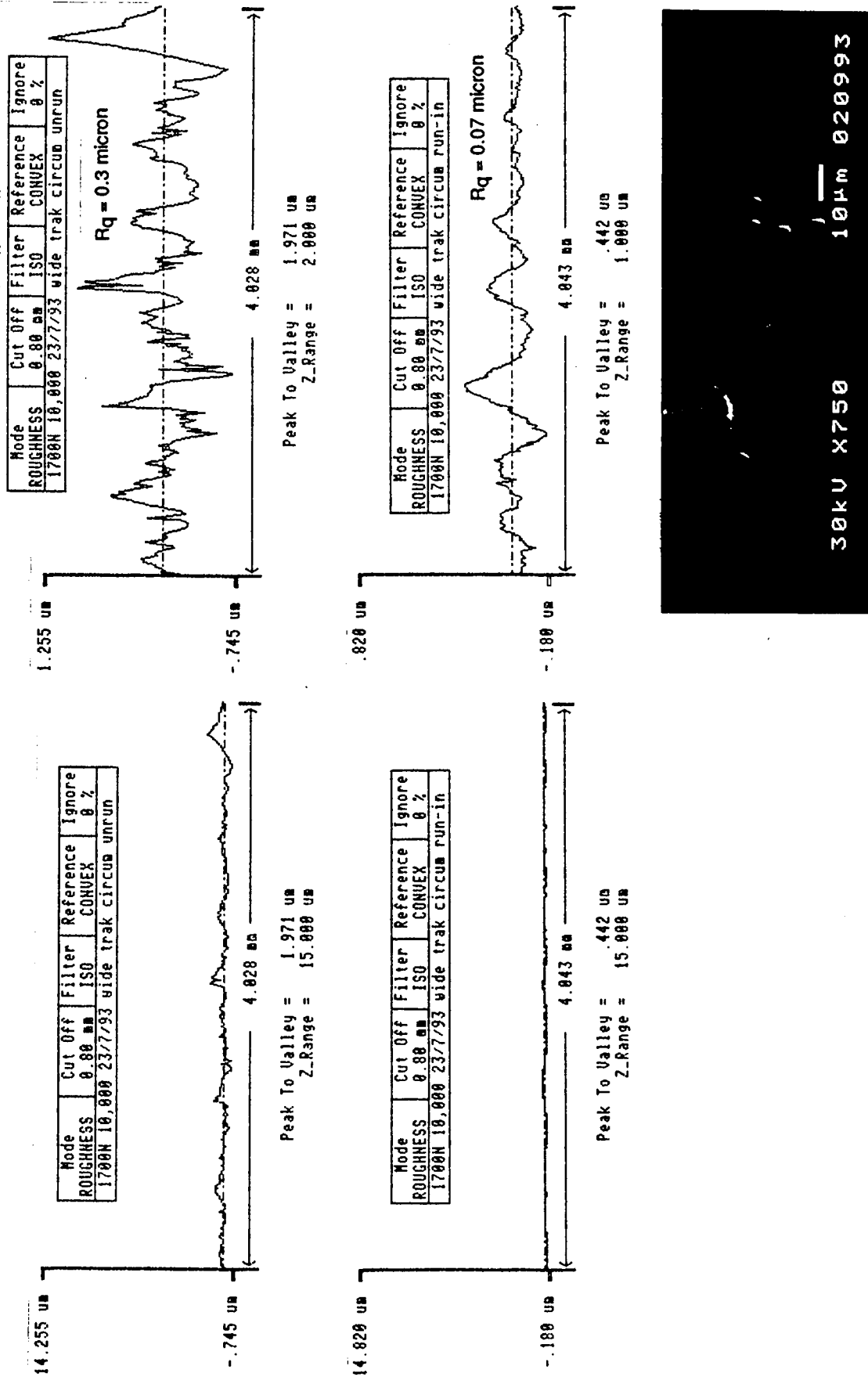
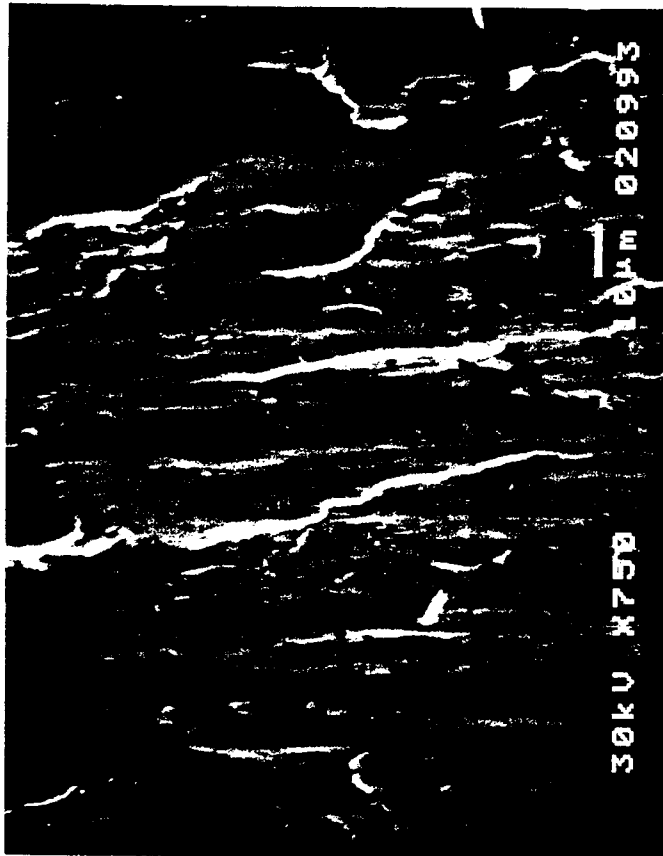


Figure 3.2 Surface Topography of Mini-Disc after Running-in

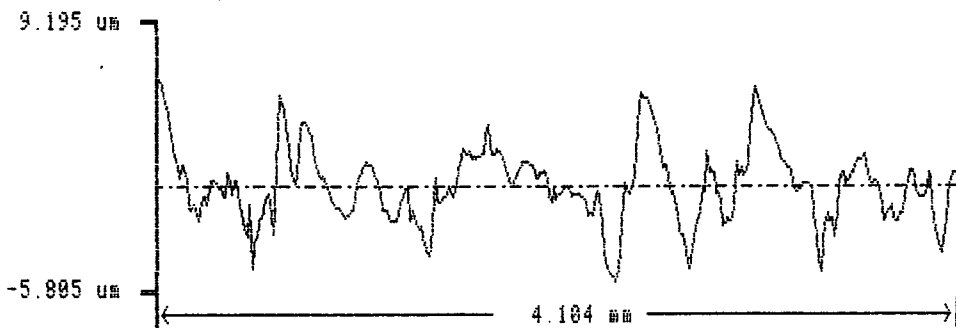


23/7/93-10,000 rpm, 37% S/R, 1700 N, Mil-L-23699B

Figure 3.3 Surface Topography of Scuffed Mini-Disc

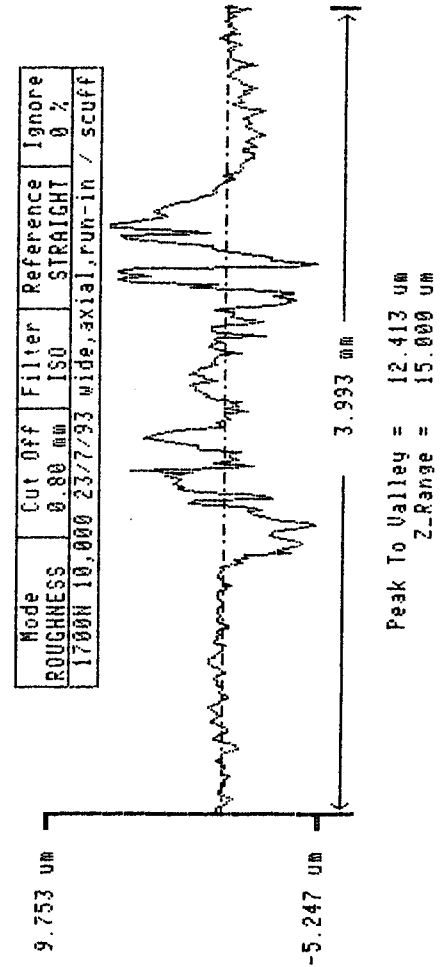


| Mode | Cut Off | Filter | Reference | Ignore |
|--------------|---------|-----------|-----------|--------|
| ROUGHNESS | 0.80 mm | ISO | CONVEX | 0 % |
| 1700N 10,000 | 23/7/93 | wide trak | circum | scuff |



Peak To Valley = 11.817 μm
Z_Range = 15.000 μm

23/7/93: 10,000 rpm , 37% S/R, 1700 N, Mil-L-23699B

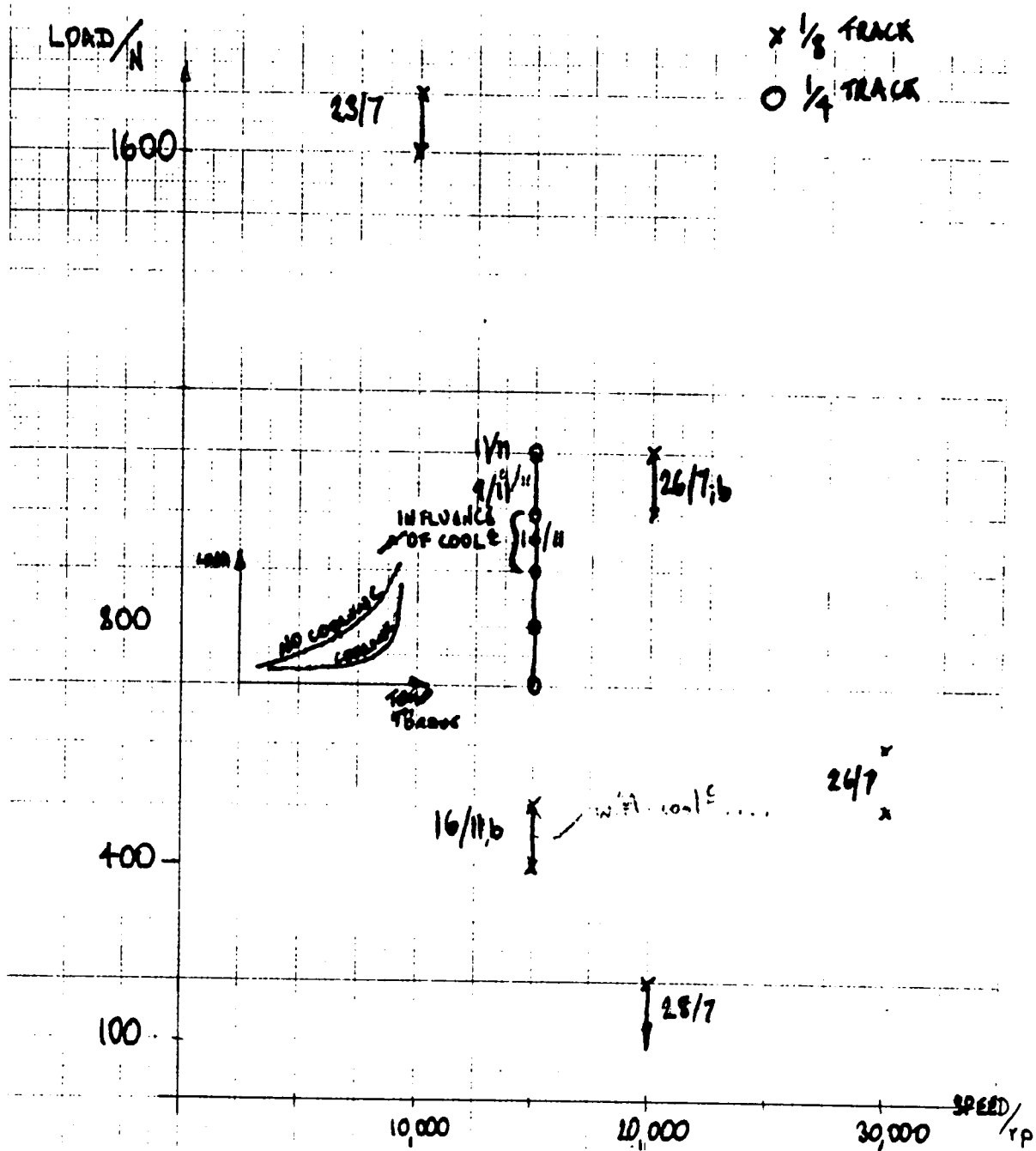


Peak To Valley = 12.413 μm
Z_Range = 15.000 μm



↓
1/8"
↑

Figure 3.4 Preliminary Scuffing Results with High Speed Mini-Disc



- ② CAUTION SHOULD BE ATTACHED TO EARLY RESULTS, $\leq 1/11$ AS THERE WERE PRIOR TO USE OF IR. THERMAL IMAGER \Rightarrow LOADS MAY BE OPTIMISTIC.

Figure 3.5 Log 10/11/93

Fluid & Contact Temperature and Armature power versus Time

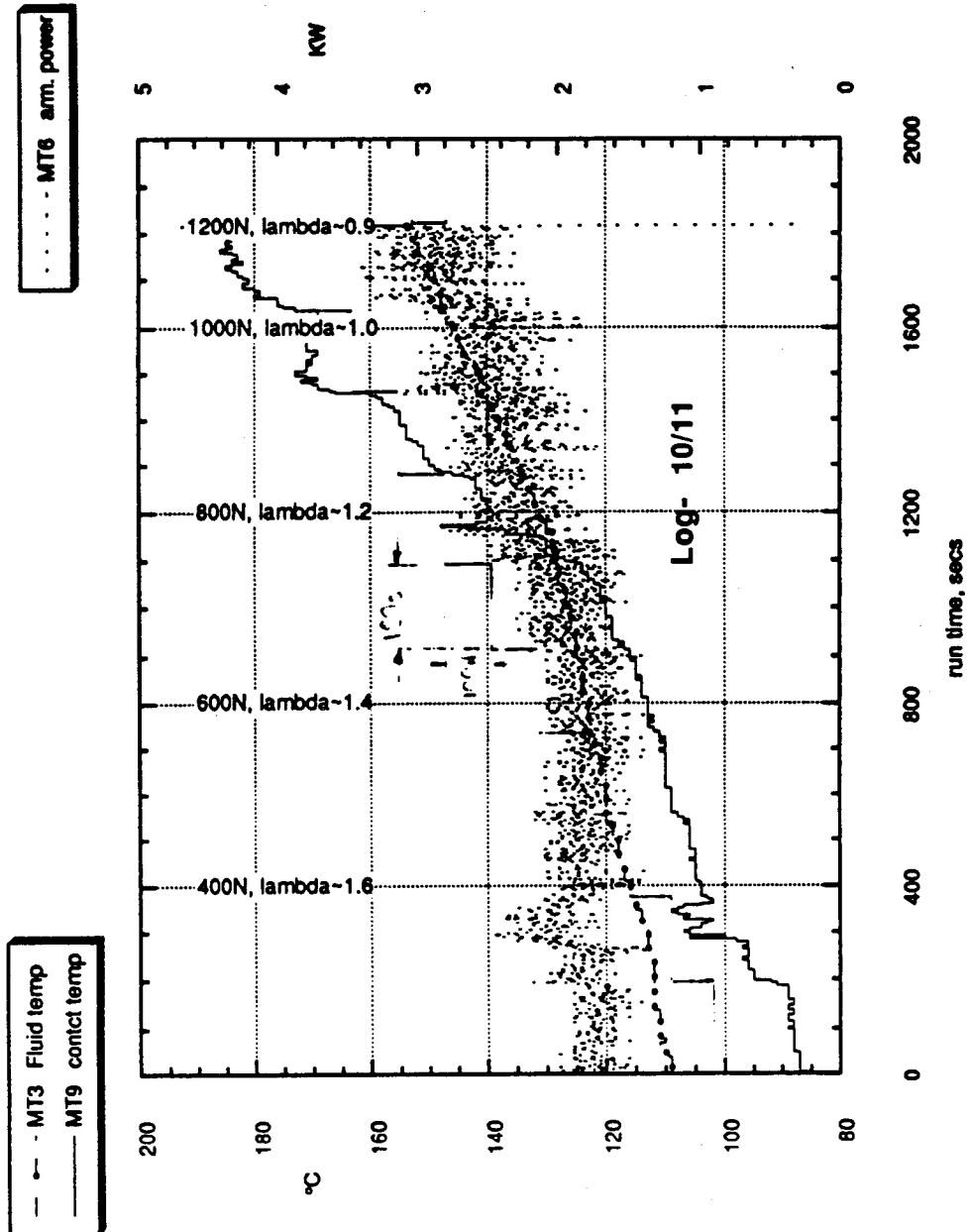
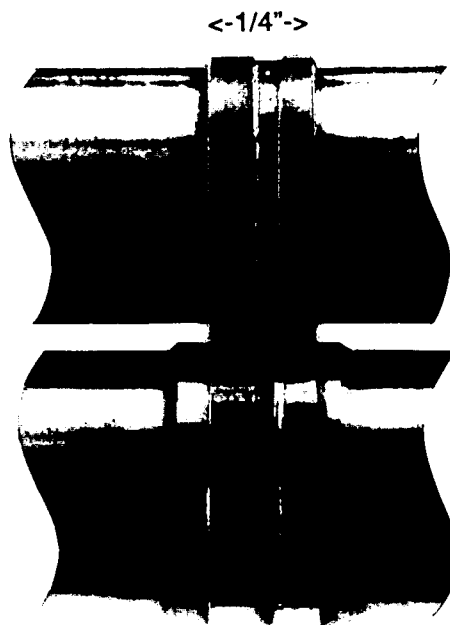


Figure 3.6 'High Speed Scuff'



11/1193: 15000 rpm, 37% slide/roll, 100 N, Mil-L-23699

Maximum temperature ~ 200°C, refer to Figure 3.6

Figure 3.7 Surface Topography of 'High Speed Scuff'

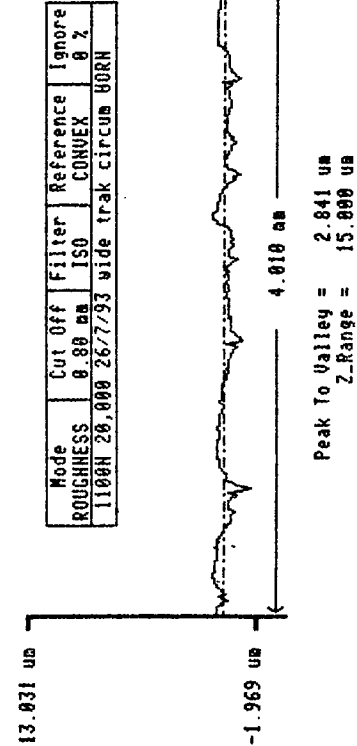
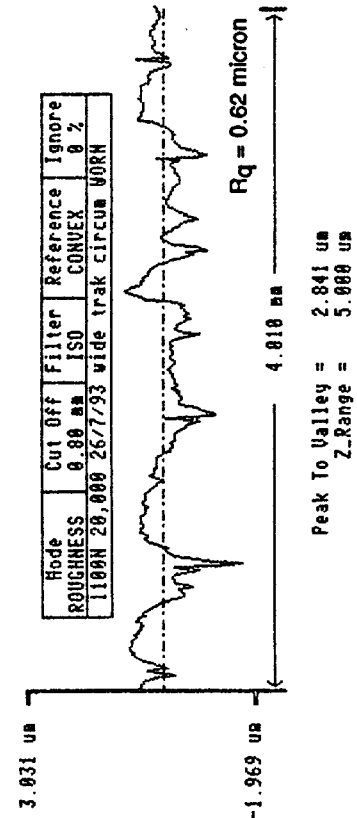
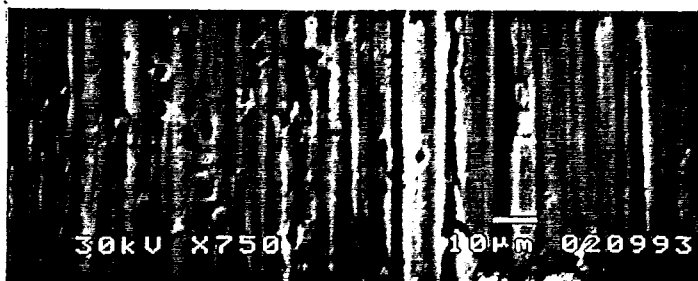
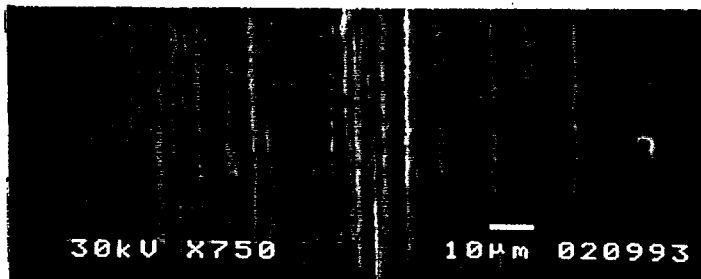
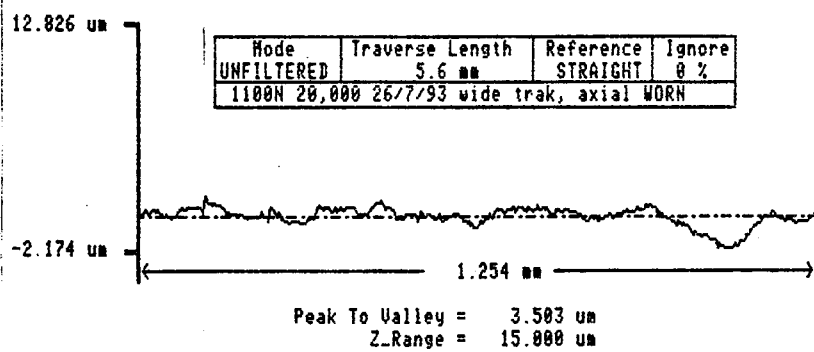
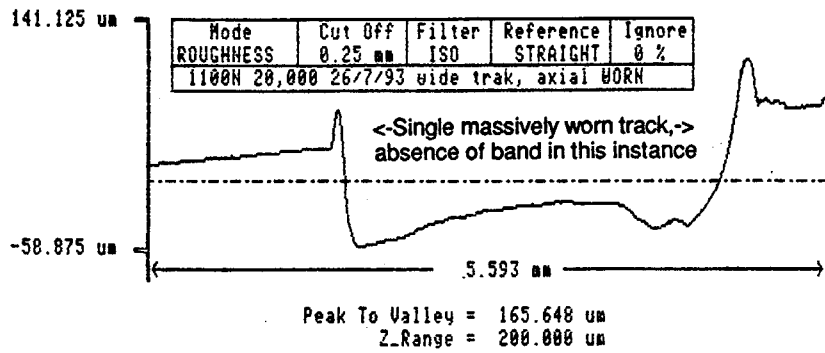


Figure 3.9 Log 11/11/93

Fluid & Contact Temperature, Armature power & Load versus Time

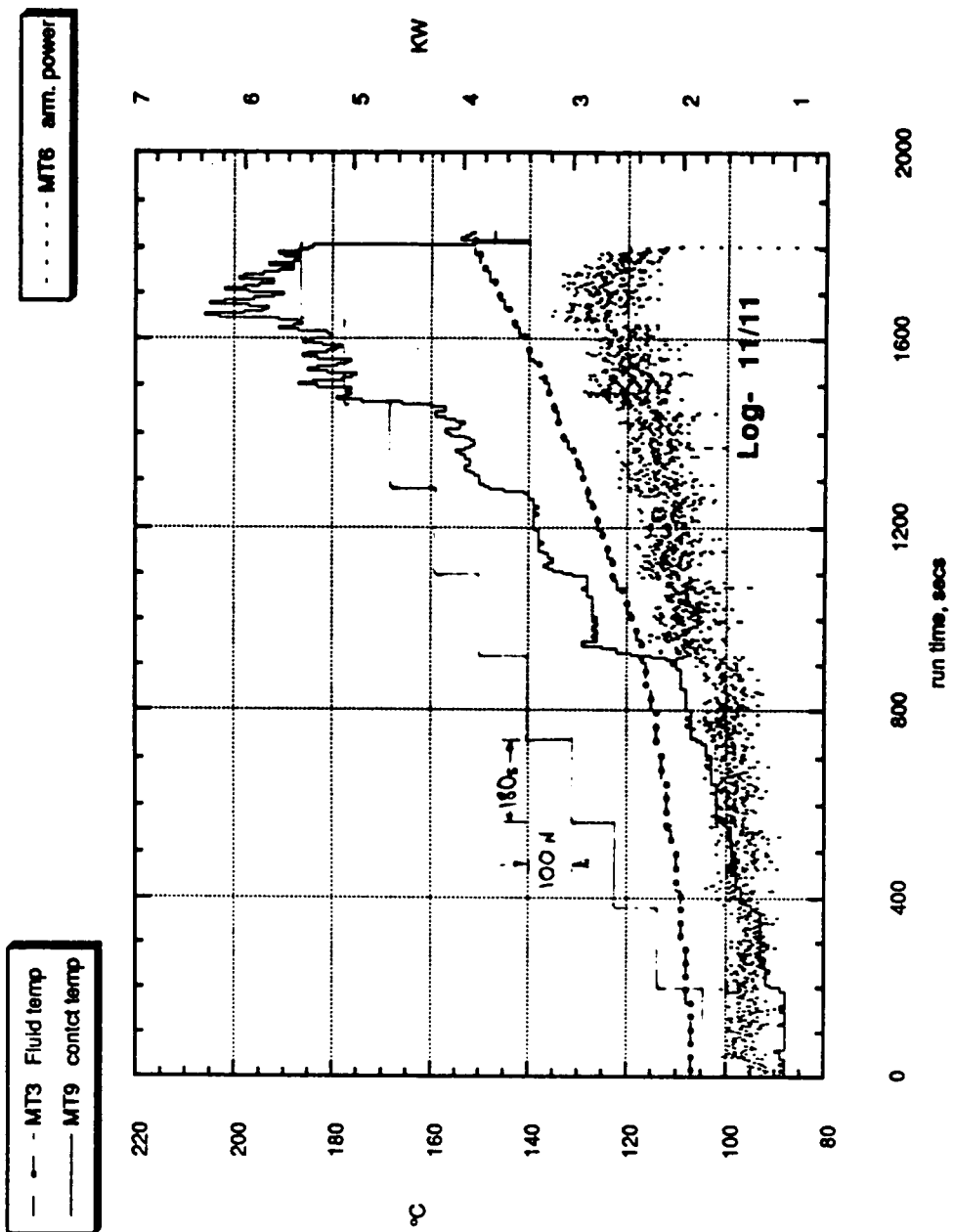
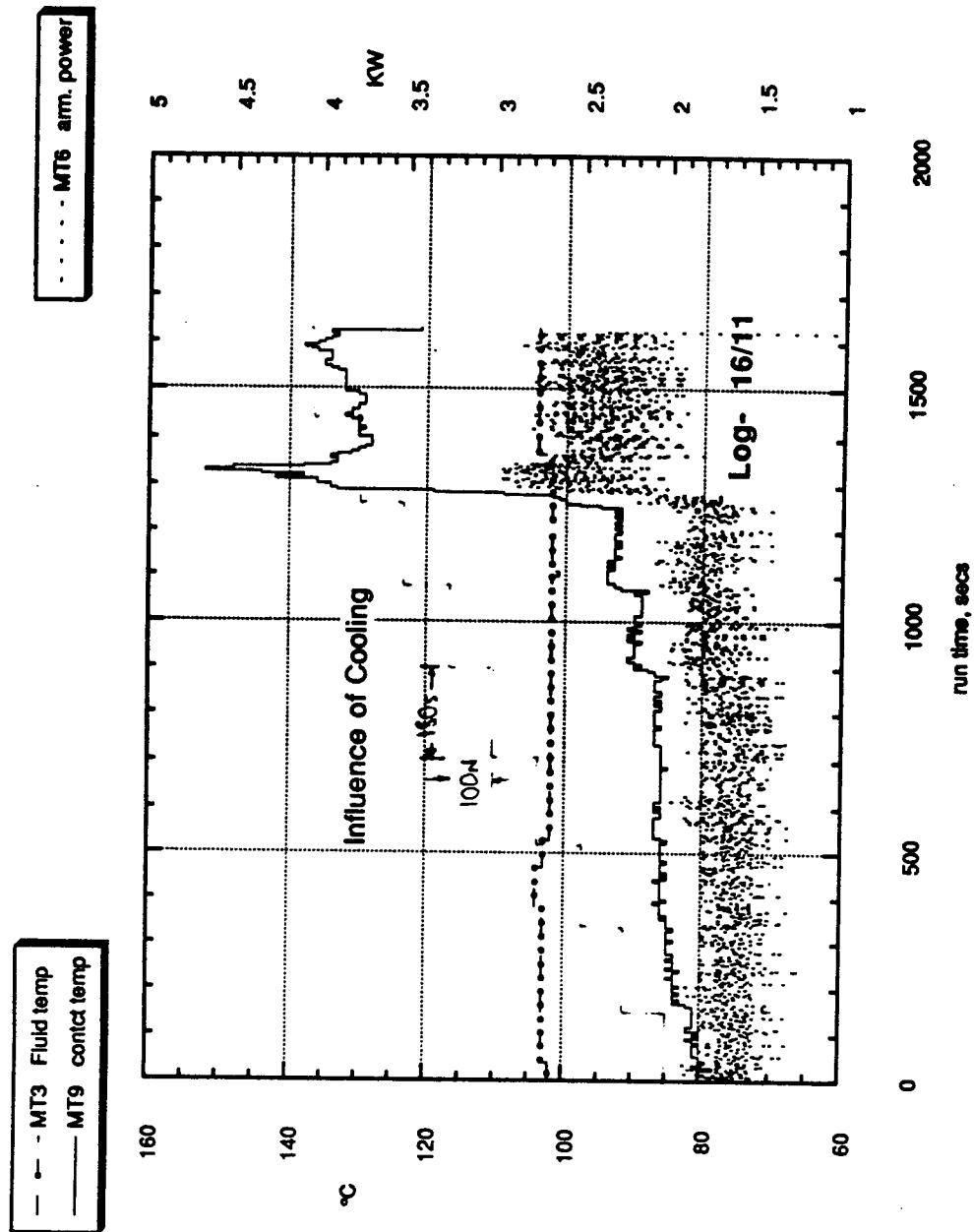


Figure 3.10 Log 16/11/93

Fluid & Contact Temperature, Armature power & Load versus Time



References

- American Gear Manufacturers Association (1980). Standard 110.04-1980
- American Gear Manufacturers Association (1965). *Gear scoring design guide for aerospace spur and helical gears*, Standard 217.01
- American Society Testing Materials. (1983). *Petroleum Products and Lubricants- 1947*, v 05.02, ASTM, Philadelphia, Pa.
- Archard, J.F. (1973). *EHD lubrication of real surfaces*, Tribology, 6, 8-14.
- Automobile Engineer(anon). (1948). *Gear Testing*, May, 191-192.
- Avery, R.W. and Hoffman, J.G. (1967). *Cylinder liner scuffing, why and how?* ASME publ. 67 DGP 12, April.
- Bair, S. & Winer, W.O. (1982). *Regimes of traction in concentrated contact lubrication*, trans. ASME, j Lub. Tech., v 104, July, 382-391.
- Bamberger, E.N., Harris, T.A., Kacmarsky, W.M., Moyer, C.A., Parker, R.J., Sherlock, J.J. and Zaretsky, E.V.(1971). *Life adjustment factors for ball and roller bearings*, ASME, New York.
- Bamberger, E.N. (1983). *Status of understanding of bearing materials*, NASA conf. Tribology in the 80's, CLEVELAND, vol II, s-publ. 2300.
- Begelinger, A. & de Gee, A.W.J. (1976). *On the mechanism of lubricant film failure in sliding concentrated steel contacts*, ASME j. Lub. Tech., 98, 4, 575-580.
- Bell, J.C. and Kannel, J.W. (1970). *Simulation of ball bearing lub. with rolling disc apparatus*, trans. ASME j. Lub. Tech., v 92, series F, 1, January, 1-15.
- Bell, K.J. & Bergelin, O.P. (1957). *Flow through annular orifices*, trans. ASME, v 79, 593-601.
- Benedict, G.H. and Kelley, B.W. (1961). *Instantaneous coefficients of Gear Tooth Friction*, trans. ASLE, 4, 59-70.
- Benedict, G.H. (1968). *Correlation of Disk machines and Gear Tests*, trans. ASLE, Dec., 591-596
- Benzing et al. (1976). *Friction & Wear devices*, 2nd ed., ASLE rpt of subcommittee on wear-lubrication fundamentals committee, ASLE, Park Ridge, Ill.
- Benzing R.J. (1964). *Experience on the IAE 3 1/4" gear rig lub. testing m/c in low temp. gear evaluation of exp. turb. oils*, Inst. Petri. Gear Lub. symp., Brighton, 29-36.
- Boner, C.J. (1971). *Gear and Transmission Lubricants*, Robert Krieger Publ.
- Brix, V.H. (~1946). *Load capacity rating of lubricants*, j. Inst. Petrol.
- Cameron, A. (1966). *Basic lubrication theory*, Longmans, London.
- Cameron, A., Lewis J.C. and Macpherson P.B. (1971). *Hydrostatic disc machine. Preliminary details*, ImechE conf. Externally pressurised bearing, Nov, C 41, 317-322.
- Carper, H.J., Anderson, E.L. and Ku P.M. (1972). *An investigation of scuffing on the AFAPL disk tester*, Tech. rpt. AFAPL-TR-72-28, June, WPAFB, Ohio.
- Carper, H.J., Anderson, E.L. and Ku P.M. (1971). *Development of the AFAPL disc tester for gear lubrication research*, Tech. rpt. AFAPL-TR-71-63, WPAFB, Ohio.
- Cocking, H. (1984). *Design of an advanced engineering gearbox*, Paper 85, Tenth European Rotorcraft Forum, The Hague, August.
- Davies, D.P. & Gittos, B.C. (1989). *Gear steels for future helicopter transmissions*, proc. IMechE, v 203 part G, 113-119.
- Dowson, D & Higginson, G.R. (1966). *Elastohydrodynamic lubrication*, Pergamon, Oxford.
- Dupont (1988). *Krytox® Fluorinated Oils sales literature*, Dupont E-77917-2 12/88.

- Dyson, A. & Naylor, H. (1961). *Application of the flash temperature concept to cam and tappet wear problems*, proc. IMechE Auto Div, April.
- Dyson, A. (1975). *Review of Scuffing*, Trib 8, 77-87, 117-121.
- Evans, E.A. and Elliott, J.S. (1941). *Hypoid gear lub. and additives*, j.Inst. Petrol., 27, 165-187.
- General Electric Fluid flow div. (1973). *Duct Systems- labyrinth seals*, 405.7, Oct., 1-20.
- Grosberg, J. (1977). *A critical review of gear scoring criteria*, Wear 43, 1-7.
- Hamrock, B.J. & Dowson, D. (1981). *Ball bearing lubrication*, Wiley, New York.
- Hopkins, V. (1962). *Development of High temperature e.p. lub. tester*, Lub. Eng. nov, 478-482.
- Hsing, F.C. & Walker, W.J. (1974). *Influence on turbine engine lubricant load carrying capacity on gear system design*, AFAPL-TR-74-94, WPAFB, Ohio.
- Hurst, G.H. (1911). *Lubricating oils and greases*, Scott Greenwood & Son, 3rd ed.
- Hyde, J.H. (1922). *Lubrication & Lubricants*, Pitman.
- Jackson, E.G., Muench, C.F. & Scott, E.H. (1960). *Evaluation of gear materials scoring at 700°F*, trans. ASLE, 3, No.1, 69-82.
- Johnson, K.L. (1987). *Contact Mechanics*, Cambridge University Press.
- Kannel, J.W. and Bupara, S.S. (1974). *Rheology of lubricants in real bearing contacts*, ASLE conf. Montreal Canada 8-10 Oct, Paper No. 74-Lub-25.
- Ku, P.M., Staph, H.E., Carper, H.J. & Anderson, E.L. (1976). *Lubricant / Metallurgy interaction effects on turbine engine lubricant load rating*, AFAPL-TR-76-27, WPAFB, Ohio.
- Kelley, B.W. (1953). *A new look at scoring phenomena of gears*, SAE trans. v 61, 175-188.
- Koshal, D. & Rowe, W.B. (1981). *Fluid-film journal bearings op. in a hybrid mode: Part I- Theoretical analysis and Design*, ASME J. Lub. Tech., v 103, oct, 558-565.
- Koshal, D. & Rowe, W.B. (1981). *Fluid-film journal bearings operating in a hybrid mode: Part II- Experimental investigation*, ASME J. Lub. Tech., v 103, oct, 566-572.
- Lane, E.A. (1979). *An analytical means for determination of scoring limited load capacity in sliding / rolling contact*, AFAPL-TR-79-2128, WPAFB, Ohio.
- Leach, E.F. and Kelley, B.W. (1965). *Temperature-the key to lubricant capacity*, trans. ASLE 8, 271-285.
- Loomis, W.R. (1982). *Overview of liquid lubricants for advanced aircraft*, ASLE Washington conf. Solid and Liquid Lub. for extreme environments, October, 33-39.
- Martin, (1916). *The lubrication of Gear Teeth*, Engineering, 11th Aug.
- Martin, H.M. (1908). *Labyrinth packings*, Engineering, Jan 10, 35-36.
- Machinery. (1948). *Machine for testing gear materials and lubricants*, May, 593-595.
- Macpherson, P.B. & Cameron, A. (1972). *Fatigue scoring, a new form of lubricant failure*, trans. ASLE, v 16, 1, 68-72.
- Macpherson, P.B. (1986). *The value of laboratory simulation testing for predicting gearbox performance*, AGARD meet. CP-394, 1, 1-11.
- Mansion, H.D. (1952). *Some factors affecting gear scuffing*, Gear Lub. symp., j. Inst. Petrol., v 38, 344, August, 633-645.
- Merritt, H.E. (1935). *Worm Gear Performance*, proc. IMechE. v 129, 127-194.
- Merritt, H.E. (1942). *Gear Lubrication*, Pitman, Bath.
- Michell, A. G. M. (1905). *Zeitschrift für Mathematik und Physik*, v 82, (Patent No. 875. 1905)
- Michell, A. G. M. (1937). *Tilting-pad bearings and their practical limitations*, Gen. discussion on Lub., Inst. Mech Eng, London, v 1, Oct, 196-203.
- Mohsin, M.E. (1981). *A hydrostatic bearing for high speed applications*, Tribology Int., Feb, 47-54.
- Musgrove, F. F., (1944), *Development and lub. of the automotive hypoid gear*, J. Inst. Pet, v 30.

- Neely, G.L. (1936). SAE trans. v 39.
- Neale, M.J. (1971). *Piston ring scuffing-a broad survey of the problems and practice*, proc. IMechE, v 185, 21-32.
- Neale, M.J. (1974). *The scuffing of piston rings*, IMechE, Chartered Mech. Engineer, Sept, 79-81.
- Nicholson, J.W. (1981). *Surface coatings to combat scuffing*, 8th Leeds-Lyon symp, Butterworths, Sept, 227-229.
- Nicolson, D.M & Sayles, R.S. (1988). *Research on a mini-disc machine for gear testing*, AFWAL-TR-87-2081, WPAFB, Ohio.
- O'Donoghue, J.P. & Cameron, A. (1966). *Friction & Temperature in rolling sliding contacts*, ASLE trans. v 9, 186-194.
- Olver, A.V. (1991). *Testing transmission lubricants: the importance of thermal response*, proc IMechE, v 205, part G, j. of Aerospace Eng., 35-44.
- Olver, A.V. (1993). *Temperature and lubrication of gears in high speed transmissions*, proc. IMechE. Aerospace Industries Div., Solihull meeting, 10th Nov.
- Orcutt et al. (1962). *Use of free energy relationships. in the selection of lubricants for high temperature applications*, Wear, 5, 345-362.
- Parker, R.J. & Kannel, J.W. (1971). *Elastohydrodynamic film thickness measurements with advanced ester, fluorocarbon and polyphenyl ether lubricants to 600°F*, NASA TN D-6608.
- Rao, N.S., Maciejewski, A.S. and Senholzi, P.B. (1981). *Precision measurement of gear lub. load carrying capacity (feasibility study)*, AFWAL-TR-81-2107 Aero prop. lab., WPAFB, Ohio.
- Rowe, W.B. (1983). *Hydrostatic and hybrid bearing design*, Butterworths, London.
- Ryder, E. (1959). *The gear rig as an oil tester*, ASLE Lub. Eng., Aug, 318-324.
- Salomon, G. (1976). *Failure criteria in thin film lubrication*, Wear, 36, 1, 1-6.
- Sayles, R.S., de Silva, G.M.S., Leather, J.A., Anderson, J.C. & Macpherson, P.B. (1981). *Elastic conformity in Hertzian contacts*, Trib. Int., Dec.
- Schlusser, A. (1963). *Development of gas entrained powder lub. for high speed and high temp. operation of spur gears*, progress rpt 3. contract AF 33(657)-8625.
- Shell (1964). *The lubrication of industrial gears*, SHELL, London.
- Sibley, L.B. and Orcutt, F.K. (1961). *Elastohydrodynamic lubrication of rolling-contact surfaces* ASLE trans, 4, 234-249.
- Smith & Macpherson, P.B. (1978). *Influence of vibrations on pitting and scuffing*, Westland Helicopters Limited, Yeovil, R.P. 588, Nov.
- Spikes, H.A. (1983). *Undergraduate Mech. Eng course notes (Lubrication)*, Dept. Mech.Eng., Imperial College, London.
- Van der Minne, J. L. (1937). *Comparison of the behaviour of various extreme pressure lub. in different testing m/c*, IMechE Gen. disc. on Lub., v 2, 1937, 429-441.
- Vermes, G. (1961). *A fluid mechanics approach to the labyrinth seal leakage problem*, j. Eng Power, April, 161-169.
- West H.J. (1946). *Mechanical testing of extreme pressure lubricants with special reference to hypoid oils*, j. Inst. Petroleum, v 32, 206-229.
- Wilson, D.S., Gray, S., Sibley, L.B., Krause, H., Allen, C.M. & Macks, F. (1959). *Development of lub. for high speed rolling contact brgs operating at 1200°F*, WADC TR 59-790
- Wilson, G. (1987). minutes of CRC Aviation Lub. Group meeting, April.
- Wolf, H.R. & Mougey, H.C. (1932). *Extreme-pressure lub. correlation of service data with lab. testing methods*, proc. Amer. Petroleum. Inst., sect. III, 118-131.
- Woodley, B.J. (1977). *Materials for Gears*, Tribology International, December, 323-330.
- Zandt, R.P. & Kelley, B.W. (1953). *Gear testing methods for the development of heavy duty gearing*, SAE Quart Trans, v 3, 354-368.